



Subduction kinematics and dynamic constraints

Carlo Doglioni ^{a,*}, Eugenio Carminati ^a, Marco Cuffaro ^a, Davide Scrocca ^b

^a *Dipartimento di Scienze della Terra, Università La Sapienza, Roma, Italy*

^b *CNR-IGAG, Roma, Italy*

Received 29 August 2006; accepted 19 April 2007

Abstract

The kinematics of subduction zones shows a variety of settings that can provide clues for dynamic understandings. Two reference frames are used here to describe the simple 2D kinematics of subduction zones. In the first, the upper plate is assumed fixed, whereas in the second frame upper and lower plates move relative to the mantle.

Relative to a fixed point in the upper plate U, the transient subduction hinge H can converge, diverge, or be stationary. Similarly, the lower plate L can converge, diverge or be stationary. The subduction rate V_S is given by the velocity of the hinge H minus the velocity of the lower plate L ($V_S = V_H - V_L$). The subduction rate 1) increases when H diverges, and 2) decreases when H converges.

Combining the different movements, at least 14 kinematic settings can be distinguished along the subduction zones. Variable settings can coexist even along a single subduction zone, as shown for the 5 different cases occurring along the Apennines subduction zone. Apart from few exceptions, the subduction hinge converges toward the upper plate more frequently along E- or NE-directed subduction zone, whereas it mainly diverges from the upper plate along W-directed subduction zones accompanying backarc extension.

Before collision, orogen growth occurs mostly at the expenses of the upper plate shortening along E–NE-directed subduction zones, whereas the accretionary prism of W-directed subduction zones increases at the expenses of the shallow layers of the lower plate.

Backarc spreading, forms in two settings: along the W-directed subduction zones it is determined by the hinge divergence relative to the upper plate, minus the volume of the accretionary prism, or, in case of scarce or no accretion, minus the volume of the asthenospheric intrusion at the subduction hinge. Since the volume of the accretionary prism is proportional to the depth of the decollement plane, the backarc rifting is inversely proportional to the depth of the decollement. On the other hand, along E- or NE-directed subduction zones, few backarc basins form (e.g., Aegean, Andaman) and can be explained by the velocity gradient within the hangingwall lithosphere, separated into two plates.

When referring to the mantle, the kinematics of subduction zones can be computed either in the deep or in the shallow hotspot reference frames. The subduction hinge is mostly stationary being the slab anchored to the mantle along W-directed subduction zones, whereas it moves W- or SW-ward along E- or NE-directed subduction zones. Surprisingly, along E- or NE-directed subduction zones, the slab moves “out” of the mantle, i.e., the slab slips relative to the mantle opposite to the subduction direction. Kinematically, this subduction occurs because the upper plate overrides the lower plate, pushing it down into the mantle. As an example, the Hellenic slab moves out relative to the mantle, i.e., SW-ward, opposite to its subduction direction, both in the deep and shallow hotspot reference frames. In the shallow hotspot reference frame, upper and lower plates move “westward” relative to the mantle along all subduction zones.

This kinematic observation casts serious doubts on the slab negative buoyancy as the primary driving mechanism of subduction and plate motions.

* Corresponding author.

E-mail address: carlo.doglioni@uniroma1.it (C. Doglioni).

W-directed subduction zones rather provide about 2–3 times larger volumes of lithosphere re-entering into the mantle, and the slab is pushed down. This opposite behavior is consistent with the down-dip extension seismicity along E–NE-directed subduction zones, and the frequent down-dip compression along the W-directed subduction zones.

Subduction kinematics shows that plate velocity is not dictated by the rate of subduction. Along the W-directed subduction zones, the rate of subduction is rather controlled i) by the hinge migration due to the slab interaction with the “easterly” trending horizontal mantle wind along the global tectonic mainstream, ii) by the far field plate velocities, and, iii) by the value of negative buoyancy of the slab relative to the country mantle.

Alternatively, E–NE–NNE-directed subduction zones have rates of sinking chiefly determined i) by the far field velocity of plates, and ii) by the value of negative buoyancy of the slab relative to the country mantle. Along this type of subduction, the subduction hinge generally advances E–NE-ward toward the upper plate decreasing the subduction rate, but it moves W–SW-ward relative to the mantle.

All this indicates that subduction zones have different origin as a function of their geographic polarity, and the subduction process is more a passive feature rather than being the driving mechanism of plate motions. A rotational component combined with mantle density and viscosity anisotropies seems more plausible for generating the global tuning in the asymmetry of subduction zones.

© 2007 Elsevier B.V. All rights reserved.

Keywords: subduction; kinematics; hinge migration; remounting slab; westward drift

52

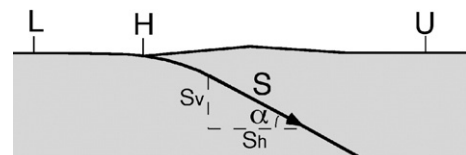
53 1. Introduction

54 The subduction process (Fig. 1) is a vital ingredient of
55 plate tectonics (Anderson, 1989, 2001; Stern, 2002;
56 Conrad and Lithgow-Bertelloni, 2003; Anderson, 2006).
57 By definition, along subduction zones, the lithosphere
58 enters into the underlying mantle (e.g., Jarrard, 1986;
59 Turcotte and Schubert, 2002). Most of the oceanic
60 lithosphere is recycled into the mantle, but also some
61 portions of continental lithosphere can subduct (Amp-
62 ferer, 1906; Panza and Mueller, 1978; Ranalli et al.,
63 2000; Hermann, 2002), usually termed as the collisional
64 stage of the process. There still are debates on the
65 initiation of the subduction process (Spence, 1987; Niu
66 et al., 2003), but once activated it may work for several
67 tens of million years. Subduction zones have a related
68 accretionary prism, or orogen, a subduction hinge that
69 can migrate (Garfunkel et al., 1986), and a large variety
70 of geophysical, magmatological and geological signa-
71 tures (Isacks and Molnar, 1971; Jarrard, 1986; Royden
72 and Burchfiel, 1989; Tatsumi and Eggins, 1995; Hacker
73 et al., 2003; Carminati et al., 2004a,b; Ernst, 2005).

74 Subduction zones may initiate when two basic param-
75 eters concur: i) the two plates have at least an initial
76 convergent component of relative plate motion and ii)
77 one of the two plates is sufficiently denser, thinner,
78 stronger and wider to be overridden. As a counterexam-
79 ple, when an oceanic rift opens to a width equal or
80 smaller than the thickness of the adjacent continen-
81 tal lithosphere, a complete subduction cannot develop
82 (Fig. 2). In other words, small oceans (150–200 km
83 wide) cannot generate normal, steady state, subduction
84 systems. This setting can rather evolve to obduction,
85 where ophiolitic slices of the oceanic realm are buckled
86 and squeezed on top of the continental lithosphere. One

example could be the Oman ophiolite complex (Nicolas 87
et al., 2000; Garzanti et al., 2002), even if it is unclear 88
whether this ocean was a narrow independent basin, or 89
rather part of a wider Tethyan branch (Stampfli and 90
Borel, 2002). 91

Regardless of the reason why the lithosphere moves, 92
e.g., slab pull (Forsyth and Uyeda, 1975) or mantle drag 93
(Bokelmann, 2002), the slab is assumed to sink at a 94
speed linearly correlated to the convergence rate (Jarrard, 95
1986) and its dip (Fig. 1). It is usually assumed that 96
the convergence rate between two plates equals the 97
subduction rate (e.g., Ruff and Kanamori, 1980; Stein 98
and Wysession, 2003; Fowler, 2005). However, the 99
behavior of the subduction hinge has been shown to be a 100
crucial parameter in subduction zones (e.g., Karig, 1971; 101
Brooks et al., 1984; Carlson and Melia, 1984; Winter, 102
2001; Hamilton, 2003). For example, a subduction hinge 103
migrating away from the upper plate, i.e. accompanying 104
the slab retreat or slab rollback, generates backarc 105
spreading (e.g., Brooks et al., 1984; Waschbusch and 106



L=lower plate
H=subduction hinge
U=upper plate
S=subduction rate=UH-UL
 S_v =vertical rate= $S \times \sin \alpha$
 S_h =horizontal rate= $S \times \cos \alpha$

Fig. 1. Basic kinematic terminology for a subduction zone used in the text. Steeper the slab, faster will be its penetration component into the mantle.

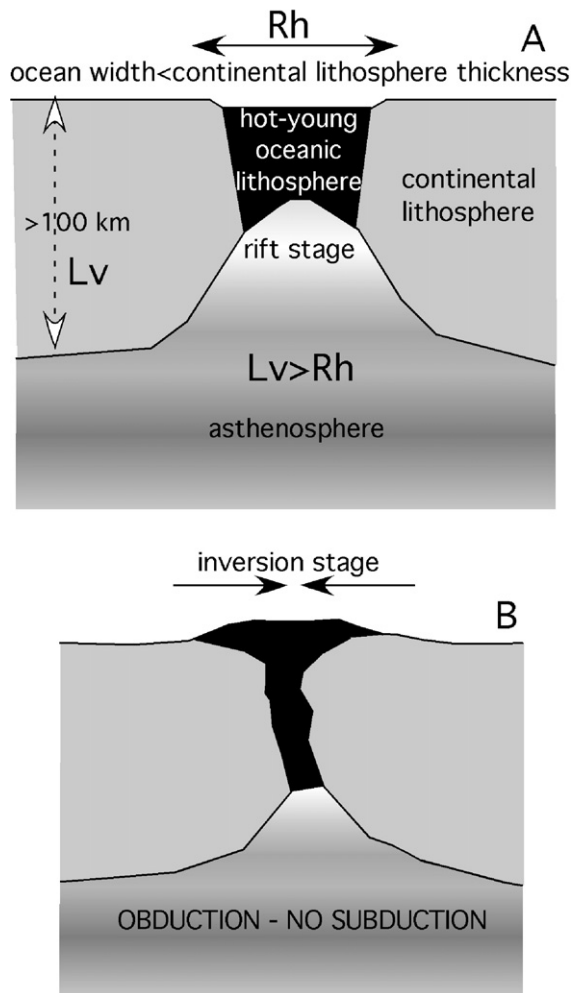


Fig. 2. An ocean basin that has a width (R_h) smaller than the thickness of the continental lithosphere (L_v) at its margins as in the upper panel A cannot evolve to a complete subduction, lower panel B. In this setting the ophiolites can be more easily obducted.

107 Beaumont, 1996; Heuret and Lallemand, 2005; Lallemand et al., 2005). Backarc basins prevail along the western Pacific supporting a geographic asymmetry of subduction zones (Dickinson, 1978; Uyeda and Kanamori, 1979; Doglioni et al., 1999a).

112 We contribute here with a simple 2D kinematic analysis of subduction zones moving the lower plate and the subduction hinge relative to the upper plate or, alternatively, moving all three points relative to the mantle. It will be shown that the subduction rate is strongly dependent on the rate and migration direction of the subduction hinge that can either converge or diverge relative to the upper plate, decelerating or accelerating the speed of subduction respectively, and a variety of different settings can be identified.

122 The model is tested with the GPS NASA data set (Heflin et al., 2005) since space geodesy data of plate motions have been shown to be equivalent to the velocities computed over the geologic time, e.g., through magnetic anomalies in the NUVEL-1 (Gordon and Stein, 1992; Robbins et al., 1993).

128 Plate kinematics is also analyzed with respect to the deep or shallow hotspot reference frames (Gripp and Gordon, 2002; Doglioni et al., 2005b; Crespi et al., 2007; Cuffaro and Doglioni, in press), supporting the notion of a westerly-polarized undulated lithospheric flow relative to the mantle, or tectonic mainstream (Doglioni, 1990; Crespi et al., 2007). In our analysis, unexpectedly against their definition, along some subduction zones directed E- or NE-ward, the slab appears to “escape” from the mantle, moving in the opposite direction to the subduction, and claiming for alternative dynamics of the subduction process.

140 On the basis of the kinematic inferences, the paradigm of the slab pull is seriously questioned. A number of counterarguments to the slab pull efficiency will be posed and critically disputed, and an alternative mechanical hypothesis is forwarded. Some basic dynamic speculations on the forces determining the subduction process and plate tectonics in general will be presented.

2. Subduction zones asymmetry

148 Subduction zones and related orogens show significant differences as a function of their polarity. It is referred here as polarity the direction of subduction with respect to the tectonic mainstream, which is not E–W, but undulates around the Earth (Doglioni, 1990; Riguzzi et al., 2006; Crespi et al., 2007).

154 Therefore, the asymmetry can be recognized not simply comparing W-directed vs. E-directed subduction zones, but subductions along the sinusoidal flow of absolute plate motions that undulates from WNW in the Pacific, E–W in the Atlantic, and NE to NNE from eastern Africa, Indian Ocean and Himalayas. In the hotspot reference frame a “westward” rotation of the lithosphere can be observed (Gripp and Gordon, 2002; Cuffaro and Jurdy, 2006). The origin of this net rotation of the lithosphere (Bostrom, 1971) is still under debate (Scoppola et al., 2006), but it should range between 4.9 cm/yr (Gripp and Gordon, 2002) and 13.4 cm/yr (Crespi et al., 2007) at its equator. This implies that the plate motions flow is significantly polarized toward the “west” (Doglioni et al., 1999a), and subduction zones follow or oppose the relative “eastward” relative mantle flow. Subduction zones following the flow are: North and South America cordilleras, Dinarides, Hellenides,

172 Caucasus, Zagros, Makran, Himalayas, Indonesia–Sunda
 173 arc, Taiwan, New Guinea, New Hebrides, southern New
 174 Zealand. Subduction zones opposing the flow are:
 175 Barbados, Sandwich, Apennines, Carpathians, Banda,
 176 Molucca, Tonga, Kermadec, Marianas, Izu–Bonin,
 177 Nankai, Philippine, Kurili, Aleutians. The Japan subduc-
 178 tion appears as a transitional subduction zone.

179 Since many subduction zones have undulations or arcs
 180 along strike, their dip and strike can be oblique or parallel
 181 to the proposed tectonic mainstream. For example, in
 182 the transfer zone between Makran and Himalayas NNE-
 183 directed subduction zones, along the Chaman left-
 184 lateral transpressive system, the tectonic mainstream is
 185 about parallel to the belt. Another emblematic case is the
 186 Aleutians arc, here considered as a subduction opposing
 187 the flow (W-directed). Along their western termination,
 188 they almost parallel the Pacific subduction direction
 189 (WNW), where the slab is a right-lateral ramp of the
 190 subduction, and it dips to the NNE.

191 The W-directed slabs are generally very steep (up to
 192 90°) and deep, apart few cases as Japan. They have a co-
 193 genetic backarc basin, and the related single verging
 194 accretionary prism has low elevation (e.g., Barbados,
 195 Sandwich, Nankai), is mostly composed of shallow rocks,
 196 and has a frontal deep trench or foredeep (Doglioni et al.,
 197 1999a). The E- or NE-directed subduction zones are less
 198 inclined (15–70°), and the seismicity generally dies at
 199 about 300 km, apart some deeper clusters close to the
 200 upper-lower mantle transition (Omori et al., 2004). The
 201 related orogens have high morphological and structural
 202 elevation (e.g., Andes, Himalayas, Alps), wide outcrops
 203 of basement rocks, and two shallower trenches or
 204 foredeeps at the fronts of the double verging belt, i.e.,
 205 the forebelt and the retrobelt. The retrobelt decreases its
 206 development when the upper plate is subject to extension
 207 (e.g., Central America, Aegena and Andaman Seas).

208 Lallemand et al. (2005) argue that the slab dip is not
 209 significantly influenced by the polarity of the subduc-
 210 tion. However their analysis is different from what was
 211 suggested in a number of alternative articles where
 212 the slab dip is measured not simply comparing E- vs. W-
 213 directed subduction zones, but is measured along
 214 the undulated flow of absolute plate motions (e.g.,
 215 Doglioni et al., 1999a,b, and references therein), and the
 216 definition of W- vs. E- or NE-directed is rather related to
 217 subductions following or contrasting this flow. More-
 218 over their analysis subdivides the slab into a shallow
 219 (<125 km) and a deeper part (>125 km). This sub-
 220 division is ambiguous for a number of reasons. The E-
 221 or NE-directed subduction zones have mostly continen-
 222 tal lithosphere in the upper plate and the dip of the first
 223 125 km is mostly constrained by the thickness and

224 shape of the upper plate. Moreover, oblique or lateral
 225 subduction zones such as the Cocos plate underneath
 226 Central America are, by geometrical constraint, steeper
 227 (>50°) than frontal subduction zones (e.g., Chile), like
 228 the oblique or lateral ramp of a thrust at shallow levels in
 229 an accretionary prism is steeper than the frontal ramp.
 230 Cruciani et al. (2005) reached similar conclusions of
 231 Lallemand et al. (2005) stating no correlation between
 232 slab age and dip of the slab, but their analysis is stopped
 233 to about 250 km depth because E- or NE-directed
 234 subduction zones do not have systematic seismicity at
 235 deeper depth, apart few areas where seismicity appears
 236 concentrated between 630 and 670 km depth, close the
 237 lower boundary of the upper mantle. The origin of these
 238 deep isolated earthquakes remains obscure (e.g., mineral
 239 phase change, blob of detached slab or higher shear
 240 stress) and therefore they could not represent the
 241 simple geometric prolongation of the shallow part of
 242 the slab. Therefore, at deep levels (>250 km) the dip of
 243 the slab based on seismicity cannot be compared
 244 between W- and E–NE-directed subduction zones,
 245 simply because most of the E- or NE-directed slabs do
 246 not show continuous seismicity deeper than 250 km.
 247 High velocity bodies suggesting the presence of slabs in
 248 tomographic images often do not match slab seismicity.

249 Moreover, Lallemand et al. (2005) note that steeper
 250 slabs occur where the upper plate is oceanic, while
 251 shallower slabs occur where the upper plate is continental.
 252 However, the majority of E- or NE-directed subduction
 253 zones worldwide have continental lithosphere in the upper
 254 plate, confirming the asymmetry. Therefore any statistical
 255 analysis on the slab dip based on seismicity cannot be
 256 done simply comparing W- and E-directed slabs because
 257 E- or NE-directed subduction zones do not have
 258 comparably deep seismicity. Moreover subduction
 259 zones juxtapose plates of different thickness and
 260 composition generating variation in the dip. The variabil-
 261 ity of the angle of obliquity of the subduction strike with
 262 respect to the convergence direction determines a further
 263 change in dip of the slab. Removing these issues, the W-
 264 directed subduction zones when compared to E- or NE-
 265 directed slabs still maintain a number of differences, such
 266 as they are steeper, they are deeper or at least they present
 267 a more coherent slab-related seismicity from the surface
 268 down to the 670 discontinuity, and they show opposite
 269 down-dip seismicity as it will be discussed later. But,
 270 even more striking, surface geology and topography of the
 271 orogens contrast dramatically with a number of differ-
 272 ences between the opposite subduction zones such as
 273 shallow vs. deep rocks, steep vs. shallow dip of the fore-
 274 land monocline, low vs. higher inclination of the topo-
 275 graphic and structural envelop, small vs. wider area above

276 sea-level, etc., respectively for W- vs. E- or NE-directed
277 subduction zones (e.g., [Lenci and Doglioni, in press](#)).

278 Moreover backarc spreading occurs mostly in W-
279 directed subduction zones. Two counterexamples are
280 proposed as proofs that this statement is not correct, i.e.,
281 the Aegean and the Andaman Seas, which are related to
282 NE- to NNE-directed subduction zones. However these
283 two cases have a different kinematics and geodynamic
284 setting with respect to the W-directed subduction zones,
285 where upper plate extension is concomitant to subduc-
286 tion hinge migrating away with respect to the upper
287 plate, being the lithospheric deficit due to subduction,
288 compensated by mantle replacement (e.g., [Doglioni,](#)
289 [1991](#)). Along the Aegean and Andaman rift zones the
290 extension rather accommodates only the differential
291 velocity within the upper lithospheric plate, which is
292 split into two plates overriding the subduction (e.g.,
293 [Doglioni et al., 2002](#)). Along the Andaman–Sunda–
294 Indonesia arc for example, the flow of plates is NE- to
295 NNE-directed ([Heflin et al., 2005](#)). Extension or
296 “backarc” spreading is not diffused along the entire
297 arc, but rather concentrated at the western margin, along
298 the transfer zone between the SW-ward faster advancing
299 of Indonesia upper plate over the lower oceanic plate
300 (about 60 mm/yr) with respect to the slower velocity of
301 Eurasia upper plate in overriding the continental Indian
302 lithosphere along the Himalayas belt (about 40 mm/yr).
303 Where upper plate extension occurs along these settings,
304 the retrobelt of the orogen is poorly developed and
305 narrower. Another example seems the Central America
306 subduction zone (e.g. Guatemala, El Salvador, Nicar-
307 agua, Costa Rica), in which the upper plate extension
308 accommodates the faster westward motion of North
309 America relative to South America.

310 [Royden \(1993\)](#) proposed that the asymmetry of
311 subduction zones is related to a convergence rate faster
312 or slower than the slab retreat. [Doglioni et al. \(2006a\)](#)
313 rather suggested that the subduction system is primarily
314 sensitive to the behavior of the subduction hinge, i.e.,
315 moving toward or away from the upper plate, regardless
316 the convergence rate. The resulting subduction rate is
317 faster than the convergence rate where the hinge migrates
318 away from the upper plate, whereas it is slower than the
319 convergence where the hinge converges or advances
320 toward the upper plate. The two end members appear
321 sensitive to the geographic polarity of the subduction
322 zones, being the asymmetry not among E–W subduction
323 zones, but following or opposing an undulated “westerly”
324 directed lithospheric flow ([Doglioni, 1993](#)), recently
325 validated by space geodesy and statistical analysis ([Crespi](#)
326 [et al., 2007](#)). This tectonic mainstream implies a relative
327 mantle undulated counterflow, “easterly” directed.

328 The result of the asymmetry among opposite sub-
329 duction zones is that along the W-directed subduction
330 zones only the shallow rocks on the subduction hinge are
331 accreted (sedimentary cover and slices of the topmost
332 basement) because the accretionary prism basal decolle-
333 ment is located at the top of the subduction, without an
334 actively thrusting upper plate. In the opposite E- or NE-
335 directed subduction hinge, the lithosphere basal decolle-
336 ment is ramping upwards, providing a mechanism for
337 uplifting deep-seated rocks ([Doglioni, 1992](#)).

338 As a consequence, the shortening is concentrated in
339 the shallow layers of the lower plate along W-directed
340 subduction zones, both during the oceanic and the
341 continental stages of subduction, providing small volu-
342 mes to the orogen and maintaining a low elevation of the
343 critical taper (e.g., [Bigi et al., 2003](#); [Lenci et al., 2004](#)).

344 The shortening is rather mostly concentrated in the
345 upper continental lithosphere in E- or NE-directed
346 oceanic subduction zones. Andean type trenches are in
347 fact often characterized by tectonic erosion (e.g., [von](#)
348 [Huene and Lallemand, 1990](#); [Ranero and von Huene,](#)
349 [2000](#); [Kukowski et al., 2001](#); [Clift et al., 2003](#)), rather
350 than accretion ([Moore et al., 1990](#); [Kukowski et al.,](#)
351 [1994](#)). It is unclear how deep it is transported the material
352 offscraped by the tectonic erosion. It could eventually be
353 re-transferred to the upper plate in the lower crust or
354 upper mantle, and later re-exhumed during shortening
355 progression.

356 However, accretion is documented along the Casca-
357 dia, Indonesia and several other segments of this type of
358 subduction zones (e.g., [Hyndman et al., 1993](#)), thus
359 providing a transfer of shallow rocks from the lower
360 to the upper plate. But it is only at a collisional stage
361 that the lower plate is eventually entirely involved and
362 shortened. During this final stage, the lower plate
363 contributes significantly to the volume increase of the
364 orogen because shear zones and decollement planes
365 enter much deeper in the continental crust of the foot-
366 wall plate.

367 No tectonic erosion has seismically been observed
368 along most of W-directed subduction zones. It has been
369 proposed along the Tonga and other western Pacific sub-
370 duction zones only on the basis of the forearc subsidence
371 (e.g., [Clift and MacLeod, 1999](#)). However such subsi-
372 dence can also be alternatively interpreted as generated by
373 the hinge retreat. In the Apennines, documented accretion
374 occurs while subduction hinge retreat-related subsidence
375 exceeds the prism uplift ([Doglioni et al., 1999a,c](#)).

376 The term accretionary prism is often confused with the
377 term forearc, which is the region between the subduction
378 trench and the volcanic arc, having not always a unique
379 tectonic meaning. The arc is also a misleading term used
379

380 both to define a volcanic belt or a structural undulation of
381 a thrust system. Moreover in the so-called forearc,
382 extension can be widespread, without active accretion.

383 The shortening in prisms of W-directed subductions
384 can be larger than the convergence rate, whereas it is in
385 general smaller than the convergence in orogens of E- or
386 NE-related subductions (Doglioni et al., 2005a, 2006a).
387 This occurs because along W-directed slabs the shortening
388 is confined in the lower plate and directly equivalent to the
389 amount of subduction, which is larger than the conver-
390 gence rate. In the E- or NE-directed slabs, the shortening is
391 smaller than the convergence because the convergence is
392 partitioned partly in the subduction rate, and partly in the
393 contraction of the upper plate. While W-subduction-
394 related prisms have a forebelt and a backarc basin, E–NE-
395 subduction-related orogens have a forebelt and a widely
396 developed retrobelt since the very early stages.

397 The different rock exhumation in the different
398 subduction settings is highlighted by peculiar petrography
399 of transported sediments (Garzanti et al., in press).

400 Regional foreland monoclines at the accretionary
401 prism fronts also show steep dip and fast subsidence
402 rates along W-directed subduction zones, and shal-
403 low dip and slow subsidence rates for E- or NE-directed
404 subduction zones (Doglioni, 1994; Mariotti and
405 Doglioni, 2000). This is a paradox because if the fore-
406 deep subsidence is generated only by the mountain load,
407 along the highest mountains as the Andes and
408 Himalayas we should expect the deepest trenches and
409 foredeeps, but we rather observe these features along the
410 opposite subduction zones where there is not a
411 significant lithostatic load, like the Marianas trench,
412 the Apennines and Carpathians foredeep. The relative
413 “eastward” mantle flow could favor the bending of the
414 slab and the foredeep fast subsidence along the hinge of
415 W-directed subduction zones. The mantle counter flow
416 should rather contrast the subsidence along the opposite
417 subduction zones, providing a force sustaining the slab
418 (Doglioni, 1994). While W-directed subduction-related
419 prisms have low-grade metamorphism, the E- or NE-
420 subduction-related orogens at the collisional stage may
421 exhibit UHP rocks (Doglioni et al., 1999a). Metallogene-
422 sis appears to be also controlled by subduction
423 style (Mitchell and Garson, 1981). The Mariana type
424 subduction is characterized by Kuroko or similar volca-
425 nogenic sulphide deposits (Nishiwaki and Uyeda,
426 1983). Porphyry copper deposits are instead concentrat-
427 ed in collisional settings and Andean type subduction
428 zones.

429 The seismicity of the slabs (Isacks and Molnar, 1971;
430 Seno and Yoshida, 2004) is mostly characterized by
431 down-dip compression along W-directed subduction

432 zones, whereas it is quite often down-dip extensional
433 along E- or NE-directed subduction zones. Japan
434 subduction shows a different case, having two separate
435 layers of slab seismicity, i.e., an upper one characterized
436 by down-dip compression, and a lower one where down-
437 dip extension prevails. However, Japan seems an
438 intermediate case of subduction, where the Neogene W-
439 directed subduction system is presently initiating to flip,
440 having the backarc basin started to shrink (Mazzotti et al.,
441 2001; Doglioni et al., 2006a). The seismicity is frequently
442 down-dip extensional all along the subduction hinges of
443 both subduction polarities, possibly related to the bending
444 of the lithosphere.

445 Within the two opposite end-members, a number of
446 different settings can occur. For example along the E–NE-
447 directed subduction zones there are oceanic slabs under
448 continental lithosphere as in the Andes, which may or
449 may not evolve to continent–continent collision such as
450 the Alps or Himalayas (Ernst, 2005). Along W-directed
451 subduction zones there also are variable compositions of
452 the lower plate (both oceanic and continental lithosphere,
453 e.g., Marianas and Apennines, Banda arc) and variable
454 depth of the basal decollement plane, determining
455 variations in the volume of the related accretionary
456 prism (e.g., Bigi et al., 2003; Lenci et al., 2004).

457 The vertical and lateral growth of orogens is strong-
458 ly asymmetric. In fact prism or orogens related to W-
459 directed subduction zones mostly generate an E-ward
460 migrating wave, never reaching high structural and mor-
461 phologic elevation, where the volumes and elevation
462 rates of the prism are constrained by the subduction rate
463 and the depth of the basal decollement plane of the
464 accretionary prism. On the other hand, orogens related to
465 E- or NE-directed subduction zones are much more
466 elevated and their growth occurs both vertically and
467 horizontally (Doglioni et al., 1999a).

468 In this article we only discuss the most striking asym-
469 metries among subduction zones and their kinematics, and
470 we speculate on how these interpretations allow alternative
471 point of view on the dynamics of plate tectonics.

472 As prototypes of different subduction zones, the Alps
473 and the Apennines (Fig. 3) are orogens formed above
474 opposite slabs (Fig. 4). Along the first belt, since the
475 Cretaceous, the European plate subducted SE-ward
476 underneath the Adriatic plate, whereas along the second
477 belt, since the Late Oligocene, the Adriatic plate sub-
478 ducted W-ward below the European plate, with fast slab
479 rollback and backarc spreading in the western Mediter-
480 ranean (Rehault et al., 1984; Rehault et al., 1985; Doglioni
481 et al., 1999b; Frizon de Lamotte et al., 2000; Faccenna
482 et al., 2004). The two belts show distinct characters
483 (Fig. 4).

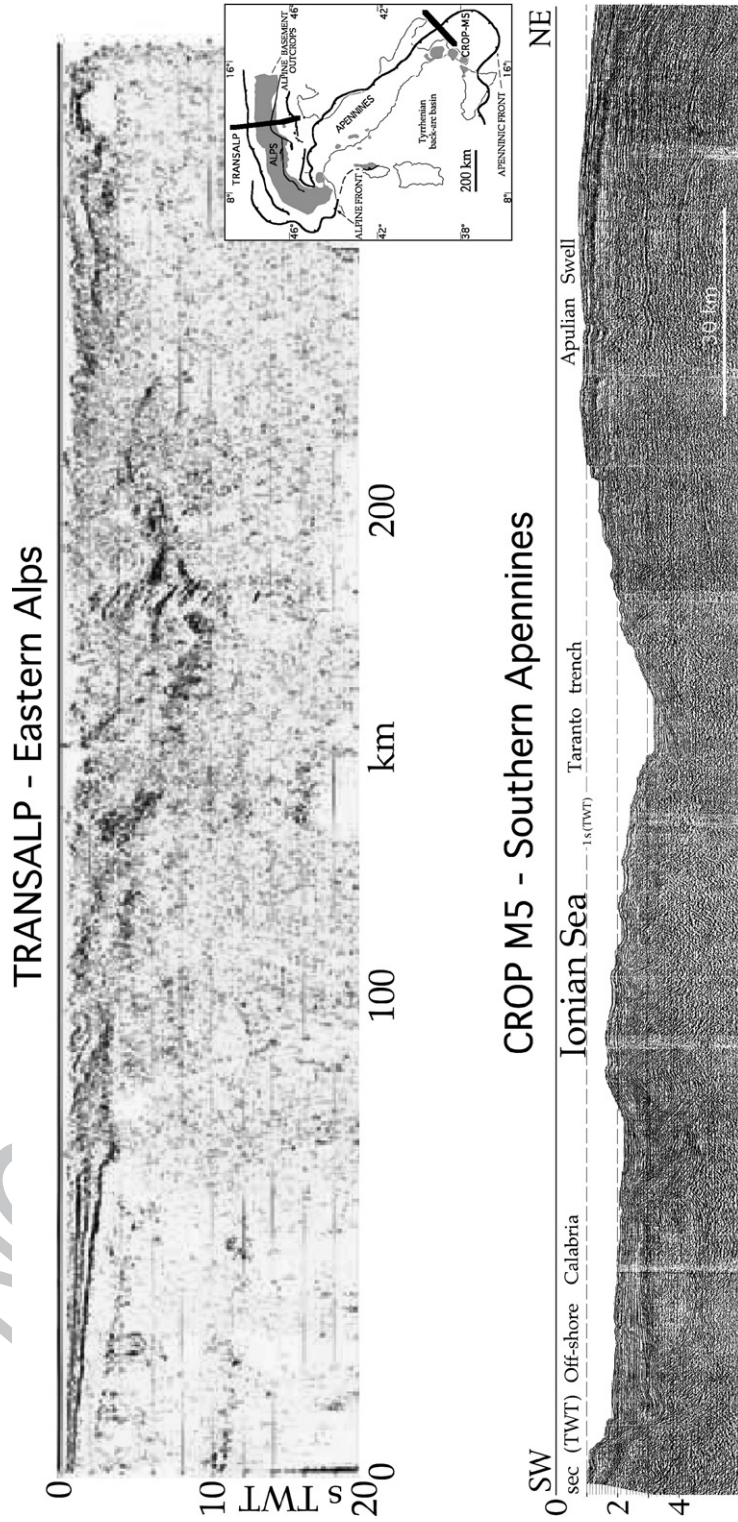


Fig. 3. Seismic sections of the Alps (Transalp, 2002) and of the Apennines (Scrocca et al., 2003).

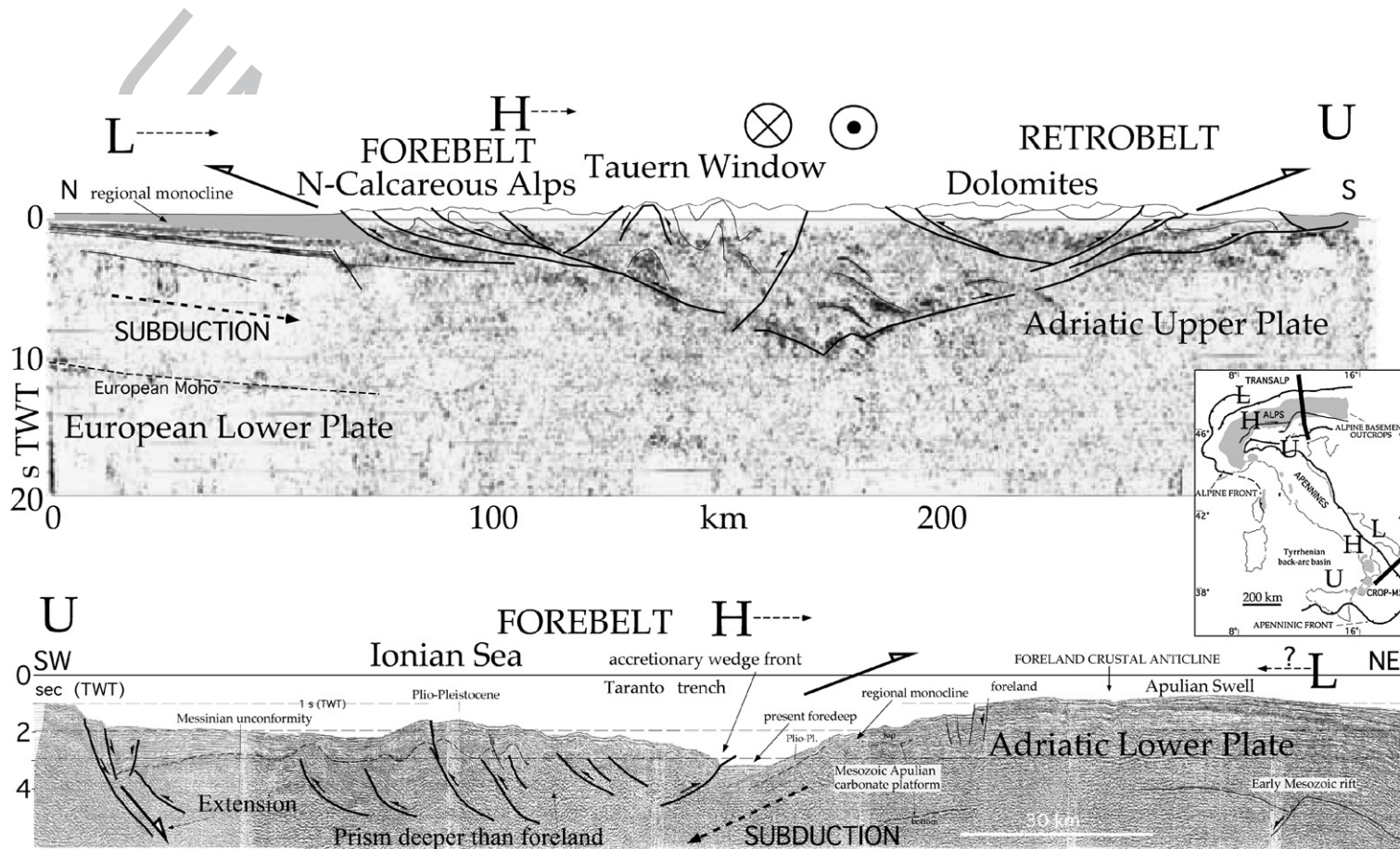


Fig. 4. Same sections as in Fig. 1 with some interpretation (modified after Doglioni et al., 1999c; Transalp, 2002). Note the Alpine double vergence vs. the single Apennines vergence, where the prism is even deeper than the foreland and followed by extension to the left. L, lower plate, H, subduction hinge, U, upper plate. In the Alps H migrated toward the upper plate, whereas it moves toward the lower plate in the Apennines. The Adriatic plate is the upper plate U in the Alps, while it is the lower plate L in the Apennines. The E–W segment of the Alps formed under right-lateral transpression.

484 The Alps, unlike the Apennines, have double vergence,
485 high structural and morphologic elevation, and no backarc
486 basin. The Alps have two shallow foreland monoclines at
487 the base of two foredeep basins, whereas the Apennines
488 have a single deep foredeep, with steeper monocline and
489 faster subsidence rates (Doglioni et al., 1999a). Beneath
490 the Alps the crust is about doubled, and the lithosphere
491 base is deeper than 100 km. Below the Apennines, a new
492 shallow Moho formed in the western backarc side, and the
493 asthenosphere is very shallow (30–40 km, Panza et al.,
494 2003). The new Moho is kinematically required by the
495 replacement of the original Moho, now subducted, on
496 which the present surface thrust sheets were originally
497 lying, being part of a pre-existing passive margin section.
498 A new mantle section from west has replaced the
499 subducted crustal section, the pre-subduction Moho and
500 the lithospheric mantle of the lower plate, since the slab is
501 eastward retreating (Doglioni, 1991).

502 The Alps have widespread outcrops of basement
503 rocks. In fact along the Alpine belt, thrusts are deeply
504 rooted, cross-cutting the whole crust and upper mantle
505 (Dal Piaz et al., 2003). Seismic tomography shows large
506 involvement of continental lithosphere in the subduction
507 system (Mueller and Panza, 1986). In the Apenninic
508 belt, the prism is rather mostly composed of shallow
509 (mostly sedimentary) crustal rocks of the lower plate
510 because the decoupling surface is traveling atop the
511 downgoing lithosphere (Bally et al., 1986).

512 The different structural settings of Alps and Apennines
513 suggest different dynamic and consequently kinematic
514 evolution of the related subduction zones. These
515 asymmetries are diffused worldwide in the orogens, and
516 appear controlled by the polarity of the subduction, i.e.,
517 following or opposing the polarized undulated flow of
518 plate motions.

519 A number of exceptions occur to these two end
520 members. For example, Japan has low elevation and other
521 characteristics of W-directed subduction zones, such as
522 the backarc basin and an accretionary prism mostly
523 composed of shallow rocks (von Huene, 1986). However
524 the slab has low dip of the subduction plane (Jarrard,
525 1986) and there is no active hangingwall extension, in
526 spite of an onshore morphology suggesting widely
527 distributed structural depressions. The GPS data confirm
528 that the Japan Sea backarc is not opening anymore, but it
529 is rather closing (Mazzotti et al., 2001). This indicates that
530 the system possibly arrived at an end, and its inversion
531 started. Unlike other living W-directed subduction zones,
532 the slab hinge in Northern Japan is moving toward the
533 upper plate.

534 W-directed subduction zones formed mostly along the
535 retrobelt of pre-existing E–NE-directed subduction

536 zones, provided that oceanic lithosphere was present in
537 the foreland to the east (Doglioni et al., 1999b). This
538 would explain why, for example, the Barbados and Sand-
539 wich arcs formed only where the Northern and Southern
540 America continental lithospheres narrow, and slices of
541 Cordillera type are boudinaged and scattered in the
542 backarc setting. Similarly, the Japanese W-directed sub-
543 duction, developed during the Neogene, to the east of a
544 retrobelt of an earlier Cretaceous Andean type orogen,
545 generated by an E-directed subduction (Cadet and
546 Charvet, 1983). This is also supported by the outcrops
547 of Andean type co-genetic porphyry copper deposits in
548 Japan and Chorea (Sillitoe, 1977; Mitchell and Garson,
549 1981).

550 W-directed subduction zones on Earth appear as short
551 lived. If the Marianas or Japan subductions were active
552 since the Cretaceous with a steady state E-ward hinge
553 retreat, they should be now positioned in the middle of the
554 Pacific. Backarc spreading in the hangingwall of W-
555 directed subduction zones are mostly Cenozoic, pointing
556 out that the related subduction should have a similar age.
557 Backarc basins probably arrive to a critical opening stage,
558 and then they become closed, until a new subduction
559 starts. The non-standard Japan subduction in fact shows
560 scattered intermediate deep seismicity, unlike it typically
561 occurs along similar slabs (e.g., Omori et al., 2004).

562 Another apparent discrepancy to the W-directed vs.
563 E–NE-directed slabs asymmetry is the occurrence of
564 backarc basins also in the hangingwall of E- or NE-
565 directed subduction zones. However these types of
566 rifts rarely arrive to oceanic spreading as W-directed
567 subduction do in their hangingwall. Moreover they may
568 be post-subduction (e.g., Basin and Range, Doglioni,
569 1995), or sin-subduction but accommodating differential
570 advancement of the upper plate over the lower plate.
571 Examples of this type are the aforementioned Aegean
572 and the Andaman rifts. The extension in western Turkey,
573 Aegean sea, Greece and Bulgaria can be interpreted as a
574 result of the differential convergence rates between the
575 NE-ward directed subduction of Africa relative to the
576 hangingwall disrupted Eurasian lithosphere (Doglioni
577 et al., 2002). Considering fixed Africa, the faster SW-
578 ward motion of Greece relative to Cyprus–Anatolia
579 determines the Aegean extension. The differences in
580 velocity can be ascribed to differential decoupling with
581 the asthenosphere. Unlike west-Pacific backarc basins,
582 where the asthenosphere replaces a subducted and re-
583 treated slab, the Aegean rift represents a different type of
584 extension associated to a subduction zone, where the
585 hangingwall plate overrode the slab at different velo-
586 cities, implying internal deformation. While W-directed
587 subductions occur with the rollback of the lower
588

588 plate relative to the upper plate, the Aegean setting
 589 needs three plates, i.e., a common lower plate, and two
 590 plates overriding at different velocities. Analogously,
 591 assuming only few mm/yr of relative motion between
 592 the Indian and Australian plates (e.g., Bird, 2003), along
 593 the Himalayas collision, the Indo-Australian plates
 594 converge relative to Asia at about 36 mm/yr, while the
 595 same Indo-Australian plates along their oceanic north-
 596 ern part are overridden by the Sumatra–Burma plate at
 597 around 64 mm/yr (Cuffaro et al., 2006). Therefore,
 598 assuming a relatively coherent lower plate, the hanging-
 599 wall plates move SSW-ward at different velocity, this
 600 gradient being responsible for the extension between
 601 Asia and Sumatra–Burma, and generating the Andaman
 602 rift. In this type of geodynamic setting the subduction
 603 hinge still moves toward the upper plate, as in the
 604 normal E- or NE-directed subduction zones.

605 There are belts that are apparently not following the
 606 global trend of plate motions, like orogens that are E–W
 607 trending, and related to N–S convergence (e.g., the
 608 Pyrenees, Venezuela–Colombia belt). They have Alpine
 609 character and may kinematically be explained as related
 610 to subrotation of plates (Cuffaro et al., 2004). Other
 611 obliquely oriented belts are the Atlas and the Maghre-
 612 bides in northwest Africa. The Atlas is not directly
 613 related to a subduction zone, but has been interpreted as
 614 an intraplate inversion structure (Laville and Petit, 1984;
 615 Warme, 1988; Doglioni, 1989; Frizon de Lamotte et al.,
 616 2000; Teixell et al., 2003; Frizon De Lamotte, 2005),
 617 while the E–W-trending Maghrebides (Frizon de
 618 Lamotte et al., 2000; Roca et al., 2004) are rather the
 619 right-lateral prolongation in northwestern Africa of the
 620 arcuate Apennines–Maghrebides subduction system.
 621 Along this segment of the belt, the right-lateral
 622 transpression coexisted with an about 5 times slower
 623 roughly N–S component of Africa–Europe convergence
 624 (Gueguen et al., 1998). The arcuate geometry of the
 625 Moroccan Riff implies local left-lateral transpression
 626 along its eastern margin, where the Maghrebides–Tell–
 627 Riff belt interferes with the inverted Middle Atlas
 628 (Doglioni, 1989). The E–W-trending Himalaya is
 629 instead almost perpendicular to the global tectonic
 630 mainstream (Doglioni, 1990).

631 3. Basic kinematics in the upper plate reference frame

632 When the subduction hinge behavior is added to plate
 633 motion, the following three end members can occur. If
 634 the hinge H is stationary, the subduction will equal the
 635 convergence (Fig. 5A). If the hinge advances as the
 636 convergence, the subduction rate will be zero (Fig. 5B),
 637 whereas in case the hinge retreats, the subduction rate

638 will be added to the convergence rate. For example, it
 639 will be twice the convergence rate if the hinge retreats at
 640 the same speed of the convergence (Fig. 5C).

641 The rate of vertical descent S_v and horizontal penetra-
 642 tion S_h into the mantle will be $S \sin \alpha$, and $S \cos \alpha$,
 643 respectively, where α is the slab dip (Fig. 1). The steeper
 644 the slab, the faster will be its descent into the mantle and
 645 viceversa.

646 Let us then consider, for a subduction zone, a reference
 647 frame with three points, one attached to the upper plate U,
 648 a second attached to the lower plate L, and the third on the
 649 transient subduction hinge H (Fig. 1). The point U located
 650 on the upper plate is taken as fixed, i.e., its velocity $V_U = 0$.
 651 The motion of the two remaining points is considered
 652 relative to the fixed upper plate, so that V_L is the velocity
 653 of the lower plate and V_H is the velocity of the hinge. If
 654 lower plate and subduction hinge move towards the fixed
 655 point in the upper plate, then V_H and V_L are assumed to be

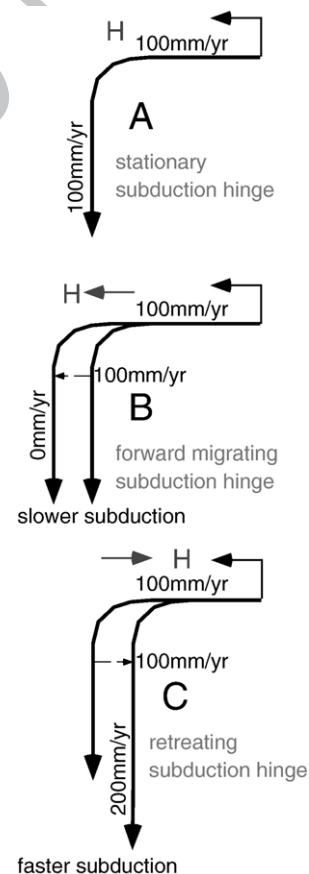


Fig. 5. Along a subduction zone, say with 100 mm/yr convergence, if the subduction hinge H is stationary (A), the subduction rate will be the same of the convergence. If H migrates left 100 mm/yr (B), then the subduction would be null. If H migrates right of the same amount, the subduction will be doubled (C).

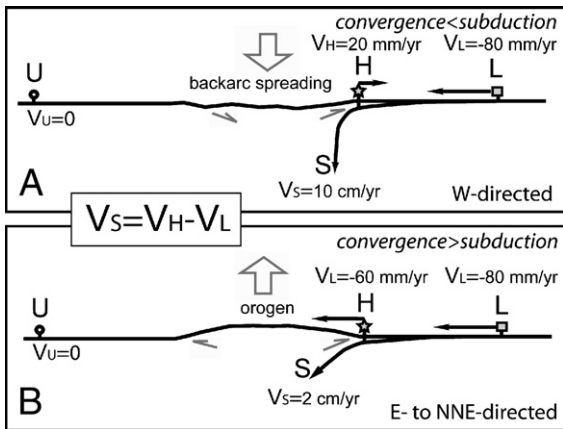


Fig. 6. Basic kinematics of subduction zones, assuming fixed the upper plate U, a converging lower plate L, and a transient subduction hinge, H. The subduction rate S is given by $V_S = V_H - V_L$. Values are only as an example. S increases when H diverges relative to the upper plate (a), whereas S decreases if H converges (b). The movements diverging from the upper plate are positive, whereas they are negative when converging. The case a) is accompanied by backarc spreading, a low prism and is typical of W-directed subduction zones, whereas in case b) double verging and elevated orogens form and is more frequent along E- to NNE-directed subduction zones. Note that in both W- and E–NE-directed subduction zones, the hinge migrates eastward relative to the upper plate, suggesting a global tuning in subduction processes.

656 negative. If lower plate and subduction hinge move away,
 657 then V_H and V_L are positive. In the following, the term
 658 convergence (of lower plate and hinge with respect to

upper plate) will be adopted for negative V_H and V_L ,
 659 whereas divergence will refer to positive V_H and V_L . V_L
 660 is easily derived from plate motion models. The exact
 661 determination of the hinge location is not that easy due to
 662 the wide rounded area of dip change from the horizontal
 663 lower plate lithosphere to the inclined downgoing slab.
 664 For sake of simplicity, the motion of the hinge zone can
 665 tentatively be assumed to be close or coincident with that
 666 of the subduction trench (this approximation has been
 667 used also in other studies of subduction zones (Heuret and
 668 Lallemand, 2005).
 669

Particular attention will be given to the effects of the
 670 kinematics of upper, lower plate and hinge on the
 671 subduction velocity (V_S). This is defined as the velocity
 672 with which the subducting lithosphere enters the
 673 subduction zone and can be calculated with the simple
 674 equation: ($V_S = V_H - V_L$). For example, in the particular
 675 case of the lower plate converging with the upper plate,
 676 the subduction rate is a function of the behavior of the
 677 subduction hinge.
 678

In this section we speculate on all the possible
 679 combinations of U, H and L, irrespective of the fact that
 680 the analyzed cases can be found in nature. For each case
 681 we describe the expected subduction velocity and the
 682 predicted deformation of the upper plate. Generally
 683 speaking, the upper plate is predicted to stretch (with the
 684 opening of backarc basins) for diverging hinges (Figs. 6,
 685 7, 8 and 9), or it is expected to shorten (or shrink) for
 686

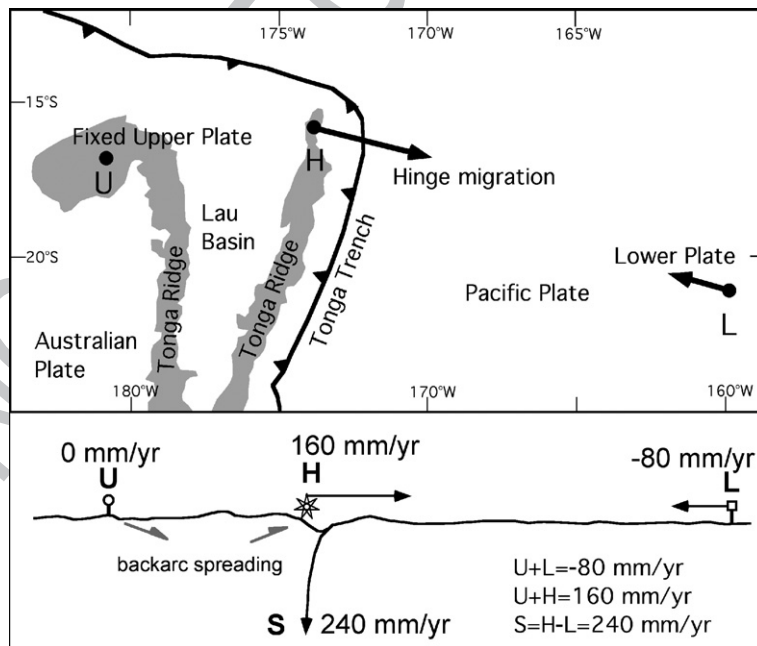


Fig. 7. GPS data of Bevis et al. (1995) along the Tonga subduction zone, taken as fixed upper plate. Note that the subduction rate is the sum of convergence between U and L, plus the motion of H. This is the fastest subduction in the world, where more than 700 km of lithosphere should sink in about 3 Ma.

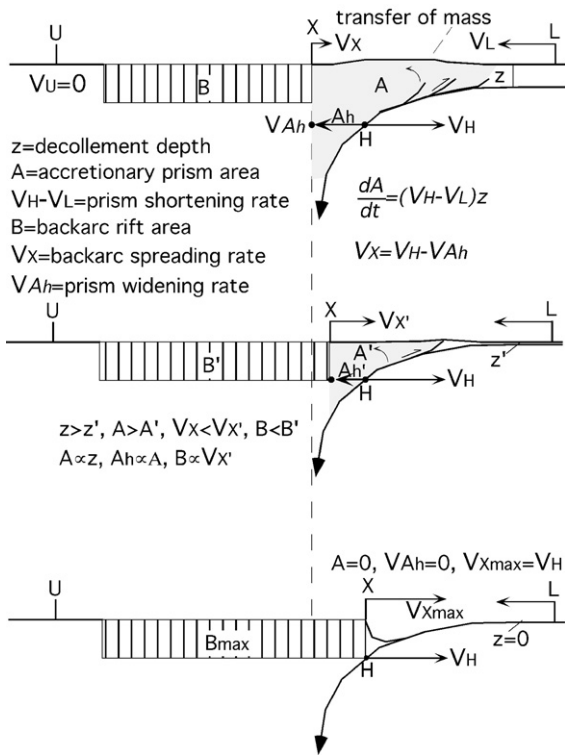


Fig. 8. In case the accretionary prism is entirely formed at the expenses of the lower plate as it occurs along W-directed subduction zones, the shortening is equal to the subduction rate ($V_S=V_H-V_L$). With given convergence (V_L) and subduction hinge (V_H) migration rates, three different cases are illustrated. The deepest position of the decollement plane depth (z) of the accretionary prism determines a larger transfer of mass per unit time from the lower to the upper plate (upper panel). This decreases the width of the backarc rift and its velocity of spreading (V_X). As a consequence, the reference point X migrates toward the foreland slower as the decollement depth and the accretionary prism width (Ah) increase. U , fixed upper plate. In case no accretion occurs at the prism front (i.e., $z=0$ and the lower plate is entirely subducted, lower panel), the backarc spreading should equal the velocity of the hinge ($V_X=V_H$). The middle panel is an intermediate case. Therefore, the reference point X might not be a reliable kinematic indicator of the subduction hinge migration rate when accretion occurs, besides all the other problems discussed in the text.

687 hinges converging toward the upper plate (Figs. 10, 11,
 688 12 and 13). These behaviors occur regardless the
 689 relative motion of the lower plate. Such subduction
 690 kinematics are summarized in Table 1. When available,
 691 we will briefly describe natural examples of the
 692 analyzed cases. We will show that some kinematics
 693 are typical of “W”-directed slabs and some others of “E-
 694 or NE”-directed subduction zones.

695 It is finally emphasized that, in this section, the
 696 analysis is purely kinematic. As a consequence, the
 697 reader could be confronted with subduction kinematics
 698 contrasting commonly accepted ideas on subduction

699 dynamics (controlled by slab pull). We show that such
 700 contrasts vanish if other plate driving forces are
 701 considered.

702 In Table 1 three major groups of kinematic settings are
 703 listed: for converging, for stationary and for diverging
 704 lower plates. For each of these three groups all the com-
 705 binations with the relative motion of the subduction hinge
 706 with respect to the upper plate are considered. The
 707 behavior of H is variable along subduction zones world-
 708 wide. Convergence rate is also changing in the different
 709 settings and even along a single subduction zone. The
 710 different kinematics are reported as a function of the main
 711 subduction polarity in Figs. 14 and 15, and the different
 712 cases are associated to regional examples. Generally
 713 speaking, along steady W-directed subduction zones, the
 714 hinge mostly diverges relative to the upper plate, and
 715 backarc basin forms. On the contrary, along E- or NE-
 716 directed subduction zones the most commonly the
 717 subduction hinge converges relative to the upper plate,
 718 and a double verging orogen develops, without backarc
 719 extension. A synoptic view is in Fig. 16, where the
 720 aforementioned fourteen kinematics are listed.

721 3.1. For converging lower plates ($L < 0$), six potential
 722 kinematics can occur

723 3.1.1. Kinematics #1

724 If the hinge diverges ($H > 0$), then backarc extension
 725 occurs in the upper plate and subduction is faster than

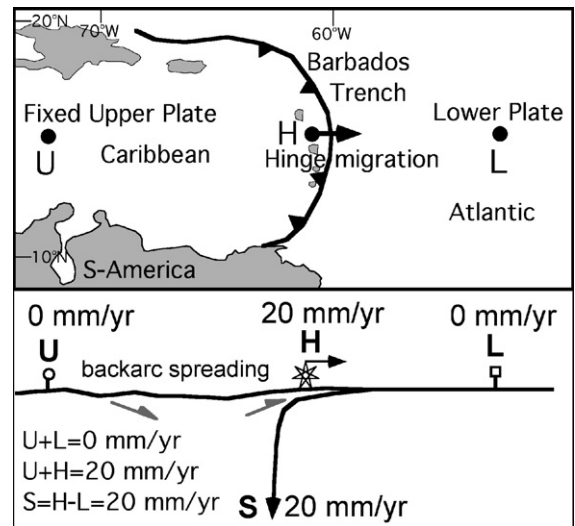


Fig. 9. Along the Caribbean subduction zone, the hinge migrates E-ward while no convergence should occur between the central parts of the backarc basin to the west and the Atlantic Ocean to the east, although no data are yet available for the interior of the backarc basin. GPS data after Weber et al. (2001).

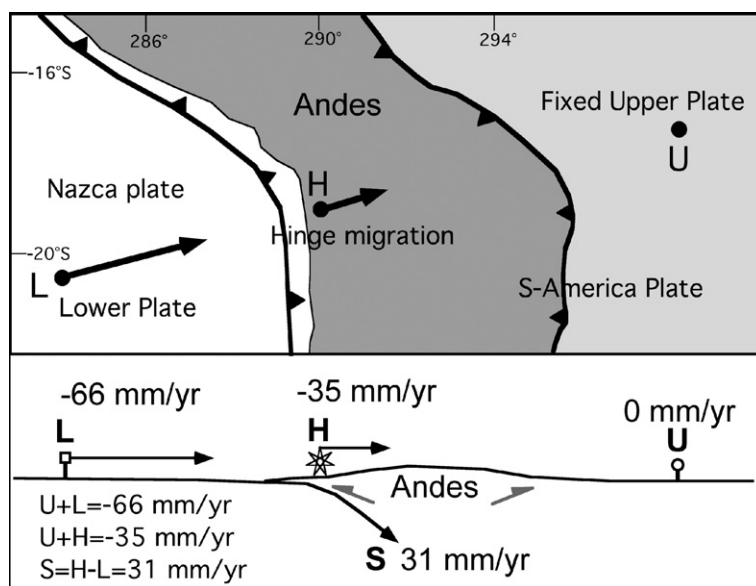


Fig. 10. The convergence between Nazca and South America plates is faster than the shortening in the Andes. The upper plate shortening decreases the subduction rate. The convergence/shortening ratio is about 1.88. GPS data after Liu et al. (2000).

726 convergence (fast sinking slab). This kinematics is
 727 typical of the western Pacific subductions, such as
 728 Tonga and Marianas. The present-day motion of the
 729 Tonga subduction zone (Fig. 7) has been investigated by

Bevis et al. (1995). In this subduction, the worldwide
 fastest plate velocities have been described. Converting
 their results in the fixed upper plate reference frame, the
 Pacific plate (L) is converging at 80 mm/yr, and the
 Tonga islands, fairly representing H, are diverging at
 about 160 mm/yr. Therefore the subduction rate S
 should be 240 mm/yr (Fig. 7).

In the case of the Marianas, we assume that variable
 rates of backarc spreading are related to different rates of
 hinge (H) migration from the upper plate. In the northern
 Mariana backarc, rates ranging from 60 to 20 mm/yr have
 been described from Pliocene to present times (Yamazaki
 et al., 2003). The related variations of H velocity should
 have determined different subduction rates, since H is
 summed to the convergent rate of the lower plate L to
 compute the slab sinking (Fig. 14, 1W). Convergence
 rates calculated using the NUVEL1A rotation poles
 (DeMets et al., 1994) vary between 90 and 95 mm/yr
 (Cruciani et al., 2005). As a consequence, subduction
 rates along the Marianas subduction zone vary between
 110 mm/yr and 150 mm/yr. Variable backarc spreading
 rates have been reported also in the Lau backarc basin, in
 the hangingwall of the Tonga subduction zone (Taylor
 et al., 1996). Other possible theoretical cases are where the
 hinge diverges in absolute value faster or slower than the
 convergence rate of the lower plate. The sum of hinge
 divergence and lower plate convergence in both cases
 determines the subduction rate. However, faster hinge
 divergence generates larger backarc spreading, whereas
 larger lower plate convergence rate should produce larger

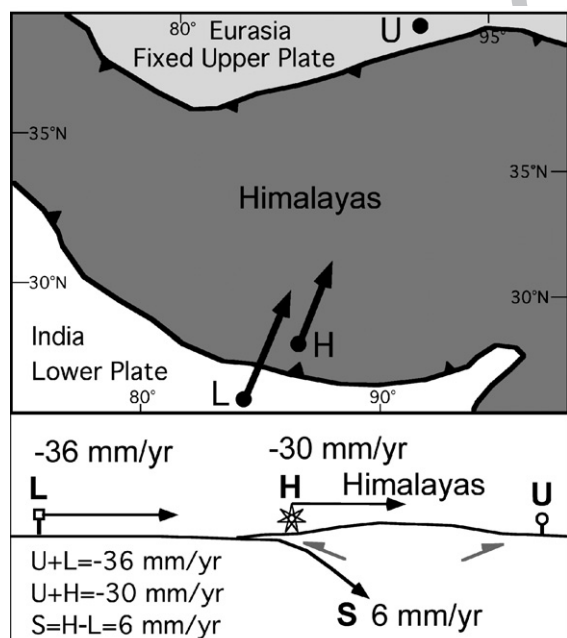


Fig. 11. The convergence between India and Eurasia plates is slightly
 faster than shortening in the Himalayas. The difference should be the
 continental subduction rate. The convergence/shortening ratio is about
 1.2. GPS data after Jouanne et al. (2004) and Zhang et al. (2004).

760 shortening rate in the accretionary prism. However we do
 761 not distinguish these cases considering them as variations
 762 of the kinematics #1.

763 3.1.2. Kinematics #2

764 If the hinge is stationary ($H=0$), then neither stretching
 765 nor shortening occur in the upper plate and subduction
 766 velocity equals the lower plate convergence ($S=|L|$)
 767 (sinking slab). It is most likely typical of the onset stages
 768 of both W-ward and E–NE-directed subduction zones. No
 769 present-day examples are available.

770 3.1.3. Kinematics #3

771 If the hinge converges ($H<0$) slower than the lower
 772 plate ($|H|<|L|$), then subduction is slower than lower
 773 plate convergence (slowly sinking slab). Shortening
 774 occurs normally along E- or NE-directed subductions
 775 (e.g., Andes, Fig. 10). In W-directed subductions, this
 776 kinematics normally follows a stage of kinematics#1,
 777 when a backarc basin opened. In this case, such as for
 778 Japan, inversion tectonics occurs in the inactive (now
 779 closing) backarc basin of the upper plate. The South
 780 Japan subduction zone (Fig. 13) is a peculiar case of W-
 781 directed subduction zone where unlike typical similar
 782 settings, H is converging rather than diverging (Fig. 13).
 783 In fact, the backarc spreading apparently ended accord-
 784 ing to seismicity and space geodesy data (Mazzotti et al.,
 785 2001). At latitude 35°N , along the Japan subduction, the

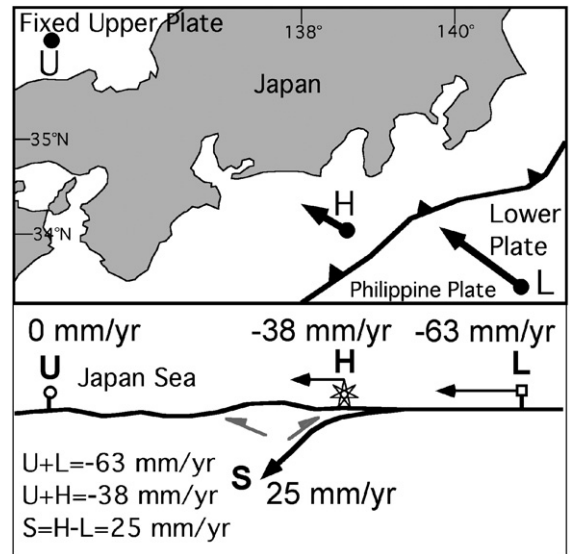


Fig. 13. The Japan subduction zone appears as a setting where a W-directed subduction zone is inverting. The hinge is not migrating away from the upper plate, but rather converging. The backarc basin is starting to shrink. GPS data of Japan stations relative to fixed Amuria plate (Eurasia), after Mazzotti et al. (2001).

786 lower plate converges at 92 mm/yr. The backarc basin is
 787 closing at rates of 25 mm/yr (Cruciani et al., 2005) and
 788 such rates can be taken as representative of the hinge
 789 convergence. As a consequence, subduction rates are

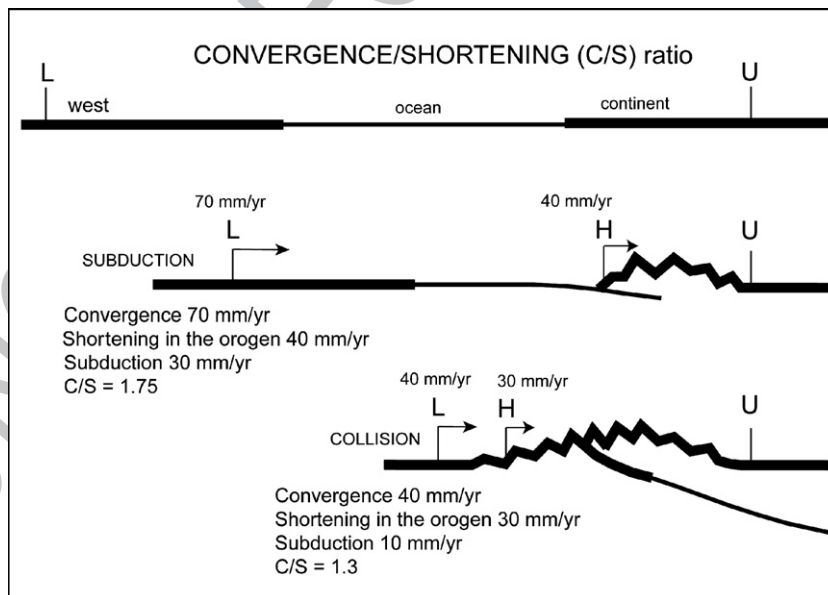


Fig. 12. During oceanic subduction, the shortening is mostly confined in the continental upper lithosphere due to its lower strength and of the coupling between upper and lower plates. At the collisional stage also the lower plate is widely involved. Larger the shortening, smaller the subduction rate, and lower the upper plate strength + greater the plate coupling. The convergence/shortening ratio decreases at the collisional stage.

t1.1 Table 1

t1.2 Main kinematic relationships of subduction zones, assuming fixed the upper plate, and moving the lower plate L and the subduction hinge H. For readability sake, $S = V_S$, $H = V_H$, $L = V_L$

t1.3	Case # and kind of subduction	Lower plate (L) and subduction hinge (H) motions and their velocities (L and H)	Subduction velocity	Kind of deformation of the upper plate	Does it occur in E–NE-directed subductions?	Does it occur in W-directed subductions?	Natural examples
t1.4	1 Fast-sinking slab	L converging ($L < 0$) H diverging ($H > 0$)	Subduction S faster than L convergence ($S > L $)	Backarc extension	No	Yes	Tonga, Marianas
t1.5	2 Sinking slab	L converging ($L < 0$) H stationary ($H = 0$)	Subduction velocity equal to L convergence ($S = L $)	Neither stretching nor shortening	Yes	Yes	Onset of subduction. No present day examples
t1.6	3 Slowly sinking slab	L converging ($L < 0$) H converging ($H < 0$) slower than L ($ H < L $)	Subduction slower than L convergence ($S < L $)	Shortening (Andes) or inversion tectonics (Japan)	Yes	Yes	Andes Japan
t1.7	4 Hanging slab	L converging ($L < 0$) H converging ($H < 0$) as fast as L ($ H = L $)	Subduction rate is null ($S = 0$)	Fast shortening	Yes	No	Final stages of continental collision
t1.8	5 “Emerging” or detaching slab	L converging ($L < 0$) H converging ($H < 0$) faster than L ($ H > L $)	Subduction rate is negative ($S < 0$)	Fast shortening	No	No	/
t1.9	6 Sinking slab and three plates	L converging ($L < 0$) Two upper plates, U–U”	Subduction faster than L convergence ($S > L $)	extension	Yes	No	Aegean Sea Andaman
t1.10	7 Sinking slab	L stationary ($L = 0$) H diverging ($H > 0$)	Subduction rate equals H retreat ($S = H $)	Backarc extension	No	Yes	Barbados
t1.11	8 Hanging slab	L and H stationary ($L = H = 0$)	Subduction rate is null ($S = 0$)	Neither stretching nor shortening	Yes	Yes (?)	Urals and Carpathians (?)
t1.12	9 “Emerging” or detaching slab	L stationary ($L = 0$) H converging ($H < 0$)	Subduction rate is negative ($S < 0$)	Shortening	No	No	/
t1.13	10 “Emerging” or detaching slab	L diverging ($L > 0$) H converging ($H < 0$)	Subduction rate is negative ($S < 0$)	Shortening	No	No	/
t1.14	11 “Emerging” or detaching slab	L diverging ($L > 0$) H stationary ($H = 0$)	Subduction rate is negative ($S < 0$)	Neither stretching nor shortening	No	No	/
t1.15	12 “Emerging” or detaching slab	L diverging ($L > 0$) H diverging ($H > 0$) slower than L ($ H < L $)	Subduction rate is negative ($S < 0$)	Post-subduction extension	Yes	Yes	Southern Apennines (?) California (Basin and Range)
t1.16	13 No sinking-laterally moving slab	L diverging ($L > 0$) H diverging ($H > 0$) as fast as L ($ H = L $)	Subduction rate is null ($S = 0$)	Backarc extension	No	Yes	Southern Apennines
t1.17	14 Slow-sinking slab	L diverging ($L > 0$) H diverging ($H > 0$) faster than L ($ H > L $)	Subduction rate is slower than H retreat ($S < H $)	Backarc extension	No	Yes	Banda

790 expected to be of 67 mm/yr. No direct measurements are
791 available for the motion of the Andean subduction hinge
792 (Fig. 10). However, along the Andean belt the calculated
793 shortening in the orogen is about half of the convergence
794 rate between the Nazca plate and the South America
795 plate (Liu et al., 2000). The unavailability of direct
796 measurements of hinge convergence velocities can be
797 overcome assuming that the shortening is approximately
798 equal to the hinge convergence. Along the Andes

subduction zone, at about 27° S, the lower plate
convergence L calculated using the NUVEL1A rotation
poles is about 66 mm/yr. Using the data by Liu et al.
(2000), the subduction hinge converges toward the
upper plate at about 35 mm/yr. As a consequence the
subduction rate S will be 31 mm/yr (Fig. 10). The hinge
convergence relative to the upper plate indicates the
amount of the upper plate shortening and is faster as the
strength of the upper plate is lower (Doglioni et al.,

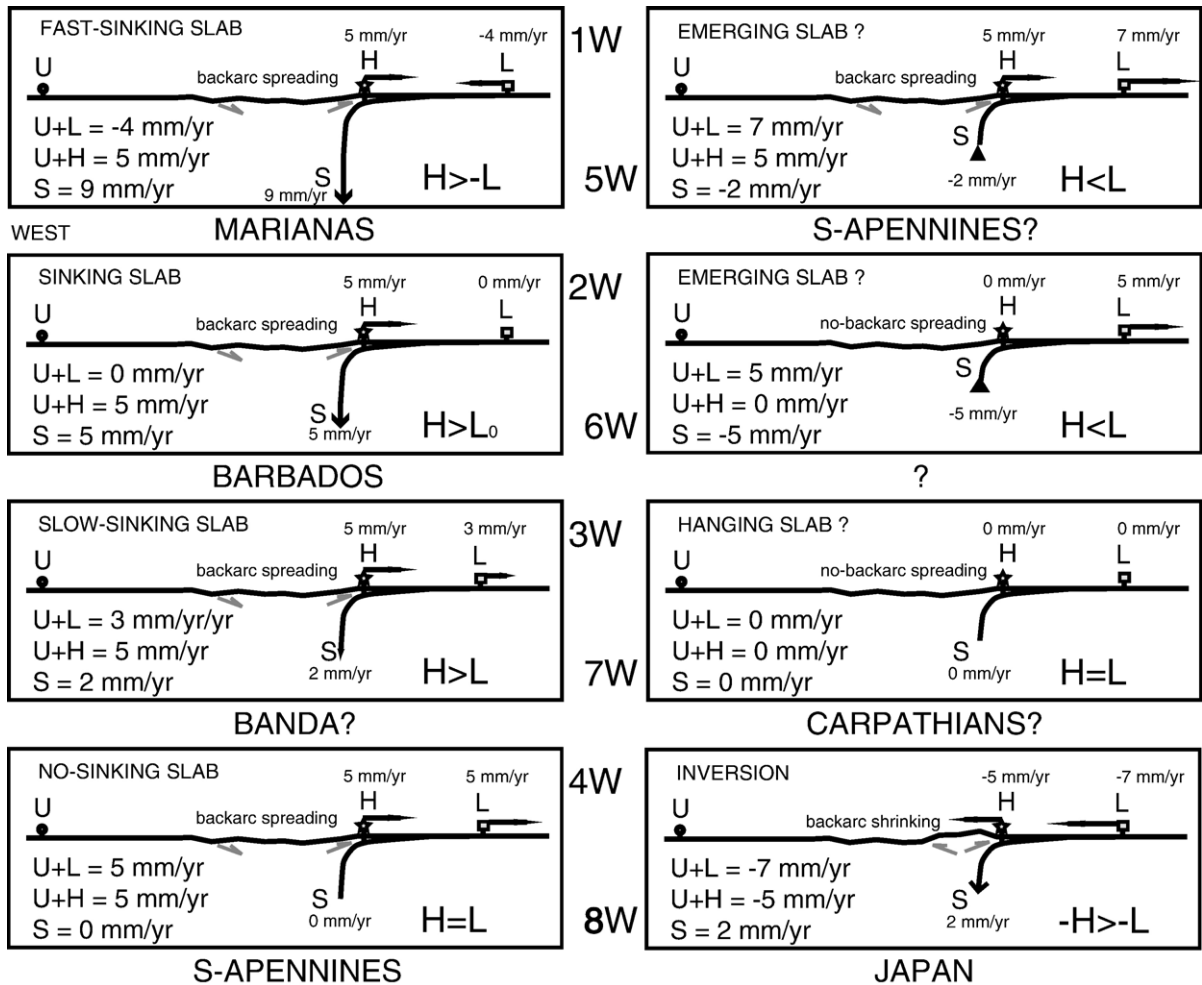


Fig. 14. Different kinematic settings of W-directed subduction zones. In the 1 to 5 sections, H is moving away from the U, in 6 and 7 H is fixed, and in section 8 is moving toward U. The site L is converging relative to U in sections 1 and 8. It is fixed to U in sections 2 and 7. The other cases have L moving away from U, but with different relationship with H, i.e., faster, slower or fixed. The different regions are interpreted as examples of the variable settings. The different regions are interpreted as examples of the variable settings. Velocities are only for relative comparison and do not apply to the example areas.

2006a). The convergence/shortening (C/S) ratio could be a useful parameter for describing the strength of the upper plate. The strength of the lithosphere is controlled by active deformation mechanisms (either brittle or plastic) and varies consistently with depth. Although on the long period the rheological behavior of the lithosphere is best described by power-law equations, the strength of the entire lithosphere is sometimes described in terms of viscosity. For example, in the section of Fig. 10, the C/S ratio is 1.88, and moving southward along the Andes it decreases, suggesting relative lower strength of the upper plate. Assuming stress balance, the viscosity of the upper plate continental lithosphere in the Andes has been computed as low as 3×10^{21} Pa s (Husson and Ricard, 2004). The

viscosity of oceanic lithosphere tends to be generally larger, and it decreases with depth. For example an oceanic lithosphere at 25 km depth might have a range of viscosity between 10^{22} and 10^{27} Pa s, increasing with its age (Watts and Zhong, 2000). This may also explain why the upper plate made by softer continental lithosphere absorbs most of the deformation.

Higher the convergence/shortening ratio (C/S), higher the strength of the upper plate (Doglioni et al., 2006a). A further parameter controlling the C/S ratio is the coupling between upper and lower plates. A strong coupling may be achieved when the friction of rocks at the interface between subducting and overriding plates is high. Strong friction will transform a consistent part of the motion of the subducting plate into deformation of

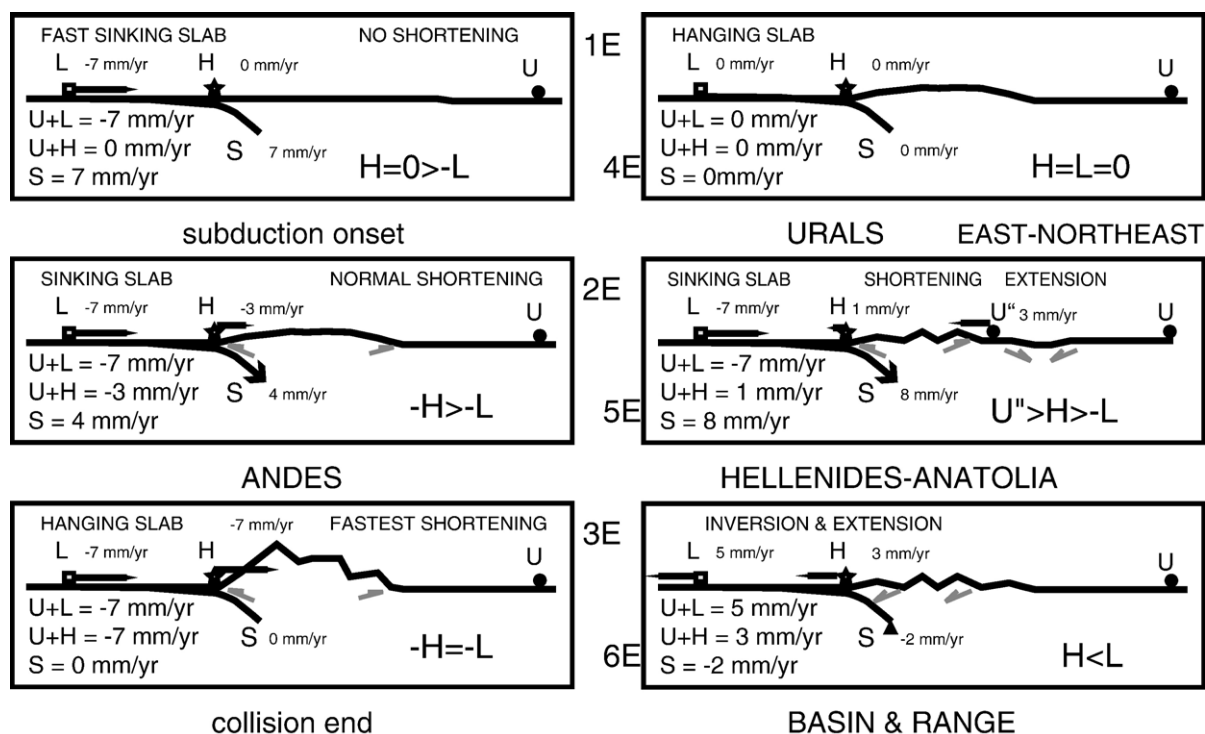


Fig. 15. Different kinematic settings of E- or NE-directed subduction zones. In the sections 1, 2, 3 and 5, L is converging relative to U, whereas it is fixed in section 4 and diverging in section 6. The hinge H is fixed relative to U in sections 1 and 4. It is rather converging in sections 2, 3 and 5, whereas it is diverging in section 6. The different regions are interpreted as examples of the variable settings. Velocities are only for relative comparison.

838 the upper plate and thus enlarge the C/S ratio. The
 839 minimum value of this ratio for E–NE-directed
 840 subduction zones should be 1, where the amount of
 841 convergence equals the amount of shortening in the belt,
 842 indicating very low strength and large coupling, and
 843 virtually no subduction. Subduction is inversely pro-
 844 portional to the amount of shortening in the upper plate,
 845 and the convergence/shortening ratio increases expo-
 846 nentially with the decrease of shortening, and the
 847 increase of the subduction rate. During collision,
 848 convergence rate slows down, and the shortening is
 849 propagating more pervasively into the lower plate
 850 (Fig. 11). Therefore the C/S ratio decreases during the
 851 final stages of the orogen life (Fig. 12).

852 The C/S ratio is 1 if convergence and shortening were
 853 equal. Therefore, as the shortening increases due to lower
 854 strength of the upper plate, the C/S ratio becomes higher.

855 The Himalayas range (Fig. 11) had an intense
 856 geodetic investigation during the last years (e.g., Bane-
 857 rjee and Bürgmann, 2002; Jade et al., 2004; Jouanne
 858 et al., 2004; Zhang et al., 2004). The convergence
 859 between the India and Eurasia plates is around 36 mm/yr,
 860 and the orogenic shortening is lower (30 mm/yr) along
 861 the selected section as in the Andes, but also the C/S ratio

862 is lower (1.2), since the shortening is relatively higher
 863 with respect to the convergence rate, possibly due to the
 864 involvement of the softer lower plate (Fig. 11).

865 As demonstrated by Zhang et al. (2004), the
 866 deformation of the Tibetan Plateau cannot be accommo-
 867 dated by single thrusts, but it is rather a diffuse
 868 deformation across the entire lithosphere. This observa-
 869 tion can be applied to most of the orogens worldwide, and
 870 it is consistent with a viscous dissipation of the shortening
 871 within the whole deeper part of the orogen, accounting for
 872 a large part of the convergence rate, but not all of it. The
 873 remaining part is expressed by the subduction rate.

874 The C/S ratio is >1 along E- or NE-directed subduction
 875 zones, whereas it is <1 along accretionary prisms of W-
 876 directed subduction zones where the subduction rate and
 877 the related shortening are faster than the convergence rate.

878 The geodynamic setting where the H migrates toward
 879 the upper plate generates a double verging Andersonian
 880 belt, no backarc basin, and high structural and
 881 morphologic elevation (Figs. 6, 10, 11 and 15).

882 Another example of convergence faster than hinge
 883 convergence is the E-directed Cascadia subduction zone
 884 (Dragert et al., 2001). Convergence rate between L and
 885 fixed U is about 35–40 mm/yr. The shortening relative

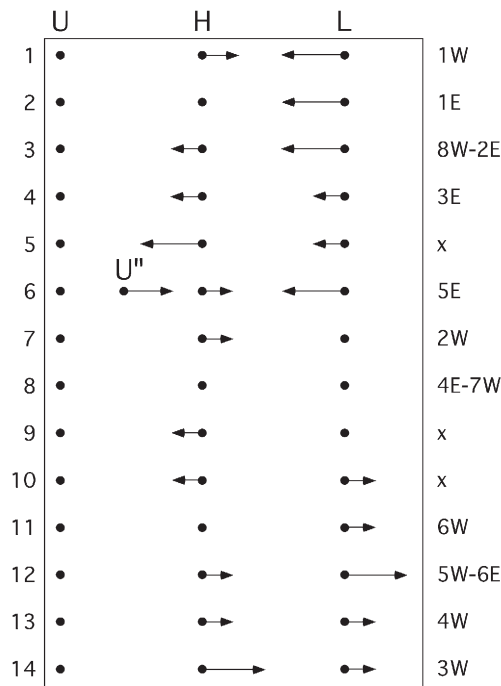


Fig. 16. Geodynamic settings where the upper plate U is considered fixed, the subduction hinge H can diverge, be fixed or converge, and the lower plate can either converge, be fixed or diverge. Case 6 occurs when the upper plate is in the third dimension split into two plates, U and U'' . Few cases are potentially not realistic, i.e., 5, 9 and 10 (X) because the subduction hinge cannot converge in case of absence of faster or equal lower plate convergence. Numbers on the left refer to the kinematics examples discussed in the text, and numbers and letters to the right refer to the cases of Figs. 14 and 15.

886 to fixed upper plate gradually decreases by means of
887 deep ductile deformation and upper crustal thrusting
888 from about 20 mm/yr at the trench, considered as the
889 hinge H , to zero in the stable plate interior.

890 3.1.4. Kinematics #4

891 If the hinge converges ($H < 0$) as fast as the lower
892 plate ($|H| = |L|$), then subduction rate is null ($S = 0$;
893 hanging slab) and the upper plate is subject to
894 shortening. This kinematics is typical of final stages of
895 continental collision.

896 3.1.5. Kinematics #5

897 If the hinge converges ($H < 0$) faster than the lower
898 plate ($|H| > |L|$), then subduction rate is negative. In other
899 words, the plate subducted during previous stages
900 characterized by other kinematics would tend to re-
901 emerge from the mantle. Since the negative buoyancy of
902 the subducted slab would prevent this, the pull-down
903 forces due to negative buoyancy and the pull-out forces
904 due to plate kinematics would induce a strong tensional

stress field in the slab. The slab could respond to such a
stress field breaking off (slab detachment, e.g., Wortel
and Spakman, 2000). The same observations will be
applicable to later cases characterized by similar
negative subduction rates. No present day examples of
this kinematics are known, and this setting seems to be
unrealistic because the hinge can converge only if the
lower plate converges as well, unless it is broken into
two diverging subplates.

3.1.6. Kinematics #6

A particular case occurs when, along a subduction
zone, the hangingwall is not a coherent single plate, but
differential velocities occur. Then the upper plate has to be
considered as composed by two upper plates (Fig. 15, 5E).
Assuming fixed the far field upper plate ($U = 0$), a segment
of the upper plate closer to the subduction zone diverging
from the far field upper plate with velocity U'' (as an
example we assume $U'' = 3$ mm/yr), a lower plate
converging for example at rates $L = -7$ mm/yr, and a
hinge diverging at $H = 1$ mm/yr, then the subduction rate
will be 8 mm/yr. In other words the subduction rate is
calculated with respect to the part of the upper plate closer
to the subduction zone. The upper plate U'' will suffer a
shortening of 2 mm/yr, and will be rifted from the upper
plate U at 3 mm/yr. These kinematics are more complex
than the other cases here analyzed, since they include
three plates (two upper plates and a lower plate). Although
not easily described by the simple relation of the two-plate
cases, this kinematic setting is particularly important since
it explains the occurrence of extension in the hanging-wall
of E- or NE-directed subduction zones such as the Aegean
and the Andaman seas, where the rift is sin-subduction,
but not related to typical slab retreat. In other words, the
two upper plates override the lower plate at different
velocities, and the velocity gradient between the two
upper plates control the rift. For example, along the
Hellenic and Cyprus–Anatolia subduction zone, Greece
is SW-ward overriding Africa faster than Anatolia
(Doglioni et al., 2002). The faster separation of Greece
relative to Anatolia in the hangingwall of the subduction
generates the Aegean extension.

3.2. For stationary lower plates ($L = 0$), three potential kinematics can occur

3.2.1. Kinematics #7

If the hinge diverges ($H > 0$) then backarc extension
occurs in the upper plate and subduction rate equals the
hinge retreat (sinking slab). This case is observed in the
W-directed Caribbean (Barbados) subduction zone
(Fig. 9). The kinematics of the Barbados–Caribbean arc

954 is well constrained by present day data (Weber et al.,
955 2001), showing 20 mm/yr of E-ward migration of H. The
956 Atlantic side, i.e., the lower plate L can be considered
957 fixed to South America. On the other hand backarc
958 spreading should increase the distance between the
959 Caribbean arc and the Central America Cordillera to the
960 west. Unfortunately there are no GPS sites in the center of
961 the Caribbean basin to validate this statement, but
962 assuming no relative eastward motion between the center
963 of the backarc basin and the Atlantic, the convergence
964 between lower and upper plate should be null ($L=0$). As a
965 consequence the subduction rate would coincide with the
966 H velocity and be equal to 20 mm/yr (Fig. 9). This
967 interpretation differs from most of the published kine-
968 matic models that assume the Caribbean plate as a single
969 coherent block (e.g., Weber et al., 2001).

970 3.2.2. Kinematics #8

971 If the hinge is stationary ($H=L=0$) then no deforma-
972 tion in the upper plate is expected to occur and the sub-
973 duction rate is null as well (hanging slab). Post-collisional
974 settings such as the Urals or other more recent presently
975 inactive alpine segments could be similar cases. Another
976 potential instance could be the northern Carpathians.

977 3.2.3. Kinematics #9

978 If the hinge is converging ($H<0$), then shortening
979 should occur in the upper plate and the subduction rate
980 should be negative (emerging or detaching slab), as in
981 case #5. No present-day examples are known.

982 3.3. For divergent lower plates ($L>0$), five potential 983 kinematics can occur

984 3.3.1. Kinematics #10

985 If the hinge converges ($H<0$) shortening should
986 occur in the upper plate and the subduction rate should
987 be negative (emerging or detaching slab). No present-
988 day examples are known, and this case seems
989 kinematically impossible, since hinge convergence
990 occurs only in the lower plate converges as well.

991 3.3.2. Kinematics #11

992 If the hinge is stationary ($H=0$), neither stretching
993 nor shortening should occur in the upper plate and the
994 subduction rate would be negative (emerging or
995 detaching slab). No present-day examples are known.

996 3.3.3. Kinematics #12

997 If the hinge diverges ($H>0$) slower than lower plate
998 ($|H|<|L|$), stretching should occur in the upper plate and
999 the subduction rate would be negative (emerging or

detaching slab). The Southern Apennines and the
California (Basin and Range) subduction zones are
present-day possible examples of this case. The
Southern Apennines front does not show active com-
pression, and the belt is dominated by extension. Deep
seismicity is also very limited. In the second case the
subduction of the Farallon plate was stopped when the
oceanic ridge bordering its western margin was sub-
ducted. Then the WNW-ward faster moving Pacific
plate west of the North America plate switched the
lower plate convergence into divergence relative to U,
and the North America Cordillera in the upper plate
started to collapse (Doglioni, 1995). Therefore the
Basin and Range is a post-subduction rift, and related
to far field velocities of the involved plates. It is not a
typical backarc basin.

3.3.4. Kinematics #13

1016 If the hinge diverges ($H>0$) as fast as the lower plate
1017 ($|H|=|L|$), then backarc extension is predicted to occur in
1018 then upper plate. Subduction rates should be null, i.e. the
1019 slab will not sink and will move laterally. 1020

3.3.5. Kinematics #14

1021 If the hinge diverges ($H>0$) faster than the lower
1022 plate ($|H|>|L|$) then the subduction rate will be slower
1023 than the subduction hinge retreat ($S<|H|$) and extension
1024 is still predicted to occur in the upper plate (Fig. 14,
1025 3W). This situation might be typical of some W-directed
1026 subductions and the northern Apennines and the Banda
1027 arc could be present-day examples. 1028

1029 In summary (Table 1), in seven cases the upper plate
1030 stretching is predicted theoretically, five along W-directed
1031 subduction zones (Fig. 14, 1W, 2W, 3W, 4W, 5W, 6E), and
1032 two along E–NE-directed subduction zones (Fig. 15, 5E,
1033 6E). Among these, two occur in post-subduction stages,
1034 i.e., 5W and 6E. Upper plate shortening is predicted in
1035 four cases. Three real cases are observed for real E- or NE-
1036 directed subductions (Fig. 15, 2E, 3E, 5E), and one for W-
1037 directed subduction (Fig. 14, 8W). In this latter case, the
1038 hinge zone that usually diverges from the upper plate, at
1039 later stages may slow down and converge (e.g.,
1040 subduction flip, N-Japan), or due to external boundary
1041 condition (e.g., plate sub-rotation, such as Africa moving
1042 relatively N-ward and deforming the southern Tyrrhenian
1043 Sea, or South America moving relatively N-ward and
1044 deforming the southern Caribbean sea).

1045 A striking feature of the above kinematic analysis is the
1046 theoretical prediction of kinematics of subduction zones
1047 in which the plate subducted at previous stages tends to
1048 move out from the mantle. However, only one potential
1049 case of emerging or detaching slab has been recognized.

1050 Such subduction zone kinematic prediction is unex-
 1051 pected and contrasts one of the main paradigms on plate
 1052 driving forces, i.e., the idea that density contrasts, in
 1053 particular the negative buoyancy of subducting plates,
 1054 provides the force (slab pull) to move horizontally the
 1055 plates. In such a scenario, the escape of a subducted plate
 1056 from the mantle seems absurd. However, if an alternative
 1057 view is considered, this inconsistency can be eliminated.
 1058 In such a scenario, subduction is a consequence of plate
 1059 motions rather than their cause and the negative buoyancy
 1060 of subducted slabs is a secondary effect of subduction and
 1061 not the primary cause.

1062 In five other cases the slab will be sinking in the mantle.
 1063 This is the far more frequently occurring case, and
 1064 examples for all five theoretical cases occur worldwide.
 1065 In the three remaining theoretical cases the slab will be
 1066 hanging and only for two cases real examples were
 1067 recognized.

1068 4. Accretionary prism and backarc spreading

1069 By definition, the tectonic accretion is the transfer of
 1070 mass from the lower to the upper plate, whereas the
 1071 tectonic erosion is the transfer of mass from the upper to
 1072 the lower plate. In case the accretionary prism is entirely
 1073 formed at the expenses of the lower plate as it occurs along
 1074 W-directed subduction zones, the shortening rate is equal
 1075 to the subduction rate ($V_S = V_H - V_L$). A backarc basin
 1076 forms when the subduction hinge retreats relative to the
 1077 upper plate. Let us assume that there is a steady state
 1078 convergence between upper ($U=0$) and lower plate
 1079 ($L=V_L$), and steady state divergence of the subduction
 1080 hinge ($H=V_H$), (Fig. 8).

1081 When the decollement depth (z) of the accretionary
 1082 prism is deep (Fig. 8, upper section), the transfer of mass
 1083 to the area (A) of the accretionary prism is larger (e.g.,
 1084 Bigi et al., 2003) than for shallow z (Fig. 8, lower
 1085 section). We may quantify this increase as a vector (V_{Ah})
 1086 indicating the rate of widening of A per unit time, being
 1087 Ah the distance between H and the backarc border. As a
 1088 consequence, the increase of width of the prism should
 1089 generate a decrease of the backarc rifting widening
 1090 rate (V_X), and a reference point (X) at the margin of
 1091 the backarc rift should move more slowly toward
 1092 the foreland. This would generate a smaller backarc
 1093 area (B) (Fig. 8, upper section). We can express
 1094 $A \propto \zeta \cdot B \propto V_X \cdot \delta A / \delta t = (V_H - V_L)z$. Therefore the speed
 1095 of X is inversely proportional to V_{Ah} (prism widening
 1096 rate), i.e., $V_X = (V_H - V_L) / V_{Ah}$, whereas Ah is in turn
 1097 proportional to the depth of the decollement. The relation
 1098 between A and Ah is variable as a function of the internal
 1099 friction, the friction on the decollement (Davis et al.,

1100 1983), and the diffuse extension affecting the prism at the
 1101 transition with the backarc.

1102 Therefore, the backarc spreading V_X can be quantified
 1103 as the velocity of H moving away from the upper plate,
 1104 minus the prism widening rate, i.e., $V_X = V_H - V_{Ah}$ (Fig. 8).
 1105 Zero accretion in the prism means $V_X = V_H$, and maximum
 1106 backarc rifting. In conclusion, this kinematic analysis
 1107 casts doubts on simplistic interpretations of GPS data as
 1108 direct indicators of deep movements, i.e., between slab
 1109 hinge and mantle; if there is accretion in the prism, surface
 1110 movements cannot represent the hinge rollback. More-
 1111 over, evidences of mantle penetrating between the upper
 1112 and lower plate have been interpreted along Pacific
 1113 subduction zones where accretion is very low or absent.
 1114 Suyehiro et al. (1996) show the presence of a serpentinitic
 1115 diapir just in front of the forearc along the trench of the
 1116 Izu–Bonin subduction zone. This volume prevents an
 1117 equivalent spreading in the backarc as well.

1118 The decrease in speed in backarc rifting settings might
 1119 then have different complementary origins: i) related to a
 1120 real slow down of the subduction hinge retreat relative to
 1121 the upper plate; ii) related to the deepening of the
 1122 decollement plane, or to a faster convergence rate and
 1123 related increase of mass transfer to the upper plate; iii) in
 1124 case of scarce or no accretion, the asthenospheric wedge
 1125 may intrude above the subduction hinge. Normal faulting
 1126 in the prism may further enlarge the upper plate close to
 1127 the subduction hinge, inhibiting the widening of the
 1128 backarc spreading.

1129 In fact, in this model, among others, three main issues
 1130 are neglected for sake of simplicity: a) the isostatic
 1131 subsidence due to the load exerted by the wedge itself, b)
 1132 the along strike lengthening generated by the arc growth
 1133 typical of W-directed subduction zones, and c) the diffuse
 1134 extension affecting the inner part of the accretionary
 1135 prism.

1136 As an application, a decrease or even a stop of the
 1137 rifting has been proposed in the Tyrrhenian Sea backarc
 1138 basin (D'Agostino and Selvaggi, 2004) in spite of
 1139 normal fault-related seismicity (Pondrelli et al., 2004)
 1140 and active convergence rate between the Ionian Sea and
 1141 the upper plate (e.g., Sardinia). Also in the Marianas
 1142 backarc basin the spreading rate has slowed down in the
 1143 Quaternary (Yamazaki et al., 2003), but an alternative
 1144 interpretation considers the transfer of mass from the
 1145 lower to the upper plate or an asthenospheric intrusion
 1146 along the subduction hinge.

1147 5. The Apennines subduction

1148 As an example, the kinematic analysis developed in
 1149 the previous section is applied to the present movements

1150 of the Apennines arc. From the analysis of GPS data, 1151 along the Apennines subduction zone at least five 1152 different kinematic settings coexist, showing how a 1153 single subduction can have internal variable velocities 1154 as a function of the combination V_H and V_L . The late 1155 Oligocene to present Apennines–Tyrrhenian system 1156 formed respectively as the accretionary prism (e.g., 1157 Bally et al., 1986) and the backarc basin (e.g., Kastens 1158 et al., 1988) in the hangingwall of an arcuate W-directed 1159 subduction system. The downgoing lithosphere has 1160 variable thickness and composition (Adriatic continen- 1161 tal, Ionian oceanic (?) and African continental, e.g., 1162 Calcagnile and Panza, 1981; Farrugia and Panza, 1981; 1163 IESG-IGETH, 1981; Calcagnile et al., 1982; Panza 1164 et al., 1982; Doglioni et al., 1999b; Catalano et al., 2001; 1165 Panza et al., 2003; Faccenna et al., 2004).

1166 Moving along strike, due to the relevant anisotropies 1167 of the downgoing lithosphere (e.g., Calcagnile and 1168 Panza, 1981), the slab had and still has different behav- 1169 iors, both in terms of seismicity, surface geology, and 1170 kinematics.

1171 We analyzed the motions of selected GPS stations of 1172 Italy, using different database. We have chosen five main

1173 sections, characterizing most of the country area (Fig. 17). 1174 We used data from D'Agostino and Selvaggi (2004) for 1175 the sections 1, 3, 5, whereas for section 2 data come from 1176 the EUREF database of July 2006 (<http://www.epncb.oma.be/>). In section 4 (Fig. 17) we used data from 1177 Hollenstein et al. (2003) for the PORO station, whereas 1178 the velocity of point A in the Ionian Sea (18.50°E 38.3°N) 1179 is computed using Africa–Eurasia relative motion para- 1180 meters from the REVEL plate kinematic model (Sella 1181 et al., 2002) (Fig. 17A). For a discussion on errors, see the 1182 related papers. We are aware that using different data sets 1183 may lead to inappropriate kinematic solutions. However 1184 for each single cross-section the data are extracted from 1185 the same solutions (apart section 4), and again, our goal is 1186 not yet to arrive to the exact determination of the velocity, 1187 but to show a methodological approach and to highlight 1188 how different kinematic and tectonic settings coexist 1189 along a single subduction zone. Error ellipses in the GPS 1190 data can be close to the estimated velocity, and we under- 1191 stand that these values might be minimum rates with 1192 respect to the real velocity field. Moreover, the location of 1193 H in our computation is ambiguous and could not repre- 1194 sent the real velocity of the hinge, but the value we use 1195

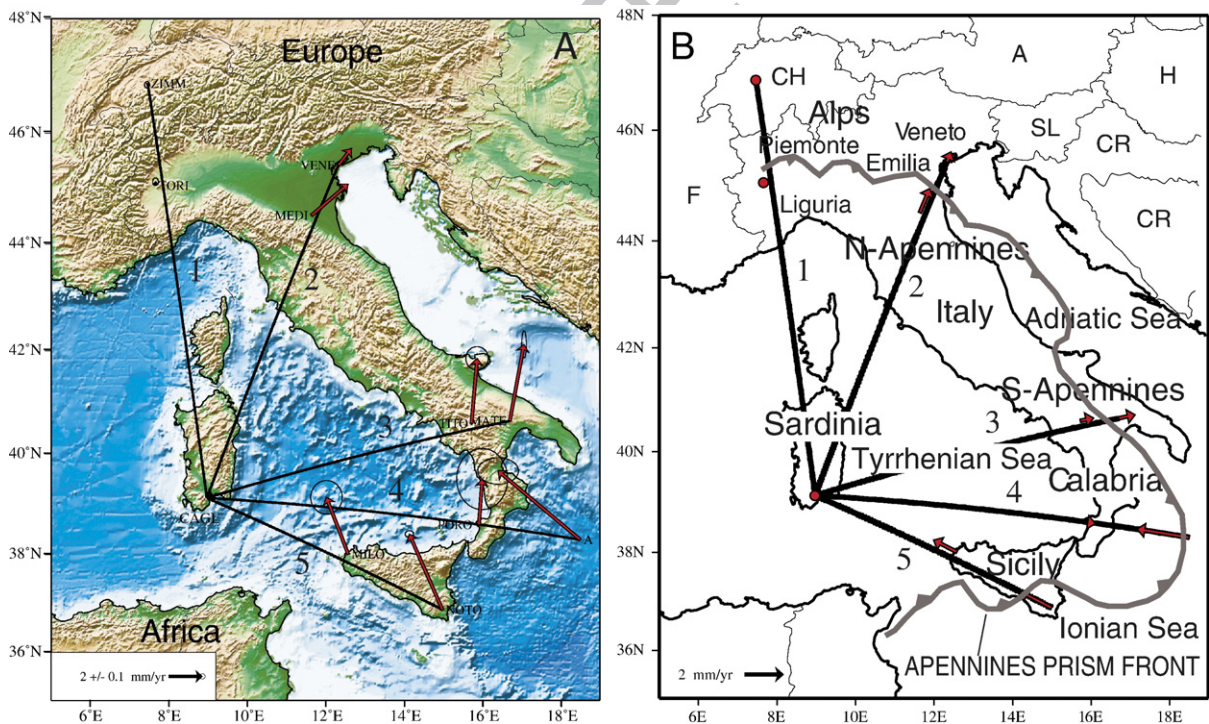


Fig. 17. A) Directions of selected GPS stations relative to Eurasia. Data are from three different databases. See text for explanation. The site of Cagliari (CAGL), which is on the Sardinia–Corsica continental boudin, is considered fixed with respect to Eurasia. B) Projections of velocity vectors on the sections connecting the stable CAGL with the other GPS stations across the Apennines subduction zone, reported in the following figure. U, upper plate; H, subduction hinge; L, lower plate; MEDI, Medicina; VENI, Venice; TITO, Tito; MATE, Matera; PORO, southwest Calabria; C, Ionian Sea, assumed fixed to Noto; MILO, Trapani; NOTO, Noto; TORI, Torino; ZIMM, Zimmerman.

1196 can be considered as a minimum rate at which H moves.
1197 This analysis aims mainly at a methodological aspect.

1198 In Fig. 17B are reported the projections on the
1199 sections of the velocity vectors. In this way, it is possible
1200 to compare relative components of the motion on the
1201 trajectories connecting the three GPS stations involved
1202 in the analysis. From the GPS data of Devoti et al.
1203 (2002), Oldow et al. (2002), Hollenstein et al. (2003),
1204 Battaglia et al. (2004), Serpelloni et al. (2005), the
1205 Sardinia plate (e.g., the Cagliari site) can be considered
1206 practically fixed relative to Eurasia. Cagliari is located
1207 in the Sardinia–Corsica micro-continent, a remnant of
1208 the upper plate boudinage in the backarc setting of the
1209 Apennines subduction (Gueguen et al., 1997). Therefore
1210 Cagliari–Sardinia can be used as reference for the upper
1211 plate of the subduction system.

1212 From Sardinia to Liguria and south Piemonte in the
1213 northern Apennines, there are no significant movements,
1214 and both H and L can be considered fixed relative to U
1215 (Fig. 17, and Fig. 14-7W). Moving from Sardinia to the
1216 northeast, through Emilia and Veneto regions, the site of
1217 Medicina (e.g., Battaglia et al., 2004), that is assumed to
1218 be coherent with the subduction hinge, is moving away
1219 from the upper plate faster than sites located more to the
1220 northeast in the foreland, so that $V_H > V_L$ (Figs. 17 and 18,
1221 section 2). Ongoing extension is documented in the
1222 central-northern Apennines (Hunstad et al., 2003), is
1223 consistent with the positive value of V_H (i.e., the hinge

migrates toward the foreland) that explains the active
1224 spreading of the Tyrrhenian backarc basin. 1225

1226 In the Southern Apennines the setting changes and,
1227 although the determination of the velocity of H it is not
1228 precise, the site used here would suggest a slower velocity
1229 of the diverging hinge with respect to the foreland,
1230 i.e., both H and L move away from the upper plate, but
1231 the lower plate L seems faster (Fig. 18-3). This setting
1232 would correspond to Fig. 14-5W, where the slab is
1233 paradoxically moving away with respect to the upper
1234 plate and subduction would result as negative (Figs. 17
1235 and 18, section 3). This is in agreement with the paucity
1236 of geological and geophysical observations supporting
1237 active compression at the Southern Apennines front,
1238 while extension is widespread in the belt (Scrocca et al.,
1239 2005).

1240 In a cross-section from Sardinia to Calabria and Ionian
1241 basin (Fig. 18-4), the setting changes again becoming
1242 similar to that of Fig. 14-1W. The Ionian (L), unlike the
1243 previous sections, is converging relative to U because it is
1244 moving with the Pelagian shelf south of Sicily, which is
1245 converging relative to Sardinia (Figs. 17 and 18, section 5).

1246 During present times, it is doubtful if and how fast
1247 Calabria (H) is still moving eastward relative to Sardinia
1248 (U), in the frame of still active extension of the Tyrrhenian
1249 (Goes et al., 2004; D'Agostino and Selvaggi, 2004;
1250 Pondrelli et al., 2004). However seismicity and seismic
1251 reflection profiles suggest active, although slow,

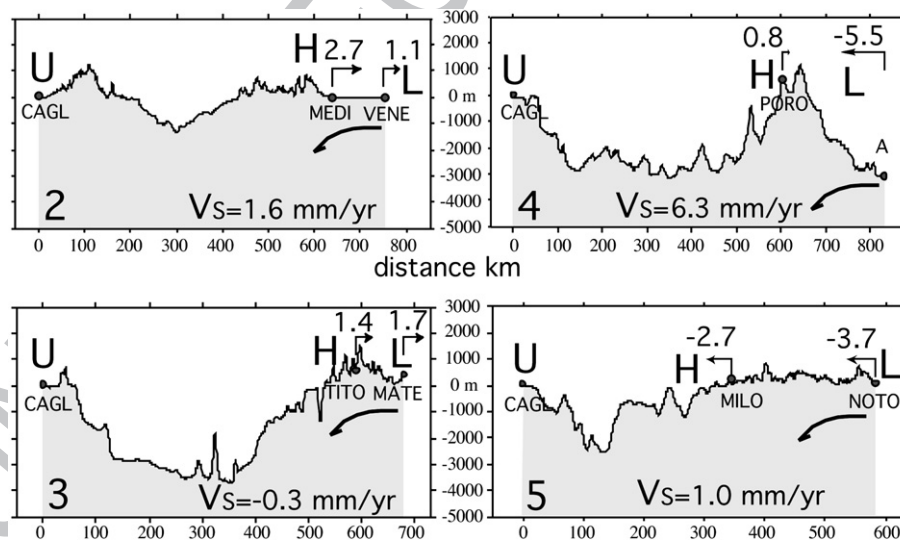


Fig. 18. Based on the data of the previous figure, along the Apenninic arc different relationships between U , H and L occur. The upper plate U is considered fixed (Sardinia–Corsica). The computed subduction rates are minimum estimates based on the approximation of a valid location of the subduction hinge H . Note that each section has different geodynamic settings and variable subduction rate, if any. The rates of H and lower plate L are in mm/yr. Section 1 is omitted since movements are close to null. Note that in section 3 the subduction is paradoxically negative, pointing for a detachment of the slab but from the surface. The variable kinematic settings are consistent with the seismicity of the area. Site and section locations in the previous figure. The fastest subduction rate is along the Calabrian arc (section 4).

PLATE MOTIONS RELATIVE TO THE MANTLE

L = Lower plate
 H = Subduction hinge
 U = Upper plate

Convergence 90 mm/yr
 Shortening in the prism 110 mm/yr
 Subduction 110 mm/yr
 Backarc spreading 20 mm/yr

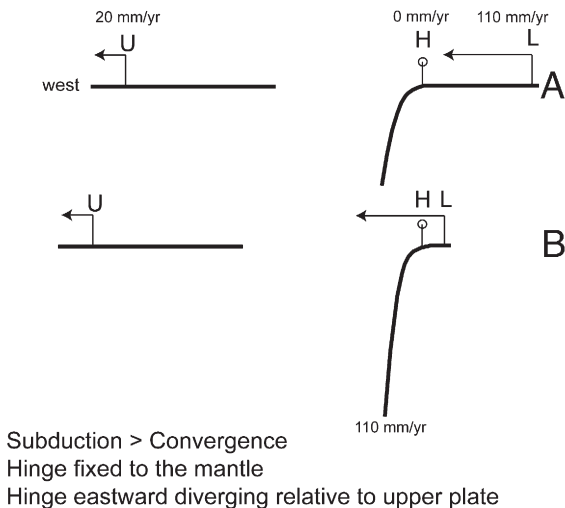


Fig. 19. Cartoon showing a two stages (A, B) absolute kinematics of a W-directed subduction zone. The slab is anchored in the mantle, and the subduction rate is faster than the convergence rate. The subduction hinge H is fixed relative to the mantle but is moving east relative to the upper plate.

1252 extension in the Tyrrhenian Sea (Scrocca et al., 2003;
 1253 Doglioni et al., 2004; Pondrelli et al., 2004; Chiarabba
 1254 et al., 2005). The Ionian (L) is converging relative to U
 1255 because it is moving with the Pelagian shelf south of
 1256 Sicily, which is converging relative to Sardinia.

1257 An increase of accretion in the Ionian prism of the
 1258 Apennines should provide an upper plate crustal thicken-
 1259 ing and widening, partly preventing the backarc exten-
 1260 sion, as previously discussed. Along this section there is
 1261 the fastest subduction rate (Figs. 8 and 18, section 4).

1262 From Sardinia to Sicily, and from Sicily foreland to the
 1263 south, the African vectors (V_L) move toward Cagliari
 1264 (Devoti et al., 2002; Goes et al., 2004), but in northern
 1265 Sicily (H) the movement is slower than in the foreland to
 1266 the south (Battaglia et al., 2004). This is the setting of
 1267 Fig. 18, section 5, and Fig. 14, 8W, where H is rather
 1268 approaching U, with a slower velocity than the L, i.e.,
 1269 $-V_H < -V_L$. This is consistent with the compressive
 1270 seismicity both south and north of Sicily (Chiarabba et al.,
 1271 2005). The backarc setting along this section is then
 1272 shrinking.

1273 However, in the southern Tyrrhenian Sea, different
 1274 settings may coexist in a single area due to the 3D nature
 1275 of the subduction. For example, in northern Sicily,

1276 convergence of the hinge relative to the upper plate in a
 1277 NW–SE section concurs with an E–W extension related
 1278 to the divergence of the hinge in Calabria. Therefore
 1279 compressive–transpressive tectonic features overlap with
 1280 extensional–transtensional faults in the southern Tyrrhe-
 1281 nian Sea. This is consistent with seismic section
 1282 interpretation (Pepe et al., 2005) and seismicity of the
 1283 area (Pondrelli et al., 2004; Chiarabba et al., 2005).

6. Basic kinematics in the mantle reference frame 1284

1285 We can now use the mantle as a reference for the
 1286 motion of the three points located in the upper plate,
 1287 lower plate and subduction hinge (Figs. 19 and 20).
 1288 Using the mantle as a reference needs either to adopt a
 1289 hotspot reference frame, or to infer other fixed mantle
 1290 frames from geological indicators. The dilemma of
 1291 choosing the most acceptable reference frame, if any, is
 1292 out of the scope of this paper. After this preamble, we
 1293 use a classic hotspot reference frame such as the one
 1294 proposed by Gripp and Gordon (2002). In this reference,
 1295 the lithosphere is moving relative to deep hotspots, and

PLATE MOTIONS RELATIVE TO THE MANTLE

L = Lower plate
 H = Subduction hinge
 U = Upper plate

Convergence 70 mm/yr
 Shortening in the orogen 50 mm/yr
 Subduction 20 mm/yr

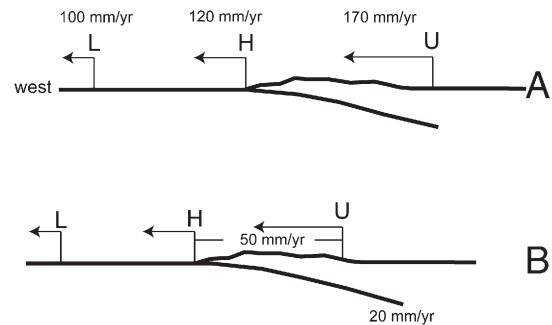


Fig. 20. Cartoon showing two stages (A, B) absolute kinematics of an E-NE-directed subduction, which has a slower subduction rate with respect to the convergence rate. The trench or subduction hinge H is moving west relative to the mantle but is moving east relative to the upper plate. Therefore in both W- and E-NE-directed subduction zones, the hinge migrates eastward relative to the upper plate. Larger the shortening in the orogen, lower the strength of the upper plate and lower the coupling between upper and lower plates. The convergence/shortening ratio in this example is 1.4 and is function of the lithospheric strength. From this analysis, plate motions are not controlled by subduction rate, but vice versa.

1296 it has a net “westward” rotation of about $0.44 (\pm 0.11)$
 1297 deg Myr^{-1} , the so-called westward drift of the litho-
 1298 sphere (Bostrom, 1971; Moore, 1973). Plate motions in
 1299 the no-net-rotation frame such as Heflin et al. (2005),
 1300 can be transferred into the net rotation frame indicated
 1301 by the motion of the lithosphere relative to hotspots.
 1302 Recently a debate arose regarding whether hotspots are
 1303 deep or shallow features (Foulger et al., 2005), and if
 1304 they can represent a fixed reference frame (e.g., Norton,
 1305 2000). In case it will be proven they are shallow
 1306 sourced, the net rotation of the lithosphere can be much
 1307 faster than presently estimated (Doglioni et al., 2005b).
 1308 Both in the deep and shallow source hypothesis, the W-
 1309 directed subduction zones have hinges fixed or
 1310 anchored to the mantle (Fig. 19). Along the opposite
 1311 E- or NE-directed subduction zones, due to the global
 1312 polarization, the hinge is moving west or southwest
 1313 (Fig. 20). For example, the Chile trench, along the
 1314 Andean subduction zone, shows a hinge moving west
 1315 relative to the mantle, while it moves eastward relative
 1316 to the upper plate.

1317 When analyzing the motion of the Nazca and South
 1318 America plate in the two reference frames (i.e., deep and
 1319 shallow hotspots), Nazca moves eastward relative to the
 1320 mantle in the deep hypothesis, whereas it would move
 1321 westward in the shallow interpretation (Cuffaro and
 1322 Doglioni, in press, Fig. 21).

1323 Along the Hellenic subduction zone, the former
 1324 speculation seems to be valid regardless the deep and
 1325 shallow models (Fig. 22). In this last case, the slab
 1326 would move out of the mantle, suggesting that it is
 1327 escaping from the mantle, but it subducts because the
 1328 upper plate is moving westward or southwestward faster
 1329 than the lower plate (Fig. 23). This kinematic constraint
 1330 is in a way indicating a paradox, i.e., along subduction
 1331 zones the slab can even move upward relative to the
 1332 mantle. This could be the rule along E- NE-directed
 1333 subduction zones in the shallow hotspot reference frame
 1334 hypothesis. But, more importantly, in the meantime it
 1335 shows that the slab pull cannot be the main cause for
 1336 subduction and the energy source of plate tectonics.

1337 The subduction almost equals the relative motion of
 1338 the upper plate over the lower plate at the trench. In fact,
 1339 in the example of Fig. 23, the upper plate overrides the
 1340 lower plate at only 10 mm/yr at the trench, in spite of a
 1341 convergence of 80 mm/yr. Moving from the base of the
 1342 slab upwards, the relative motion between upper and
 1343 lower plates decreases because part of the converge is
 1344 adsorbed by the upper plate shortening (Fig. 23). Note
 1345 that in these shallow settings there should occur the
 1346 slowest subduction rates. It is interesting that the
 1347 tectonic erosion (e.g., von Huene and Lallemand,

1348 1990; Ranero and von Huene, 2000) has been described
 1349 more frequently along this type of geodynamic
 1350 environment. Tectonic erosion means that the basal
 1351 decoupling surface of the orogen is in the upper plate
 1352 rather than in the lower plate when accretion occurs.
 1353 This is also logical during oceanic subduction because
 1354 of the higher strength of the oceanic rocks with respect
 1355 to the continental crust. In these settings, most of the
 1356 shortening is in fact concentrated in the upper plate.

7. The Hellenic subduction 1357

1358 Along the Hellenic trench the Africa plate subducts
 1359 NE-ward underneath Greece. The Hellenic subduction
 1360 zone is active as evidenced by seismicity, volcanism,
 1361 space geodesy data, etc. (Innocenti et al., 1982, 1984;
 1362 Christova and Nikolova, 1993; Clément et al., 2000;
 1363 Doglioni et al., 2002). Along slab, seismicity shows
 1364 down-dip extension (Papazachos et al., 2005). Using the
 1365 hotspot reference frame of Gripp and Gordon (2002),
 1366 Africa is moving west slower than Greece. This is even
 1367 more evident in the shallow hotspot reference frame, but
 1368 the directions are more southwestward directed
 1369 (Fig. 22). Therefore, regardless the mantle reference
 1370 frame, Africa moves relatively west or southwest, in the
 1371 opposite direction with respect to the direction of
 1372 subduction under the Hellenic trench. Therefore, the
 1373 mantle should move eastward with respect to the slab,
 1374 i.e., the slab would move west or southwestward relative
 1375 to the mantle. The deep seismicity of the slabs under the
 1376 Apennines and the Hellenides shows opposite behavior,
 1377 i.e., the slab is under down-dip compression along the
 1378 W-directed subduction zone (Frepoli et al., 1996), and
 1379 down-dip extension along the Hellenides (Papazachos et
 1380 al., 2005). These kinematics (Fig. 24) suggest that the
 1381 slab under the Apennines resists the sinking, whereas
 1382 the Hellenic slab is pulled either from below (slab pull)
 1383 or from above (W-ward drift of the lithosphere). The
 1384 relative eastward mantle flow would be consistent with
 1385 these observations, pushing down the Apennines slab,
 1386 and moving eastward with respect to the Hellenic slab,
 1387 attached to the Africa plate which is due west.

1388 A mantle flowing to the east or northeast in the
 1389 Mediterranean is consistent with a number of observa-
 1390 tions, such as the shear-wave splitting analysis (Mar-
 1391 gheriti et al., 2003; Barruol et al., 2004), S-wave mantle
 1392 tomography (Panza et al., 2007), the fast eastward
 1393 Neogene to present retreat of the Apennines–Maghre-
 1394 bides subduction zone, the shallow dip and depth of the
 1395 Hellenic slab vs. the steeper and deeper W-ward directed
 1396 Apennines subduction, plus another number of geolog-
 1397 ical asymmetries such as the shallow vs. the deep trench

1398 or foreland basin, the shallow vs. the steep regional
1399 monocline, etc. (Doglioni et al., 1999b).

1400 In this interpretation, the Hellenic subduction is
1401 moving out of the mantle (Fig. 23), no matter the hotspot
1402 reference frame. Subduction occurs because the upper
1403 plate (Greece) is overriding the lower plate Africa faster.
1404 This setting appears as a prototype of a subduction not
1405 driven by the negative buoyancy of the slab because the
1406 kinematic observation is not biased by the reference
1407 frame, and seems consistent with the corollary of
1408 geological and geophysical observations.

8. What drives subduction?

1409
1410 One paradigm of plate tectonics relates the dip of the
1411 slab to the buoyancy of the downgoing lithosphere along
1412 subduction zones, being the negative buoyancy propor-
1413 tional to the age of the oceanic lithosphere, length of the
1414 slab and length of the trench (Forsyth and Uyeda, 1975;
1415 Jarrard, 1986; Anderson, 2001; Conrad and Lithgow-
1416 Bertelloni, 2003). Carlson et al. (1983) found an
1417 important correlation between the absolute velocity of
1418 plates and the age of the oceanic crust, pointing out for a

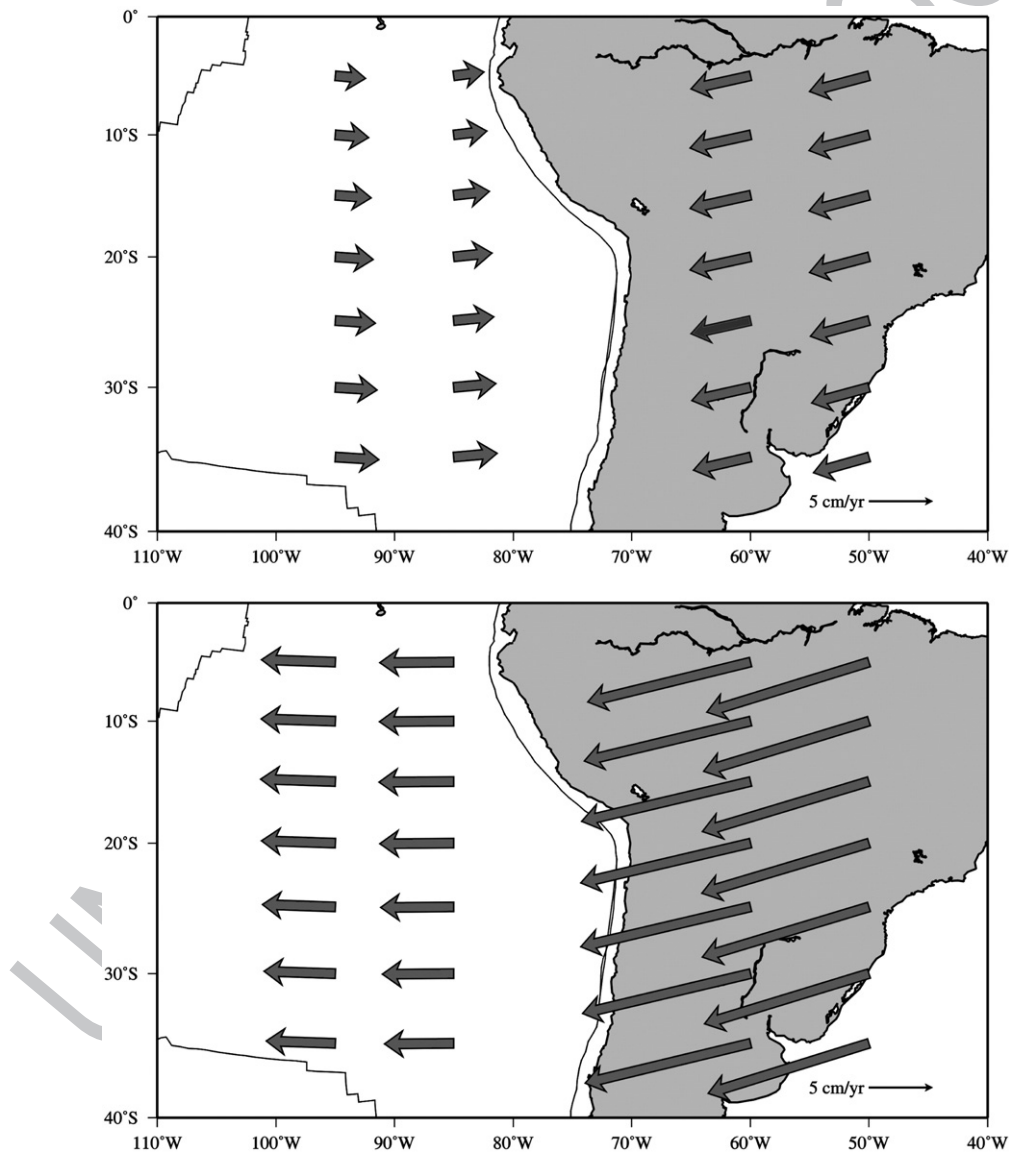


Fig. 21. Plate motions of South America and Nazca relative to the mantle in the deep (above) and in the shallow hotspot reference frames (below). Note that in the shallow hotspot reference frame, the Nazca plate is moving westward faster than the underlying mantle, escaping from the subduction.

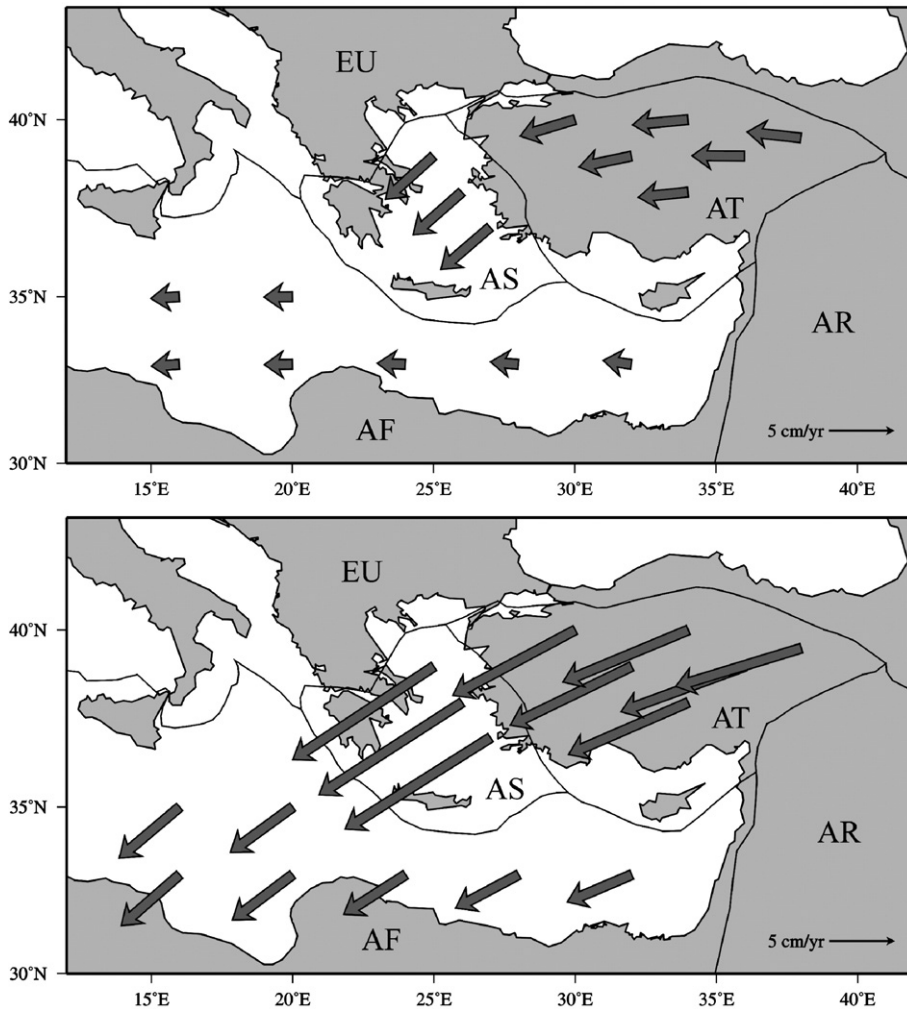


Fig. 22. Plate motions of Africa, Greece and Anatolia relative to the mantle in the deep (above) and in the shallow hotspot reference frames (below). Note that in both reference frames, Africa is moving westward faster than the underlying mantle, escaping from the subduction. This setting refers to the case of the frame SE of Fig. 15.

1419 fundamental role of the slab pull as the driving
 1420 mechanism: the older and cooler oceanic lithosphere
 1421 should result in a denser and faster sink along the
 1422 subduction zone driven only by its negative buoyancy.
 1423 However there is no correlation between convergence
 1424 rates and age of the oceanic crust (Fig. 25). Moreover,
 1425 when plate motions are computed in the deep and in the
 1426 shallow hotspot reference frame, few plates move out of
 1427 the trench along E–NE-directed subduction zones
 1428 (Figs. 21 and 22), indicating only the negative buoyancy
 1429 of the slab does not drive that subduction. In their
 1430 analysis, Carlson et al. (1983) have a strong weight of the
 1431 Pacific plate which is the fastest plate surrounded by a
 1432 number of subduction zones (Marianas, Izu–Bonin,
 1433 Japan, Kurili, Tonga, Kermadec). But is the plate fast
 1434 because driven by the slab pull at the margin, or are there

1435 other forces acting on the plate and the subduction is a
 1436 consequence of this speed? It is worth noting that the
 1437 Pacific plate has the lowest asthenosphere viscosity
 1438 values (Pollitz et al., 1998), i.e., it is the most decoupled
 1439 plate with respect to the asthenosphere. Moreover the
 1440 Pacific plate has a single angular velocity, it has no
 1441 relevant internal strain, but nevertheless is treated by
 1442 Carlson et al. (1983) as several independent plates to
 1443 which different slabs are attached. Along the regression
 1444 line computed in their research, W-directed subduction
 1445 zones are generally faster than the opposite E to NNE-
 1446 directed slabs. This is predicted by the simple afore-
 1447 mentioned kinematics. Moreover, due to the “westerly”
 1448 directed rotation of the lithosphere, the plates located to
 1449 the west of a rift (e.g., the Pacific plate to west of the
 1450 East Pacific Rise) tend to be preserved longer. For example

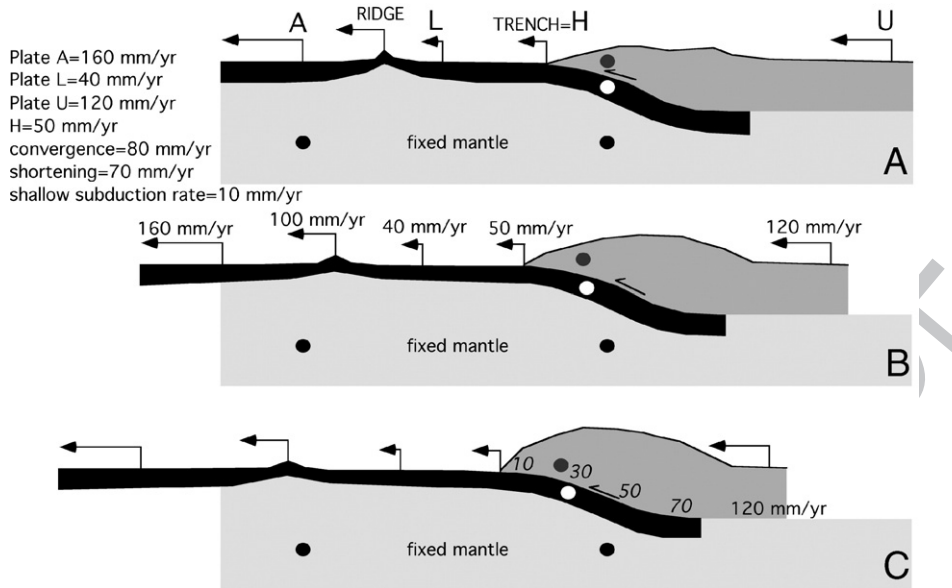


Fig. 23. When plate motions are considered relative to the hotspot reference frame, i.e., assuming fixed the mantle, the slabs of E- or NE-directed subduction zones may move out of the mantle. In the three stages sketch (a, b, c), the white circle moves leftward relative to the underlying black circle in the mantle. Subduction occurs because the upper plate dark gray circle moves leftward faster than the white circle in the slab. In this model, the slab moves west at 40 mm/yr relative to mantle. The subduction rate is the convergence minus the orogenic shortening. With different velocities, this seems to apply to the Hellenic subduction and, in the shallow hotspot reference frame, also to the Andean subduction. This kinematic evidence of slabs moving out of the mantle casts doubts on the slab pull as the driving mechanism of plate motions. In the lower section, the numbers in italic from 10 through 70 indicate the relative velocity in mm/yr between the upper and the lower plate. Note that the subduction rate should increase with depth, where the upper plate shortening is decreasing. This is consistent with the down-dip tension seismicity of this type of subduction.

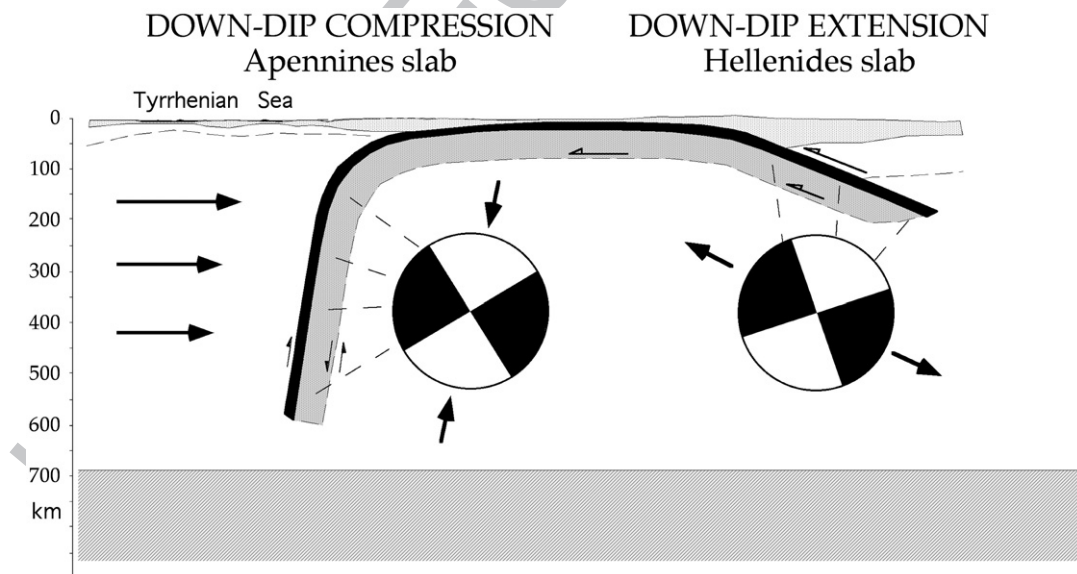


Fig. 24. The deep seismicity along the Apennines and Hellenides slab shows opposite behavior, being steeper and deeper vs. shallower and less inclined respectively. Moreover the Apennines slab is undergoing down-dip compression (Frepoli et al., 1996), whereas the Hellenic slab suffers down-dip extension (Papazachos et al., 2005). This opposite behavior mostly occurs also comparing the western and the eastern margins of the Pacific subduction zones. This asymmetry is consistent with the W-ward drift of the lithosphere relative to the mantle.

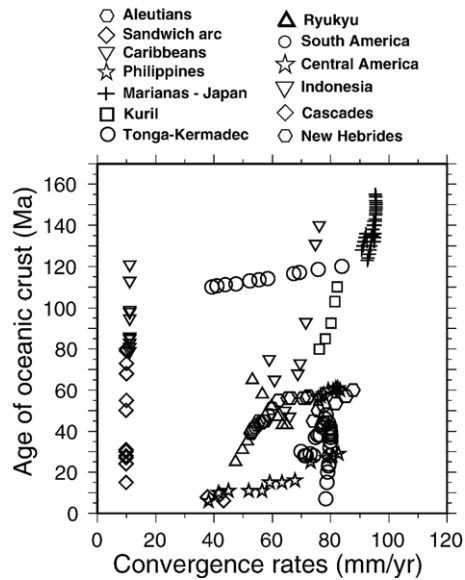


Fig. 25. Age of oceanic lithosphere entering the trench (after Mueller et al., 1997) vs. velocity of convergence calculated using the NUVELIA (DeMets et al., 1994) rotation poles. The diagram shows a plot obtained for 13 subduction zones. Note the absence of correlation suggesting no significant relation between plate motions speed and negative slab buoyancy. Data taken after Cruciani et al. (2005).

1451 the plates in the hangingwall of the western margin of the
1452 Pacific ocean also move west, but in the eastern margin,
1453 since again both upper and lower plates move west, the
1454 lower plate will be gradually overridden by the upper
1455 plate. This could explain why the age of the Pacific
1456 Ocean is older in the western side, and the lithosphere is
1457 characterized by the oldest ages along the western trench.

1458 We have seen in the previous sections that the
1459 subduction rate depends both on the absolute velocity of
1460 the lower and upper plates, plus the velocity and
1461 direction migration of the subduction hinge. Therefore
1462 the absolute velocity of the lower plate does not provide
1463 direct information on the subduction rate, which is
1464 considered in the slab pull model only constrained by the
1465 negative buoyancy.

1466 Several analogue and finite element models have been
1467 carried out in order to reproduce subduction mechanisms
1468 (e.g., Sheena, 1993; Regard et al., 2003). However all these
1469 models a priori impose a denser lithosphere with respect to
1470 the underlying mantle. This assumption is questionable
1471 because there are no direct density constraints on the
1472 hosting mantle, which is considered denser than the
1473 lithosphere in all models at least below the asthenosphere
1474 (Dziewonski and Anderson, 1981; Kennett et al., 1995).

1475 The larger negative buoyancy has been invoked to
1476 explain the steeper dip of the western Pacific subduction
1477 zones because the subducting western Pacific oceanic

1478 lithosphere is older, cooler and therefore denser. However,
1479 the real dip of the slabs worldwide down to depths of
1480 250 km shows no relation with the age of the downgoing
1481 lithosphere (Cruciani et al., 2005; Lallemand et al., 2005).
1482 In fact there are slabs where moving along strike the age of
1483 the downgoing lithosphere varies, but the dip remains the
1484 same (Barbados), or vice versa, the age remains constant
1485 while the dip varies (Philippines). There are cases where
1486 the age decreases and the dip increases (W-Indonesia),
1487 and other subduction zones where the age increases and
1488 the dip decreases (Sandwich). This shows that there is not
1489 a first order relationship between slab dip and lithospheric
1490 age. This suggests that supplemental forces or constraints
1491 have to be accounted for, such as thickness and shape of
1492 the hangingwall plate, relative and absolute plate velocity,
1493 presence of lateral density variations in the hosting upper
1494 mantle, effects of accretion/erosion, subduction of
1495 oceanic plateaus and slab deformation due to the motion
1496 of the mantle relative to the subducting plate (Cruciani
1497 et al., 2005). Seismicity illuminating the slab geometry is
1498 strongly influenced by the composition, thermal state and
1499 velocity of the downgoing plate (e.g., Carminati et al.,
1500 2005).

1501 In the following sections we will analyze the
1502 alternative mechanisms that have been proposed to
1503 drive plate tectonics, namely slab pull, mantle convec-
1504 tion and the forces generated by the Earth's rotation.

1505 8.1. On the efficiency of the slab pull

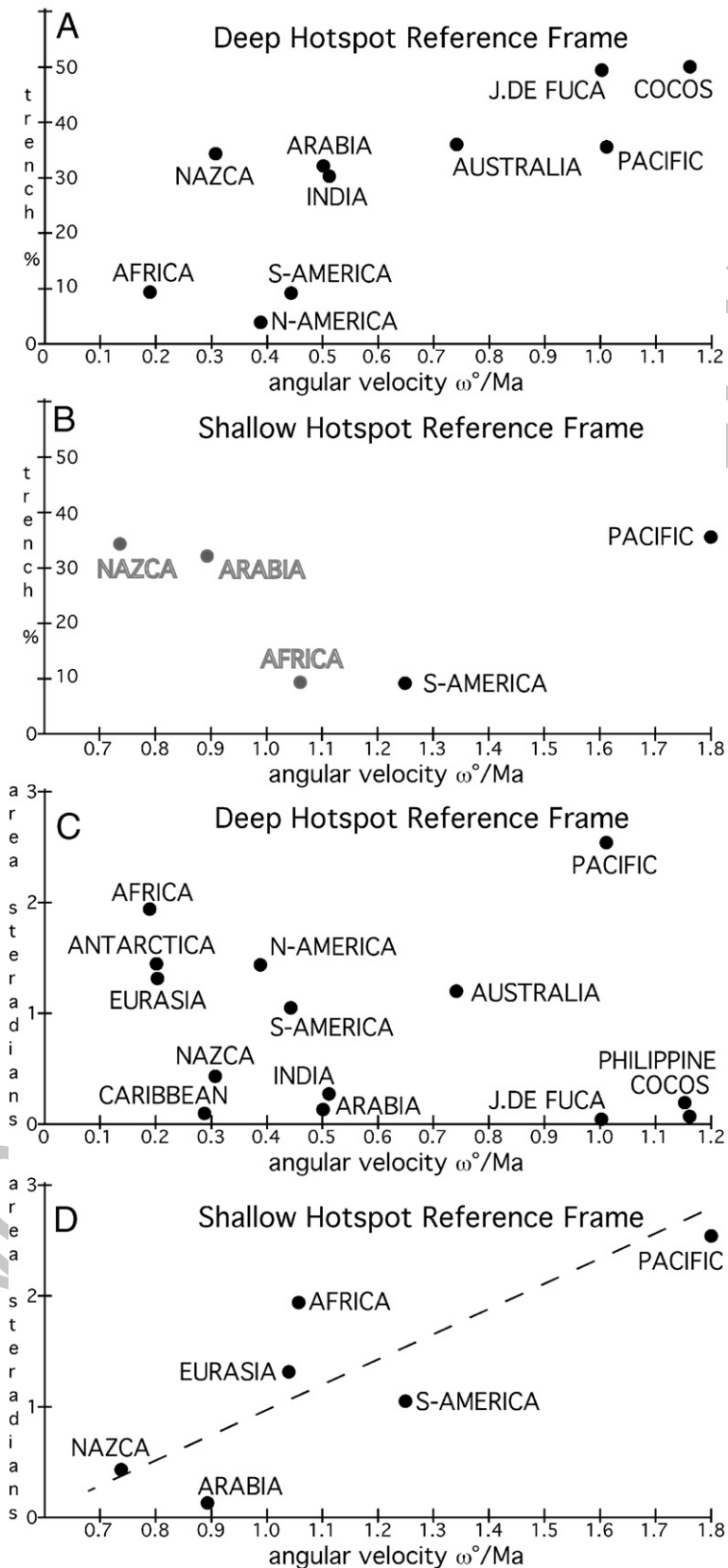
1506 The negative buoyancy of slabs should determine the
1507 pull of plates, but it has been shown that the dip of the
1508 subduction zones is not correlated with the age and the
1509 thermal state of the down going plates (Cruciani et al.,
1510 2005). Moreover relative convergence rates at subduc-
1511 tion zones do not correlate with age of oceanic
1512 lithosphere at the trench (Fig. 25). One statement used
1513 to corroborate the slab pull is the trench length with
1514 respect to the plate velocity (Forsyth and Uyeda, 1975).
1515 On the basis of a similar observation it could be argued
1516 that fast spreading ridges generate fast plate motions.
1517 However these relations may be a circular reasoning,
1518 e.g., longer subduction zones and faster ridges form
1519 when plates move faster (Doglioni et al., 2006b). The
1520 relationship between trench length and plate velocity is
1521 also questionable for other reasons; for example the
1522 absolute plate velocity can be recomputed either in the
1523 deep hotspot (Fig. 26, A) or in the shallow hotspot
1524 reference frame (Fig. 26, B), and the different results do
1525 not support a correlation between slab length percentage
1526 (length of the trench with respect to the length of the
1527 boundary surrounding the plate) and plate velocity.

1528 The relationship between the area of plates (Schettino,
1529 1999) and the angular velocity of plates in the deep
1530 hotspot reference frame (HS3-NUVEL1A, Gripp and
1531 Gordon, 2002) shows no correlation (Fig. 26, C), as
1532 already observed by Forsyth and Uyeda (1975). However,
1533 when plotting the area vs. the absolute angular velocities
1534 of plates in the shallow hotspot reference frame, a
1535 correlation seems to be present, being bigger plates
1536 generally faster (Fig. 26, D). When comparing similar size
1537 of plates, the oceanic or continental plus oceanic, oceanic
1538 plates travel faster than purely continental.

1539 Both analyses do not support a significant correlation
1540 casting more doubts on the importance of the slab pull,
1541 which has a number of further counterarguments. For
1542 example, the assumption that the slab is heavier than the
1543 country mantle remains debatable, particularly because
1544 there are not constraints on the composition of both slab
1545 and mantle at variable depth (e.g., the amount of Fe in
1546 the lower asthenosphere and the lower upper mantle). Is
1547 the slab pull the energetic source for plate motions? Is it
1548 large enough? Is it correctly calculated? Are the
1549 assumptions reliable? Most of the literature indicates
1550 that the slab pull is about $3.3 \times 10^{13} \text{ N m}^{-1}$ (e.g.,
1551 Turcotte and Schubert, 2002). This is a force per unit
1552 length parallel to the trench. However this value is very
1553 small when compared to other energetic sources for
1554 Earth, such the energy dissipated by tidal friction, heat
1555 flow emission, and Earth's rotation (e.g., Denis et al.,
1556 2002). Moreover the slab pull would be even smaller if
1557 chemical and mineralogical stratification are introduced
1558 in the upper mantle. Most of the Earth's volcanism is
1559 sourced from above 200 km: the subduction zones
1560 release magmatism at about 100–150 km depth
1561 (Tatsumi and Eggins, 1995); mid-oceanic ridges are
1562 sourced by even shallower asthenosphere melting (100–
1563 30 km, e.g., Bonatti et al., 2003); hotspots are also
1564 debated as potentially very shallow, and sourced by the
1565 asthenosphere (Bonatti, 1990; Smith and Lewis, 1999;
1566 Doglioni et al., 2005b; Foulger et al., 2005). Since even
1567 xenoliths in general and kimberlite chimneys originated
1568 at depth not deeper than the asthenosphere, we have no
1569 direct sampling of the composition of the standard lower
1570 part of the upper mantle. Therefore we cannot exclude
1571 for example a more Fe-rich fayalitic composition of the
1572 olivine, heavier and more compacted than the Mg-rich
1573 olivine (forsterite, which is presently assumed as the
1574 more abundant mineral of the upper mantle. In case
1575 more iron is present in the upper mantle olivine, the
1576 density of the ambient mantle would be slightly higher,
1577 making the slab pull smaller, if any. The slab pull
1578 concept is based on the hypothesis of a homogeneous
1579 composition of the upper mantle, with the lithosphere

sinking only because it is cooler (e.g., Turcotte and
Schubert, 2002). However, the oceanic lithosphere is
frozen shallow asthenosphere, previously depleted
beneath a mid-oceanic ridge. Depleted asthenosphere
is lighter than the “normal” deeper undepleted asthenosphere
(see Oxburgh and Parmentier, 1977; Doglioni
et al., 2003, 2005a,b for a discussion). Therefore the
assumption that the lithosphere is heavier only because
it is cooler might not be entirely true, and the slab pull
could be overestimated. Phase transitions within the
subducting lithospheric mantle would enhance the slab
pull in the transition zone (300–400 km; Stern, 2002;
Poli and Schmidt, 2002), but again, the occurrence of
higher density country rocks due to chemical and not
only phase transitions could make the effect of the slab
pull smaller and smaller. Moreover, the occurrence of
metastable olivine wedges in fast subducting oceanic
lithosphere is considered to create positive density
anomalies that should counteract the effects of slab pull
(Bina, 1996). A further density anomaly that is sug-
gested to drive slab pull is expected to come from the
eclogitization of the subducting oceanic crust. This
process involves only a thin layer (5–8 km thick) and
not the entire downgoing lithosphere (70–90 km thick).
Nevertheless, this type of metamorphic transition is
often assumed to be able to determine the slab pull. The
eclogites reach densities of about 3440–3460 kg m^3
only at depths of about 100 km (Hacker et al., 2003;
Pertermann and Hirschmann, 2003). The density of the
country mantle at comparable depths according to the
PREM model is 3370 kg m^3 (Anderson, 1989), i.e., only
slightly lighter than the eclogitized oceanic crust. Both
eclogite and mantle densities are quite speculative. The
small density contrast between subducting crust and
country mantle casts doubts on the potential effect of the
negative buoyancy of oceanic crust. Therefore we do not
have hard constraints on the depth at which the slab pull
should turn on and at what depth it should turn off since
the mineralogy of the slab and the hosting mantle is still
largely unknown. Why then a slab should maintain its
shape and coherence down to the 670 km discontinuity?
The easiest explanation would be its higher stiffness.
Since seismic wave velocity is inversely proportional to
density, the high velocity of the slab detected by
tomography could be related not to its higher density,
but to its higher rigidity. Certainly the slab becomes
heavier during sinking for phase transformations, but is
it a priori denser, or does it become heavier on the way
down? Is it continuously reaching density equilibrium
while moving down (Doglioni et al., 2006b)?

Trampert et al. (2004) have recently demonstrated
that low velocity volumes of the mantle detected by



1632 tomography can be due to lateral variations in compo-
 1633 sition rather than in temperature, i.e., they can be even
 1634 higher density areas rather than hotter lighter buoyant
 1635 material as so far interpreted. In fact, considering the
 1636 main low velocity zones in the mantle such as the
 1637 asthenosphere or the liquid core, their decrease in speed
 1638 of the P waves is related to their lower rigidity (e.g.,
 1639 Secco, 1995) either generated by CO₂ content in the
 1640 asthenosphere, or higher density — low viscosity iron
 1641 alloys in the liquid core. As extreme examples, gold or
 1642 lead have high density but low seismic velocity.
 1643 Therefore the interpretation of tomographic images of
 1644 the mantle where the red (lower velocity) areas are
 1645 assumed as lighter and hotter rocks can simply be wrong,
 1646 i.e., they may even be cooler and denser (Van der Hilst,
 1647 2004). With the same reasoning, blue (higher velocity)
 1648 areas, which are assumed as denser and cooler rocks may
 1649 even be warmer and lighter.

1650 Trampert et al. (2004) also suggest that the low
 1651 velocity in the lower mantle could for example be due to
 1652 higher concentrations in iron. Minerals containing more
 1653 iron are more conductive, and at that depth the coefficient
 1654 of thermal expansion must be very low. Both factors
 1655 decrease the Rayleigh number, making the convection
 1656 very sluggish (e.g., Anderson, 2002). The onion structure
 1657 of the Earth with shells compositionally homogeneous
 1658 (e.g., the PREM, see Anderson, 1989) is a misleading
 1659 oversimplification, since the occurrence of lateral hetero-
 1660 geneities in the whole Earth layers has been widely
 1661 demonstrated.

1662 The main geometric, kinematic and mechanical
 1663 counterarguments on the slab pull as the primary mecha-
 1664 nism for moving plates and for triggering subduction are
 1665 listed:

- 1666 1) The dip of the slab is independent from the age of
 1667 the oceanic lithosphere (Cruciani et al., 2005).
 1668 Therefore, the supposed larger negative buoyancy
 1669 determined by the cooler oceanic lithosphere does
 1670 not control the slab dip.
 1671 2) We have no hard constraints of the real compo-
 1672 sition of the upper mantle: there could be more

fayalite, making the upper mantle more dense and
 the slab negative buoyancy smaller.

- 3) Subduction processes involve also continental
 lithosphere descending to depths deeper than
 100–150 km (Ampferer, 1906; Dal Piaz et al.,
 1972; Trümpy, 1975; Ranalli et al., 2000; van
 Hinsbergen et al., 2005), although subducted
 average continental crust is most probably buoyant
 with respect to mantle rocks (Hermann, 2002).
- 4) The oceanic lithosphere is frozen shallow (30–
 100 km deep) asthenosphere, previously depleted
 below ridges. Therefore the oceanic lithosphere is
 the differentiated lighter upper part of the mantle.
 Then why should it be a priori heavier than the
 undepleted deeper (100–300 km) asthenosphere?
 A pyrolite density of 3400 kg m³ in the asthenosphere
 lying beneath the old oceanic lithosphere
 has been inferred (Jordan, 1988; Kelly et al.,
 2003). Moreover, hydrothermal activity generates
 serpentinization of the mantle along the ridge that
 decreases even more the density.
- 5) If oceanic lithosphere is heavier than the under-
 lying mantle, why are there no blobs of litho-
 spheric mantle (LID) falling in the upper mantle
 below the western older side of the Pacific plate?
- 6) Within a slab, eclogitization is assumed to make the
 lithosphere denser. However, eclogitization is
 concentrated in the 6–8 km thick oceanic crust,
 whereas the remaining 60–80 km thick lithospheric
 mantle does not undergo the same transformation.
 Therefore only 1/10 of the slab is apparently
 increasing density, but the main mass of the slab
 (90%) does not change significantly.
- 7) The density increase due to eclogitization is
 in contrast with the exhumation of the eclogitic
 prism that is usually detached with respect to the
 “lighter” lithospheric mantle (G.V. Dal Piaz,
 pers. comm.).
- 8) Why the lithosphere should start to subduct? This
 crucial point arises particularly when considering
 an oceanic hydrated and serpentinized lithosphere
 that has not yet been metamorphosed by the

Fig. 26. A) Relationship between absolute plate motions angular velocity vs. trench percent in the deep hotspot reference frame. There is not evident correlation between the two values. For example, the Nazca and Pacific plates have about the same percentage of trench length with respect to the plate circumference, but the Pacific is much faster. Angular velocities after Gripp and Gordon (2002). B) Relationship between absolute plate motions angular velocity vs. trench percent in the shallow hotspot reference frame. The absence of correlation between the two values is even more evident, but the gray points on the left show a negative motion of the plates, i.e., away from the trench. Therefore, in this reference frame, plates cannot be moved by the slab pull. Angular velocities after Crespi et al. (2007). C) Plot of plate areas and absolute angular velocities in the deep hotspot reference frame. Areas of plates after Schettino (1999). As already shown by Forsyth and Uyeda (1975), no relation is observable. D) Plot of plate areas and absolute angular velocities in the shallow hotspot reference frame. Angular velocities after Crespi et al. (2007). Unlike the previous figure, a correlation seems to exist, i.e., larger plates move faster, even if oceanic plates still move relatively faster than continental plates for comparable areas.

- 1715 subduction process, and consequently it is still
 1716 less dense (G.V. Dal Piaz, pers. comm.).
- 1717 9) Down-dip compression affects most of the slabs,
 1718 all below 300 km (Isacks and Molnar, 1971), most
 1719 of them even at shallower depth (e.g., Frepoli
 1720 et al., 1996), pointing out for a slab forced to sink
 1721 rather than actively sinking.
- 1722 10) The 700 km long W-Pacific slab, where only the
 1723 upper 300 km show some potential down-dip
 1724 extension seismicity (but it could be generated
 1725 also by horizontal shear in the mantle, Giardini
 1726 and Woodhouse, 1986) should pull and carry the
 1727 10,000 km wide Pacific plate, 33 times bigger,
 1728 winning the shear resistance at the plate base, and
 1729 the opposing basal drag induced by the relative
 1730 eastward mantle flow inferred from the hotspots
 1731 migration (Doglioni, 2006b).
- 1732 11) Kinematically, subduction rollback implies that the
 1733 volumes left in the hangingwall of the slab have to
 1734 be replaced by horizontal mantle flow, whether
 1735 this is a consequence or the cause of the retreat
 1736 (Doglioni et al., 1999b). However, in order to allow
 1737 the slab to move back, the slab retreat needs that
 1738 also the mantle in the footwall of the slab moves
 1739 away in the direction of the slab retreat. This is true
 1740 regardless this motion is generated by the slab pull
 1741 or it is an independent mantle horizontal flow. But
 1742 the energy required to push forward the mantle is
 1743 much greater than the slab pull can effort. Where
 1744 there is no convergence or rather divergence occurs
 1745 between upper and lower plates, the slab pull has
 1746 been postulated as the only possible driving
 1747 mechanism. However the slab pull has not the
 1748 energy to push back eastward the whole section of
 1749 mantle located east of the slab, in order to allow the
 1750 slab rollback. A relative eastward motion of the
 1751 mantle would be much more efficient in terms of
 1752 scale of the process and mass involved, to generate
 1753 the eastward slab hinge retreat, determining active
 1754 subduction without plates convergence (e.g.,
 1755 Apennines, Barbados).
- 1756 12) Are plates surrounded by long slabs and trenches
 1757 faster? It might be a circular reasoning because
 1758 long subduction zones might be a consequence of
 1759 fast movements of plates. Moreover plates are
 1760 considered fast in the no-net-rotation (NNR)
 1761 reference frame (Conrad and Lithgow-Bertelloni,
 1762 2003). For example, measuring plate motions in
 1763 the hotspot reference frame, i.e., relative to the
 1764 mantle, Nazca is very slow relative to mantle, so
 1765 the relation between plate velocity, slab age and
 1766 length of a subduction zone is not that simple.
- 13) Some plates in the hotspot reference frame move
 without any slab pulling them, e.g., the westward
 movements of North America, Africa and South
 America (Gripp and Gordon, 2002). Trench
 suction has been proposed to explain these move-
 ments, but beneath both North and South America
 the mantle is relatively moving eastward, opposite
 to the kinematics required by the trench suction
 model.
- 14) Plate velocities in the hotspot reference frame seem
 to be inversely proportional to the viscosity of the
 asthenosphere rather than to the length of the
 subduction zones and the age of the downgoing
 lithosphere. In fact the Pacific, which is the fastest
 westerly moving plate (Gripp and Gordon, 2002),
 has the lowest viscosity values (Pollitz et al., 1998).
- 15) The lateral velocity of plates is 10–100 times
 faster than vertical velocity (subduction related
 uplift or subsidence) suggesting that vertical
 motions are rather passive movements. Moreover,
 the kinematic analysis of section 3 shows that
 subduction rates appear controlled by rather than
 controlling horizontal plate motions.
- 16) The energy for shortening an orogen is probably
 larger than the one supposed for the slab pull.
- 17) When describing the plate motions relative to the
 mantle, e.g. in the hotspots reference frame, along
 E- or NE-directed subduction zones the slab might
 move out of the mantle, e.g., in the opposite
 direction of the subduction. It is sinking because
 the faster upper plate overrides it.
- 18) There are rift zones formed between plates not
 surrounded by oceanic subduction to which the
 pull for moving the lithosphere can be attributed
 (e.g., the Red Sea).
- 19) Although the knowledge of the rheological be-
 havior of subducted lithosphere is very poor, it can
 be conjectured that the downgoing slab, being
 progressively heated, could potentially lose
 strength, diminishing the possibility to mechani-
 cally transfer the pull (Mantovani et al., 2002).
- 20) The folding and unfolding of the lithosphere at the
 subduction hinge makes the slab even weaker for
 supporting the slab pull.
- 21) Slab pull has been calculated to be potentially
 efficient only at a certain depth (e.g. 180 km,
 McKenzie, 1977); and shallower than that? How
 does subduction initiate?
- 22) At the Earth's surface, oceanic lithosphere has low
 strength under extension (e.g., $8 \times 10^{12} \text{ N m}^{-1}$, Liu
 et al., 2004) and is able to resist a force smaller than
 that requested by slab pull ($3.3 \times 10^{13} \text{ N m}^{-1}$,

1819 Turcotte and Schubert, 2002). If the slab pull is the
 1820 cause for the motion of the Pacific plate, this
 1821 observation argues for a stretching of the Pacific
 1822 lithosphere before slab pull being able to move the
 1823 plate. In other words, the plate cannot sustain the
 1824 tensional stresses eventually due to slab pull. The
 1825 low lithospheric strength problem could be,
 1826 however, partly counterbalanced by the mantle
 1827 flow and viscous tractions acting on the plates
 1828 induced by slab sinking (e.g., Lithgow-Bertelloni
 1829 and Richards, 1998). Due to low temperature and
 1830 high pressure, the strength of subducted oceanic
 1831 lithosphere rises to some 2×10^{13} – 6×10^{13} N m⁻¹
 1832 (Wong A Ton and Wortel, 1997) and would make
 1833 sustainable the eventual pull induced by density
 1834 anomalies related to phase changes at depth. In
 1835 summary the subducted slab is probably able to
 1836 sustain the load induced by slab pull but probably
 1837 this load cannot be transmitted to the unsubducted
 1838 portion of the plate without breaking it apart.
 1839

1840 This long list casts doubts on the possibility that the
 1841 slab pull can actually trigger subduction, slab rollback,
 1842 and drive plate motions. Density anomalies due to
 1843 phase changes occurring at depth within the slab could
 1844 enhance the sinking of the slab. However, the slab pull
 1845 alone, even if efficient at some depth, is apparently
 1846 unable to explain the initiation of the subduction, and
 1847 the mechanism perpetuating plate motions in general.

1848 The slab detachment model is conceived as a
 1849 consequence of the negative buoyancy of the slab and it
 1850 has been invoked many times to explain the supposed
 1851 rupture of the slab in tomographic images (e.g., Wortel
 1852 and Spakman, 2000) and to fit the geochemistry of
 1853 magmatism (e.g., Lustrino, 2005). However, tomographic
 1854 images are based on velocity models that often overes-
 1855 timate the velocity of the asthenosphere where usually the
 1856 detachment is modeled. Therefore the detachment
 1857 disappears when using slower velocity for the astheno-
 1858 sphere in the reference velocity model, or generating
 1859 regional tomographic images with better accuracy (e.g.,
 1860 Piromallo and Morelli, 2003). Recently, Rychert et al.
 1861 (2005) have shown how the base of the lithosphere — top
 1862 of the asthenosphere (LVZ, e.g., Panza, 1980) is
 1863 characterized by unexpected, few km thick, extremely
 1864 low velocities beneath northwestern North America, far
 1865 from subduction zones. This implies a revision of the
 1866 velocity models used for mantle tomography, particularly
 1867 in areas characterized by strong lateral variations in
 1868 composition of the subducting lithosphere (e.g., conti-
 1869 nental vs. oceanic) that cannot be 3D modeled with a 1D
 1870 velocity model.

8.2. Mantle convection 1871

1872 It is obvious that convection occurs in the mantle, not
 1873 only from modeling, but also from the kinematics of plate
 1874 boundaries, where mantle upraises along ridges and
 1875 lithosphere sinks along subduction zones. It is also evident
 1876 that oceanic lithosphere circulates in the mantle much
 1877 more easily than the continental lithosphere, since only
 1878 relatively young (180–0 Ma) oceans cover the Earth's
 1879 surface, comparing to the much older cratons (> 3000 Ma),
 1880 being the thick continental lithosphere buoyant over the
 1881 mantle. Convection is required to cool the Earth. But
 1882 convection models are necessarily oversimplified and
 1883 possibly overvaluated. The mantle is considered compo-
 1884 sitionally quite homogeneous, but is not, having both
 1885 vertical and lateral significant heterogeneities. The whole
 1886 Earth is intensely stratified both in density and chemistry
 1887 from the topmost atmosphere down to the core. The
 1888 supposed convection cells should be made of an uprising
 1889 warmer buoyant mantle, laterally accompanied by down-
 1890 welling cooler currents. In the view of convection mode-
 1891 lers, the surface expression of cells should be the plates.
 1892 But the Atlantic, E-Africa and Indian rifts have no
 1893 intervening subductions; there are also several cases of
 1894 paired subduction zones without rifts in between: this
 1895 shows the inapplicability of the convection cells to the
 1896 simple superficial plate tectonics kinematics.

1897 In most of the convection models, uprising and down-
 1898 welling mantle currents are stationary, but we know that all
 1899 plate margins rather migrate. Convection styles frequently
 1900 generate polygonal shapes for cells, but plate margins can
 1901 be very linear e.g., the Atlantic ridge, in contrast with the
 1902 typical mushroom shape of mantle plumes.

1903 The fastest W-ward moving plate relative to the
 1904 mantle (the Pacific plate) has the lowest asthenosphere
 1905 viscosity value (Pollitz et al., 1998), and it is the most
 1906 decoupled plate, but mantle convection should rather
 1907 predict that faster moving plates are more coupled
 1908 (higher viscosity) with the mantle.

1909 The Hawaii hotspot volcanic chain indicates that the
 1910 underlying mantle is moving E–SE-ward. Beneath the
 1911 East Pacific Rise, an eastward migrating mantle has
 1912 been modeled by Doglioni et al. (2003) and Hammond
 1913 and Toomey (2003). An eastward migrating mantle has
 1914 been suggested also beneath the Nazca plate by Russo
 1915 and Silver (1994) through shear wave splitting analysis.
 1916 An eastward relative mantle flow beneath the South
 1917 America plate is imposed by the hotspot reference frame
 1918 (Van Hunen et al., 2002). A relatively moving eastward
 1919 mantle flow has been proposed also beneath North
 1920 America (Silver and Holt, 2002) and beneath the
 1921 Caribbean plate (Negredo et al., 2004). Beneath the

1922 Tyrrhenian Sea a similar west to east flow of the mantle
 1923 can be inferred from mantle anisotropy (Margheriti
 1924 et al., 2003). A global reconstruction of the anisotropy in
 1925 the asthenosphere (Debayle et al., 2005) fits quite well
 1926 the sinusoidal flow of plate motions (e.g., Doglioni
 1927 et al., 1999a), apart along subduction zones where the
 1928 shear wave splitting anisotropy shows orthogonal trend
 1929 compatible with the re-orientation of a flow encroaching
 1930 an obstacle.

1931 8.3. Earth's rotation

1932 The lithosphere is decoupled relative to the mantle as
 1933 indicated for example by the hotspots tracks. The
 1934 anisotropy detected by shear wave splitting supports a
 1935 shear zone active in the asthenosphere (Gung et al., 2003).
 1936 Sheared asthenospheric xenoliths confirm decoupling at
 1937 that depth (Kennedy et al., 2002), and the migration of
 1938 plate boundaries in general (Garfunkel et al., 1986;
 1939 Doglioni et al., 2003). But what is forcing the lithosphere
 1940 relative to the mantle? The decoupling is polarized toward
 1941 the west (Rittmann, 1942; Le Pichon, 1968; Bostrom,
 1942 1971; Wang, 1975), although along a sinusoidal flow
 1943 (Doglioni et al., 1999a; Crespi et al., 2007).

1944 Scoppola et al. (2006) recently proposed a combined
 1945 model where the net westward rotation of the lithosphere
 1946 relative to the underlying mantle is a combined effect of
 1947 three processes: 1) Tidal torques act on the lithosphere
 1948 generating a westerly directed torque decelerating the
 1949 Earth's spin; 2) The downwelling of the denser material
 1950 toward the bottom of the mantle and in the core decreasing
 1951 the moment of inertia and speeding up the Earth's
 1952 rotation, only partly counterbalancing the tidal drag; 3)
 1953 The development of thin (3–30 km) layers of very low
 1954 viscosity hydrate melt rich channels in the asthenosphere.
 1955 Scoppola et al. (2006) suggested that shear heating and the
 1956 mechanical fatigue self-perpetuate one or more channels
 1957 of this kind which provide the necessary decoupling zone
 1958 of the lithosphere. This can account for the geological and
 1959 geophysical asymmetry characterizing W-directed vs. E-
 1960 or NE-directed subduction zones and related orogens
 1961 (Marotta and Mongelli, 1998; Doglioni et al., 1999a).
 1962 The fastest westerly moving plate (Pacific) is the slowest
 1963 toward the east possibly due to the more effective
 1964 decoupling in the asthenosphere generated by the Earth's
 1965 rotation.

1966 9. Horizontal vs. vertical movements at 1967 subduction zones

1968 The comparison between horizontal speed of plates
 1969 and their vertical rate at plate boundaries could provide

some insight on plate dynamics. Slab pull is widely
 considered the engine of plate motions (e.g., Anderson,
 2001; Conrad and Lithgow-Bertelloni, 2003; Sabadini
 and Vermeersen, 2004). Most numerical models for
 vertical motions in subduction zones use this assumption,
 although the excess mass of subducted slabs predicted by
 slab pull models is greater than that predicted by geoid
 models (Chase, 1979). Such models might be able to
 reproduce surface topography and subsidence rates of
 trenches (e.g., Zhong and Gurnis, 1992; Giunchi et al.,
 1996; Sabadini and Vermeersen, 2004) and suggest that
 topography could be a dynamic feature depending on the
 balance between tectonic and buoyancy forces (Melosh
 and Raefsky, 1980; Wdowinski, 1992). However, a
 sensitivity analysis of the effects of slab buoyancy
 showed that typical trench bathymetries are obtained
 with both positive and negative density anomalies of the
 slab (Hassani et al., 1997). According to this modeling
 slab buoyancy controls overriding plate topography, but
 overriding plate topography is dramatically influenced by
 parameters not included in calculations, such as the
 accretional (Karig and Sharman, 1975) or erosional (von
 Huene and Lallemand, 1990) nature of the subduction, the
 amount of shortening and the depth of the decollement
 (Woodward et al., 1989), the deformation partitioning
 between brittle and ductile levels and erosion (Willett and
 Brandon, 2002).

The present (Fig. 27) and past motions along
 subduction zones, as in any other plate boundary (Cuffaro
 et al., 2006), have the horizontal component in average 10
 to 100 times faster (10–100 mm/yr) than the vertical
 component (0.01–1 mm/yr; Fig. 28).

Vertical movements along subduction zones such as
 uplift in the overriding plate and subsidence in the
 subducting plate accompany respectively the growth of an
 orogen and the deepening of a trench or foreland basin.
 Bernet et al. (2001) used apatite fission-track grain-age
 distributions for detrital zircons to infer a steady-state
 exhumation in the Alps at rates of 0.4–0.7 mm/yr since at
 least 15 Ma. Subsidence rates in the alpine foredeep are in
 the order of 0.1–0.3 mm/yr (Doglioni, 1994). Rates
 along the Andean subduction zone are of the order of 1–
 4 mm/yr for uplift and less than 0.5 mm/yr for subsidence.
 Fission-track analysis in the Peruvian Andes suggests
 1.1 mm/yr uplift (Montario, 2001). Convergence rates
 along the same subduction zone are in the order of 30–
 100 mm/yr.

In Alaska, exhumation rates of about 3 mm/yr have
 been suggested (Spotila et al., 2004). Faster (5–10 mm/
 yr) uplift rates have been computed in Taiwan and Papua
 New Guinea (Liu, 1982; Dadson et al., 2003; Baldwin
 et al., 2004).

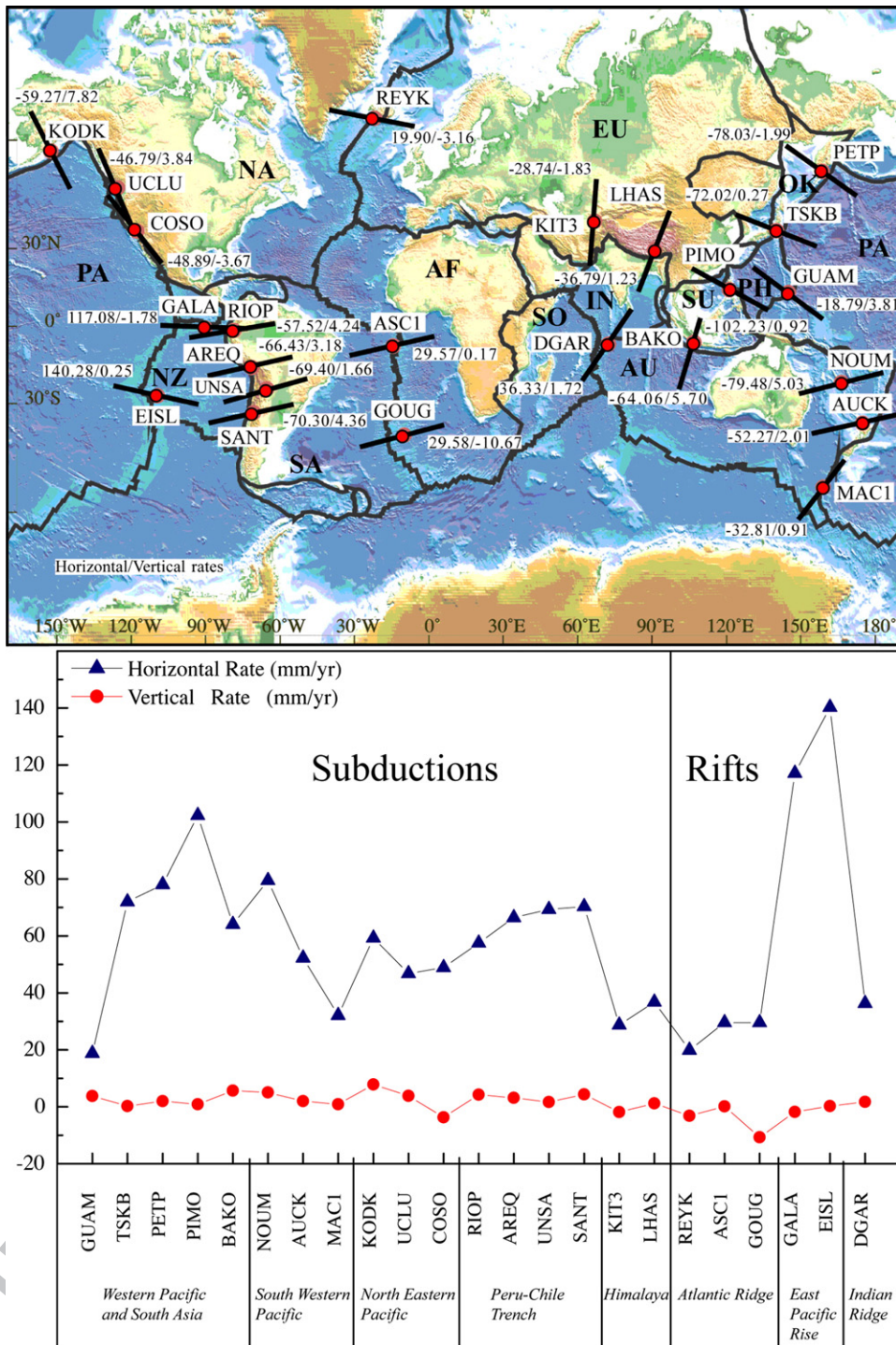


Fig. 27. Comparisons between relative horizontal and vertical motions of selected GPS stations. The oriented segments in the upper panel show relative motion directions. Units are in mm/yr, and show horizontal and vertical velocities respectively. The dot indicates the location of the vertical motion on the plate boundary. About horizontal velocities, negative signs show contraction and positive signs show extension. About vertical velocities, negative signs show subsidence and positive signs show uplift. Site localities are from Heflin et al. (2005). PA, Pacific plate; PH, Philippine plate; AU, Australia plate; IN, Indian plate; SO, Somalia plate; EU, Eurasia plate; SU, Sunda plate; OK, Okhotsk plate; NZ, Nazca plate; NA, North America plate; SA, South America plate; AF, Africa–Nubia plate (after Cuffaro et al., 2006).

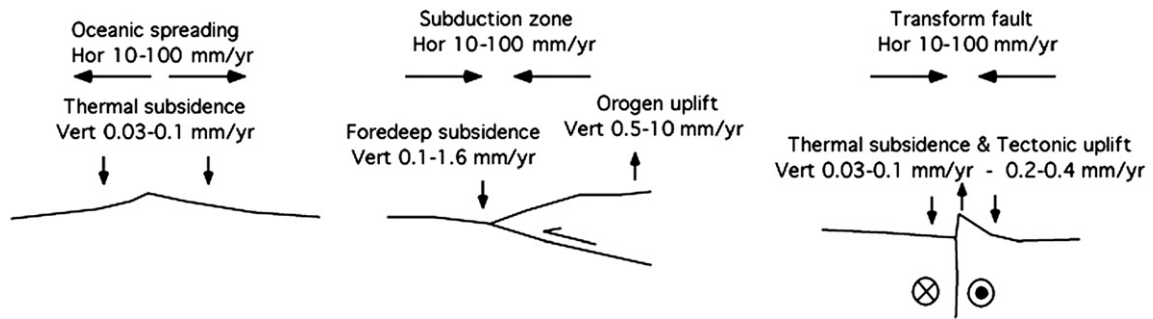


Fig. 28. Present and past horizontal relative plate motions are about 10–100 times faster with respect to vertical movements in all geodynamic settings.

2022 Foredeeps and trenches during the last 100 Ma have
 2023 worldwide subsidence rates spanning on average from
 2024 0.1 to 1.6 mm/yr (Doglioni, 1994), with the fastest rates
 2025 located along the west-directed subduction zones. Along
 2026 the Marianas subduction zone, where the slab pull is
 2027 theoretically the highest on Earth, the Pacific plate
 2028 moves WNW-ward faster than 100 mm/yr, whereas the
 2029 subsidence in the trench is in the order of few mm/yr
 2030 maximum.

2031 The slow uplift of an orogen is partitioned through-
 2032 out the belt, while the two convergent plates move 10–
 2033 100 times faster. Plate boundaries can in fact be several
 2034 hundreds km wide (e.g., Gordon, 2000). Moreover, the
 2035 subduction rate can be even smaller than the conver-
 2036 gence rate (Doglioni et al., 2006a).

2037 If plate velocity is controlled by the plate boundary
 2038 itself (i.e., slab pull or trench suction), how is it possible
 2039 for the fastest down going plate to have such relatively
 2040 smaller uplift in the belt and smaller subsidence rate in
 2041 the trench, or to have a plate moving faster than the
 2042 energetic source? This would rather support a passive
 2043 role of plate boundaries with respect to far field forces
 2044 determining the velocity of plates. The faster horizontal
 2045 velocity of the lithosphere with respect to the upward or
 2046 downward velocities at plate boundaries supports
 2047 dominating tangential forces acting on plates. These
 2048 forces acting on the lithosphere can be subdivided in
 2049 coupled and uncoupled, as a function of the shear at the
 2050 lithosphere base. The higher the asthenosphere viscos-
 2051 ity, the more significant should be the coupled forces,
 2052 i.e., the mantle drag and the trench suction. The lower
 2053 the asthenosphere viscosity, the more the effects of
 2054 uncoupled forces might result determinant, i.e., the ridge
 2055 push, the slab pull and the tidal drag. Although a
 2056 combination of all forces acting on the lithosphere is
 2057 likely, the decoupling between lithosphere and mantle
 2058 suggests that a torque acts on the lithosphere indepen-
 2059 dently of the mantle drag. The Earth's rotation might

rather have a primary role if the viscosity of the upper
 asthenosphere is sufficiently low.

Slab pull and ridge push are candidates for generating a
 torque on the lithosphere, but few counterarguments are
 presented. For example, no significant correlation exists
 between trench percentage and plate velocity (Fig. 26, A,
 B). Moreover, unlike these boundary forces, the advan-
 tage of the tidal drag is to be a volume force, acting
 simultaneously on the whole of the plate, and being the
 decoupling at the lithosphere base controlled by lateral
 variations in viscosity of the low-velocity layer.

10. Upper mantle circulation

Subduction zones represent part of the mantle con-
 vection. Hamilton (2003) proposes a restricted upper
 mantle circulation driven from the cooler plates. Regard-
 less the slabs penetrate or not into the lower mantle,
 we observe that W-directed subductions enter in the
 mantle on average at least 2–3 times faster than the
 opposite E–NE-directed subduction zones. There are
 two reasons for this kinematic asymmetry: 1) most of
 the W-directed subductions have the subduction rate S
 increased by the hinge subduction retreat; 2) they are
 steeper and have therefore a higher $S_v = S \sin \alpha$.

Therefore W-directed subduction zones contribute
 more efficiently to mantle recycling; for example along
 the northern Tonga subduction zone the subduction rate
 can be as high as 240 mm/yr (Bevis et al., 1995),
 whereas the central Andes subduction rate can be of
 about 31 mm/yr (Fig. 10).

Along oceanic ridges, melting produces a residual
 depleted asthenosphere that is also more viscous than
 the undepleted one. Braun et al. (2000) have shown that
 water extraction during melting leads to higher viscosity
 in the residual mantle up to 2 orders of magnitude. The
 mantle, once depleted along the transit beneath the ridge
 should be cooler, less dense and more viscous. The most

2096 shallow, depleted asthenosphere will eventually become
 2097 lithospheric mantle with the progressive cooling,
 2098 shifting away from the ridge. In this view, moving
 2099 horizontally within the asthenosphere, the viscosity
 2100 distribution could be due more to lateral compositional
 2101 variations rather than temperature gradients.

2102 Since the Pacific plate has the lowest viscosity of the
 2103 underlying asthenosphere and it is the fastest plate, there
 2104 seems to be a positive correlation between asthenospheric
 2105 viscosity, lithospheric decoupling and plate velocities.

2106 Plate variable velocities seem controlled by the
 2107 lithosphere–asthenospheric decoupling, which is a func-
 2108 tion of the asthenospheric viscosity. Subduction zones and
 2109 oceanic ridges contribute to upper mantle convection. The
 2110 W-directed subductions clearly reach the lower boundary
 2111 of the upper mantle. The E- or NE-directed subduction
 2112 zones are rather shallower and less inclined. Most of their
 2113 seismicity terminates into the asthenosphere, apart fewer
 2114 deep earthquakes at the upper–lower mantle transition.
 2115 These earthquakes are considered either related to phase
 2116 transition, or to remnants of cold detached slabs. An
 2117 alternative interpretation would be that they represent the
 2118 faster shear and related strain rate between upper and
 2119 lower mantle, triggered by the Bernoulli principle, for the
 2120 narrower upper mantle section beneath the E–NE-
 2121 directed subduction zones.

2122 Most of the Earth's subduction-related magmatism is
 2123 sourced from a top slab depth range of 65–130 km
 2124 (England et al., 2004). As shown in the previous chapters,
 2125 the Andean subduction rate should be slower than the
 2126 convergence rate. Moreover, the slab along some
 2127 segments of the Andes becomes almost flat, indicating
 2128 the insertion of the slab into the asthenosphere. At that
 2129 depth, the slab shares the pressure and temperature that
 2130 allow partial melting of the asthenosphere. Therefore the
 2131 oceanic lithosphere might re-enter the source mantle,

2132 becoming ductile, and gradually melting, refertilizing the
 2133 mantle that generated it (Fig. 29). Note that in the mantle
 2134 reference frame, assuming shallow hotspots and the faster
 2135 W-ward drift of the lithosphere, the Nazca plate is coming
 2136 out of the mantle, but subduction occurs because the
 2137 South America plate moves westward faster than Nazca
 2138 (Fig. 21).

2139 The W-directed subduction zones are penetrating
 2140 and geochemically modifying the lower upper mantle
 2141 (Fig. 29), whereas the E- or NE-directed subduction
 2142 zones are more suitable for regenerating the shallow
 2143 upper mantle that is the most favorable candidate for
 2144 sourcing MORB along mid-oceanic ridges (e.g., Bonatti
 2145 et al., 2003).

2146 For the aforementioned kinematic constraints, the
 2147 rate of subduction is expected to be generally 2–3 times
 2148 higher along W-directed subduction zones than along
 2149 the opposite settings (Fig. 30). The different kinematics
 2150 also generate different geometries and depth of the
 2151 1300 °C isotherm assumed to mark the lithosphere–
 2152 asthenosphere boundary. Therefore, the asthenosphere
 2153 is much shallower along W-directed subduction zones
 2154 than along the opposite slabs (Fig. 31). Moreover, in the
 2155 hangingwall of the slab, the asthenospheric section cross
 2156 cut by the fluids released by the slab at about 100–
 2157 130 km (Syracuse and Abers, 2006) to generate the
 2158 magmatic arc, is thicker along W-directed subduction
 2159 zones than again along the opposite subduction zones
 2160 (AW>AE, Fig. 30), possibly providing geochemical
 2161 differences among the two subduction end members.

2162 11. Dynamic speculations

2163 As discussed earlier, orogens and related features
 2164 show marked asymmetries (Fig. 32). The topography
 2165 and the foreland monocline are lower and steeper for the

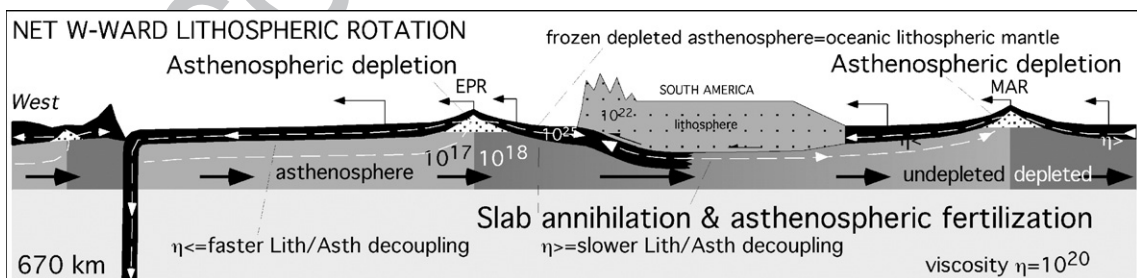


Fig. 29. Model for the upper mantle cycle. Lower the asthenospheric viscosity, faster the W-ward displacement of the overlying plate. The asthenospheric depletion at oceanic ridges makes the layer more viscous and decreases the lithosphere/asthenospheric decoupling, and the plate to the east is then slower. The oceanic lithosphere subducting E-ward enters the asthenosphere where it is molten again to refertilize the asthenosphere. W-directed subductions provide deeper circulation. Note that the E-directed subduction (the Andes) tends to escape out of the mantle, but it is overridden by the upper plate (South America, after Doglioni et al., 2006a).

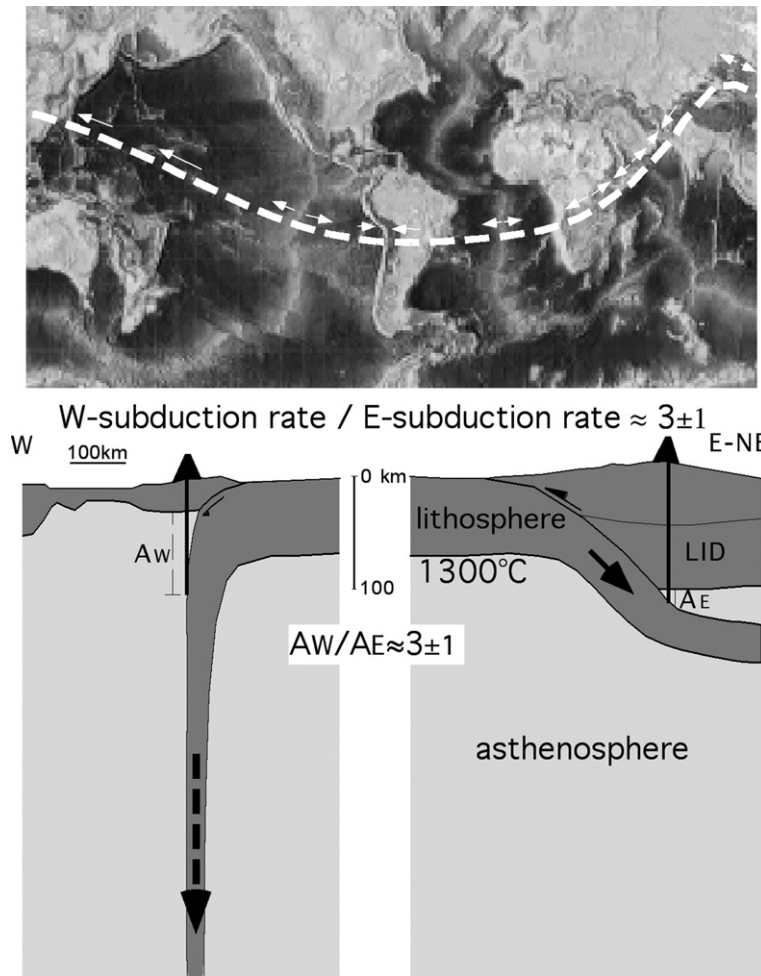


Fig. 30. The main differences between orogens are a function of the subduction polarity along the tectonic mainstream (Doglioni, 1993; Crespi et al., 2007). The volumes recycled along W-directed subduction zones is about 2–3 times higher than along the opposite settings due to the aforementioned kinematic constraints. Moreover, the asthenospheric wedge above slabs is thicker along W-directed subduction zones (AW) with respect to the E–NE-directed subductions (AE).

2166 W-directed subduction zones (Fig. 33) and the area
 2167 above sea level is remarkably higher for the opposite E-
 2168 to NNE-directed subduction zones (Fig. 34). The
 2169 aforementioned kinematic and geometric observations
 2170 allow us to make a few dynamic considerations. All
 2171 types of tectonic-geodynamic settings at plate bound-
 2172 aries show 10–100 times faster horizontal velocity with
 2173 respect to the vertical motion (Cuffaro et al., 2006). Is
 2174 this a trivial observation, or is it rather telling us some-
 2175 thing fundamental on the dynamics of plate tectonics?
 2176 Does slower vertical motion imply strain partitioning
 2177 and passive role of plate boundaries, as suggested, for
 2178 example, by the gradual decrease in shortening from the
 2179 subduction hinge to the fixed upper plate (Fig. 10)?
 2180 The mechanisms driving plate motion, e.g., plates
 2181 driven by ‘the boundary forces’, slab pull and ridge push

(Forsyth and Uyeda, 1975), vs. plates actively dragged by
 the asthenosphere flow (e.g., Bokelmann, 2002) seems
 not relevant to the preceding discussion of horizontal vs.
 vertical motion rates, because the rates themselves do not
 provide evidence for or against any particular mechanism.
 Both ‘active plates and passive asthenosphere’ and ‘an
 active asthenospheric flow dragging passive plates’ may
 be consistent with faster horizontal motions. The inertia of
 plates is negligible, and each plate must be in dynamic
 equilibrium, so the sum of the torques acting on a plate
 must be zero (Forsyth and Uyeda, 1975).

The main forces acting on the lithosphere can be
 subdivided into coupled and uncoupled forces (Fig. 35).
 Mantle drag and trench suction (e.g., Bercovici, 1998;
 Conrad and Lithgow-Bertelloni, 2003) need high
 coupling (higher viscosity) between the lithosphere

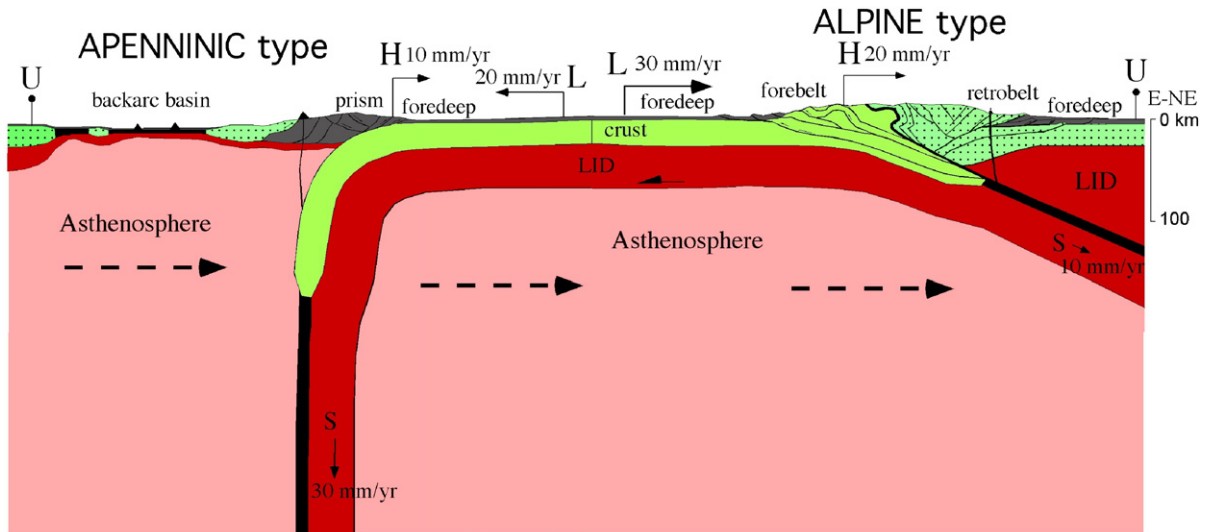


Fig. 31. Schematic sections showing how in an Alpine setting, the subduction rate is decreased by the migration of the hinge H toward the upper plate U , and the orogen in the final collisional stage is composed both by the upper and lower plate L rocks. In the opposed Apenninic setting, the subduction rate is rather increased by the migration of H away from U , and the accretionary prism is made of shallow rocks of the lower plate. Note also the shallower asthenosphere in the hangingwall, which is typical of W-directed subduction zones.

2198 and the asthenosphere to be more effective. The ridge
 2199 push, the slab pull and the tidal drag should rather need
 2200 low coupling (lower viscosity) to be efficient (Fig. 35).
 2201 The down-dip extension along E–NE-directed slab
 2202 can be generated either by the slab pull from below, or
 2203 by the tidal drag acting on the surface plate.
 2204 Among the uncoupled forces, the ridge push is at
 2205 least one order of magnitude lower than the slab pull
 2206 (e.g., Ranalli, 1995). The dissipation of energy by tidal
 2207 friction is even larger (1.6×10^{19} J/yr) than the energy

released by tectonic activity (1.3×10^{19} J/yr, Denis et al., 2208
 2002). The tidal drag can effectively move plates only if 2209
 very low viscosity intra-asthenospheric layers occur 2210
 (Scoppola et al., 2006). In this case, tidal forces, 2211
 combined with mantle convection, could trigger plate 2212
 tectonics. A very low velocity layer at the very top of the 2213
 asthenosphere (100–150 km) has been recently demon- 2214
 strated (Panza et al., 2007). 2215
 Therefore the viscosity of the upper layers of the 2216
 asthenosphere plays a crucial role in controlling plate 2217

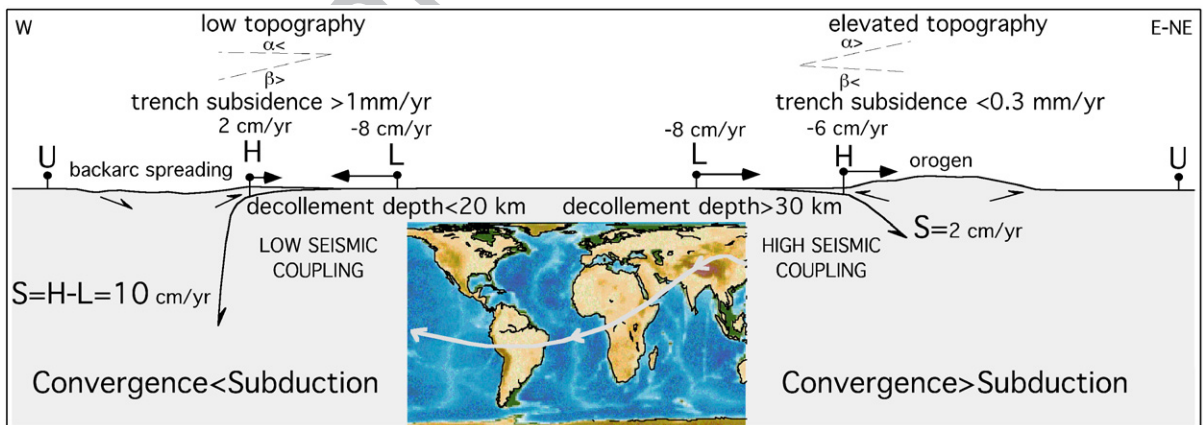


Fig. 32. Assuming fixed the upper plate U , along west-directed subduction zones the subduction hinge H frequently diverges relative to U , whereas it converges along the opposite subduction zones. L , lower plate. Note that the subduction S is larger than the convergence along W-directed slabs, whereas S is smaller in the opposite case. The two end-members of hinge behavior are respectively accompanied in average by low and high topography, steep and shallow foreland monocline, fast and slower subsidence rates in the trench or foreland basin, single vs. double verging orogens, etc., highlighting a worldwide subduction asymmetry along the flow lines of plate motions indicated in the insert (after Lenci and Doglioni, in press).

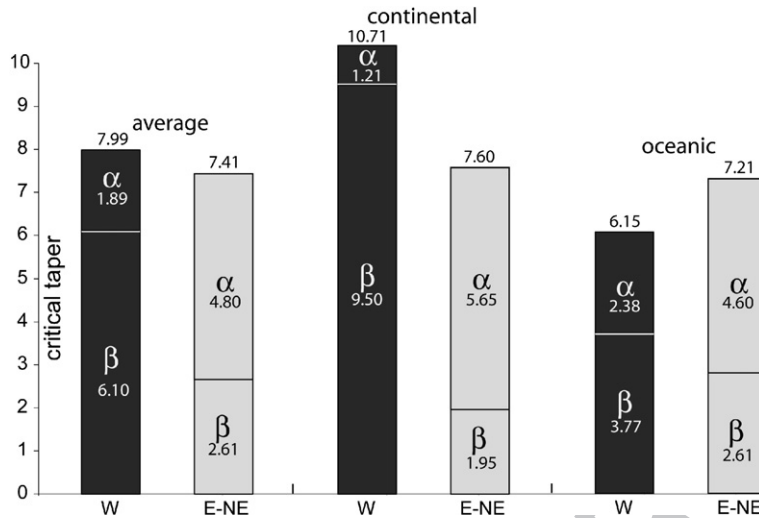


Fig. 33. Average values of the topographic envelope (α), dip of the foreland monocline (β), and critical taper ($= \alpha + \beta$) for the two classes of subduction zones, i.e., W-directed and E- or NE-directed. Note that the “western” classes show lower values α and steeper values of β .

2218 tectonics. Moving from the highest viscosity (10^{19-20} Pa
 2219 s) to the lowest (10^{12-14} Pa s), the most likely mechanisms
 2220 able to move plates are in order: the mantle drag, the
 2221 trench suction, the slab pull, the ridge push and the tidal
 2222 drag.

2223 Relatively small forces can move a floating plate fast
 2224 horizontally, because no work has to be done against
 2225 gravity, whereas non-isostatic vertical motions require
 2226 work to be done against gravity. However this can be
 2227 true when at the base of the lithosphere there is a very
 2228 low viscosity in the decoupling layer, i.e., the weaker

low velocity zone in the upper asthenosphere. Increasing
 2229 the asthenosphere viscosity, larger forces are
 2230 required to decouple the lithosphere. On the other
 2231 hand, if the lithosphere is not moved by lateral forces
 2232 such as the slab pull, but rather passively dragged by the
 2233 mantle, the higher viscosity will enable a better
 2234 coupling. Then, what is generating the decoupling of
 2235 the lithosphere (Fig. 36)? Are there external tangential
 2236 forces acting on the lithosphere?
 2237

There are lines of evidence that the lithosphere is partly
 2238 decoupled from the mantle as suggested for example by
 2239

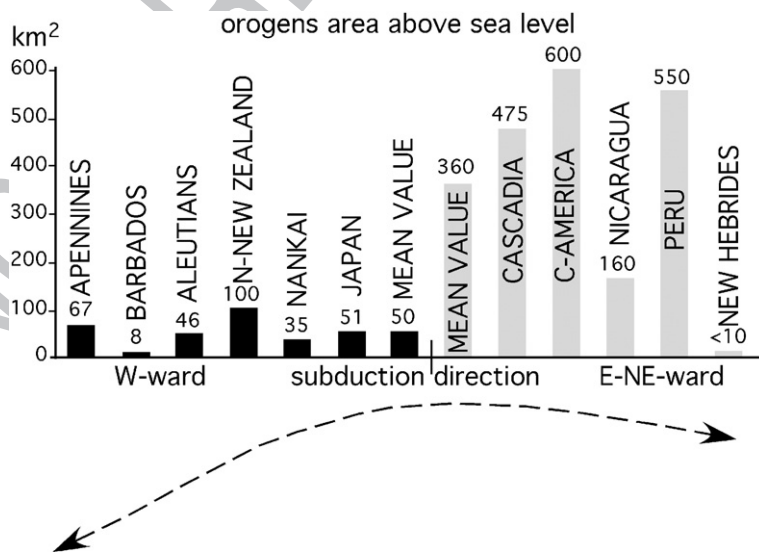


Fig. 34. Average values of the area above sea-level of the main subduction zones, showing how orogens above E- or NE-directed subduction zones are about 6–8 times larger than the W-directed subduction zones-related accretionary prisms. After Lenci and Doglioni (in press).

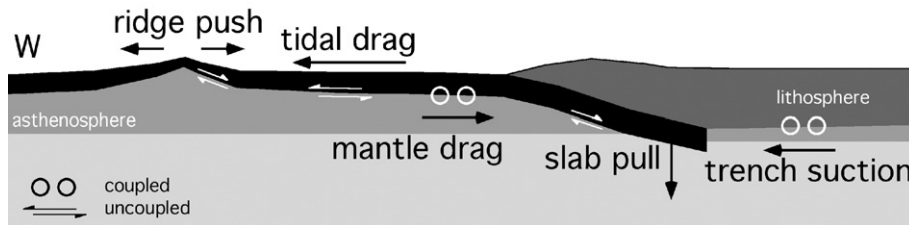


Fig. 35. Main forces acting on the lithosphere. Mantle drag and trench suction need high coupling (higher viscosity) between lithosphere and asthenosphere to be more effective. Ridge push, slab pull and tidal drag should rather need low coupling (lower viscosity) to be efficient. Since the lithosphere is decoupled with respect to the asthenosphere, possibly more than one force is actively forcing plate motions. Circles indicate coupled forces, white half arrows show the uncoupled forces. See text.

2240 the hotspot tracks and by the asthenosphere anisotropy
 2241 (e.g., Silver and Holt, 2002). A super fast net rotation of
 2242 the lithosphere relative to the mantle has been proposed by
 2243 Crespi et al. (2007), assuming a shallow origin of the
 2244 Pacific plumes used as reference frame (Fig. 36). If so,
 2245 where does the energy providing this torque come from?
 2246 What is moving plates relative to the mantle? The net
 2247 westerly directed rotation of the lithosphere has been
 2248 attributed either to lateral variations in asthenosphere
 2249 viscosity (Ricard et al., 1991), or to the Earth's rotation
 2250 (Scoppola et al., 2006). The westward drift (Le Pichon,
 2251 1968) is consistent with the asymmetry of subduction and
 2252 rift zones worldwide along an undulated plate motions
 2253 flow (Doglioni et al., 2006a). A number of authors (e.g.,
 2254 Dickinson, 1978; Uyeda and Kanamori, 1979; Doglioni,

1990) proposed a shear at the lithosphere base driven by
 mantle drag or relative mantle flow.

Plate motions are driven either by coupled or
 uncoupled forces. A comparison between horizontal
 and vertical motions does not allow to state which plate
 tectonics driving mechanism prevails. However, the
 steady 1 or 2 order of magnitude faster horizontal over
 vertical motion at plate boundaries points to a stronger
 tangential component in plate tectonics.

However, if ridges and subduction zones trigger con-
 vection, but are nevertheless still passive features, what
 does move the plates? Whatever the mantle convection
 works, it cannot explain the lithosphere decoupling alone.
 Therefore the uncoupled forces appear to dominate, but
 we cannot exclude that possibly more than one force, both

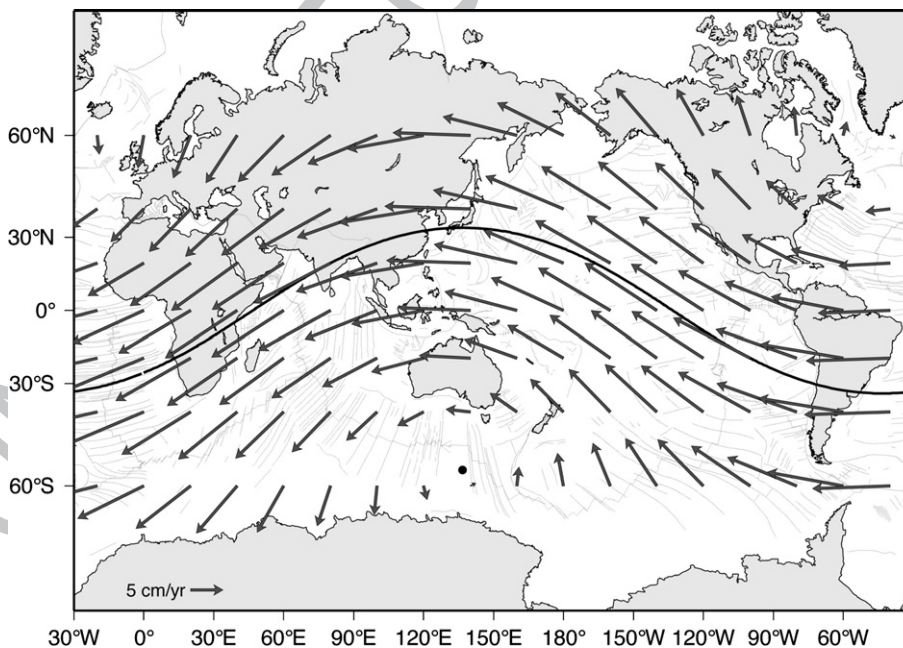


Fig. 36. Global lithospheric net rotation relative to the mantle assuming a mid-asthenospheric source of the Pacific plumes, after Crespi et al., 2007. Subduction asymmetries should not be considered as E–W related, but following or opposing the absolute tectonic mainstream.

2270 coupled and uncoupled, energize plate motions. Earth's
2271 rotation cannot work alone because mantle convection is
2272 required to maintain the mantle fertile and the low
2273 viscosity in the asthenosphere. Moreover density gradi-
2274 ents (e.g., slab pull) allow differential sinking of plates at
2275 convergent margins.

2276 Are plates dragged horizontally by mantle convection
2277 (e.g., [Bercovici, 1998](#))? Are they dragged and sheared at
2278 the base by a faster moving mantle ([Bokelmann, 2002](#))?
2279 Are they rather pulled by slab pull forces ([Forsyth and](#)
2280 [Uyeda, 1975](#); [Anderson, 2001](#))? Could they be driven by
2281 Earth's rotation and tidal drag ([Scoppola et al., 2006](#))?
2282 We do not have a final word, but further studies on the
2283 composition, water content and viscosity of the astheno-
2284 sphere might significantly contribute to answer these
2285 basic questions.

2286 12. Discussion and conclusions

2287 A subduction zone should be analyzed considering at
2288 least three points, i.e., two located in stable areas of both
2289 the upper and the lower plate, and one located at the plate
2290 boundary, along the subduction hinge. Two main types
2291 of subduction zones can be distinguished, i.e., 1) those
2292 where the subduction hinge migrates away from the
2293 upper plate, and 2) those in which the subduction hinge
2294 migrates toward the upper plate ([Fig. 31](#)). This
2295 distinction recalls what [Laubscher \(1988\)](#) defined as
2296 pull arc and push arc respectively. Apart few excep-
2297 tions, this distinction seems to apply particularly for W-
2298 directed and E- or NE-directed subduction zones respec-
2299 tively (e.g., Apennines, Marianas, Tonga and Car-
2300 pathians for the W-directed, Andes, Alps, Dinarides
2301 and Hellenides for the opposite case). In either W- and
2302 E-NE-directed subduction zones, the hinge migrates
2303 eastward or northeastward relative to the upper plate
2304 ([Table 2](#)).

2305 In the literature it is often referred to retreating or
2306 advancing slab. However this terminology might
2307 generate confusion because a retreating hinge or slab
2308 retreat in the upper plate reference frame might become
2309 a fixed hinge in the mantle reference frame (e.g.,
2310 Barbados). On the other hand, an advancing hinge
2311 relative to the upper plate is a retreating hinge relative to
2312 the mantle (e.g., Andes).

2313 The rate of subduction is generally larger than the
2314 convergence rate along W-directed subduction zones,
2315 whereas it is smaller along E- or NE-directed subduction
2316 zones. Therefore the subduction rate is decreased or
2317 increased as a function of whether the subduction hinge
2318 converges or diverges relative to the upper plate. Along
2319 W-directed slabs, the subduction rate is the convergence

2320 rate plus the slab retreat rate, being the latter close to the
2321 backarc extension rate, if no accretion occurs in the
2322 upper plate, which is a rare case.

2323 As a result, in eastern Pacific subduction zones, and
2324 in the E- or NE-directed subduction zones in general
2325 such as the Alps or Himalayas, the subduction rate
2326 should be lower than the convergence rate. On the other
2327 hand, along the western Pacific subduction zones, and
2328 the W-directed subduction zones in general such as the
2329 Apennines, the subduction rate has to be faster than the
2330 convergence rate since it is incremented by the hinge
2331 retreat.

2332 In this interpretation, the far field velocities of the
2333 upper and lower plates control the subduction rate, and
2334 the subduction is a passive process. In fact, the rates of
2335 subduction do not determine plate velocities, but are
2336 rather a consequence of them.

2337 The convergence/shortening ratio along W-directed
2338 subduction zones is instead generally lower than 1.
2339 Along E- or NE-directed slabs, the shortening in the
2340 upper plate decreases the subduction rate, and typically
2341 no backarc basin forms. The convergence/shortening
2342 ratio in this type of orogens is higher than 1 and is
2343 inversely proportional to the strength of the upper plate
2344 and is directly proportional to the coupling between
2345 upper and lower plates. Higher the strength and lower
2346 the coupling, smaller the shortening, and faster is the
2347 subduction rate.

2348 Along both W- and E- NE-directed subduction zones,
2349 the hinge migrates eastward relative to the upper plate,
2350 apart few exceptions like Japan. Therefore, most fre-
2351 quently along the W-directed subduction zones the hinge
2352 migrates away with respect to the upper plate, whereas the
2353 hinge migrates toward the upper plate along E- NE-
2354 directed subduction zones. In this interpretation, the far
2355 field velocities of the upper and lower plates control the
2356 subduction rate, and the subduction is a passive process.

2357 Along E- or NE-directed subduction zones, the
2358 convergence rate is partitioned between upper plate
2359 shortening and subduction. The shortening is mainly
2360 concentrated in the upper plate until it is continental and
2361 less viscous than the lower oceanic plate. At the
2362 collisional stage even the lower plate is extensively
2363 shortened. However, the observation that, say 80 mm/yr
2364 convergence are transferred to 60 mm/yr shortening in
2365 the upper plate and 20 mm/yr only are reserved to
2366 subduction, point out a fundamental result, i.e., the lower
2367 values of shortening and subduction rates with respect to
2368 the convergence rate are hierarchically a consequence
2369 of the far field plate motion. This means that the
2370 driving primary source of energy for determining the
2371 convergence is neither with the slab, nor in the related

t2.1 Table 2

Few main geometric, kinematic and dynamic differences between orogens and subduction zones following or opposing the tectonic mainstream.
 Subduction zones parallel to the mainstream (e.g., Pyrenees) have similar characters as the subduction zones following it

t2.3		Subductions opposing the tectonic mainstream (W-directed)	Subductions following the tectonic mainstream (E–NE–NNE-directed)
t2.4	Elevation average	–1250 m	+1200 m
t2.5	Foreland monocline average dip	6.1°	2.6°
t2.6	Trench or foredeep subsidence rate	>1 mm/yr	<0.3 mm/yr
t2.7	Prism envelope average dip	1.9°	4.8°
t2.8	Orogen-prism vergence	Single verging	Mostly Double verging
t2.9	Type of prism rocks	Mostly sedimentary cover & volcanics	Largely basement, sedimentary cover & volcanics
t2.10	Prism decollement depth	0–10 km; (rarely up to 20 km) offscraping the top of the lower plate	>30 km; Oceanic subduction, affecting mostly the whole section of the upper plate; continental subduction affecting also the lower plate
t2.11	Seismic coupling	Mainly low	Mainly high
t2.12	Moho	Shallow (<30 km) new upper plate Moho	Deep (>40 km) doubled old Mohos
t2.13	Asthenosphere depth	Shallow (<20–50 km) beneath the arc	Deep (>70–100 km) beneath the arc
t2.14	Seismicity	0–670 km; intra-slab mostly down-dip compression and horizontal shear	0–250 km and scattered 630–670 km; intra-slab mostly down-dip extension
t2.15	Slab dip	25°–90°	15°–50°, steeper up to 70° along oblique subductions and thicker upper plate
t2.16	Subduction hinge motion relative to upper plate	Mainly diverging Eastward (except Japan where subduction started to flip)	Mainly converging Eastward or northeastward
t2.17	Subduction hinge motion relative to mantle	Fixed	Westward or southwestward
t2.18	Subduction rate	S=H–L, faster than convergence rate; mainly slab retreating and entering the mantle	S=H–L, slower than convergence rate; slab “escaping” relative to the mantle, overridden by the upper plate
t2.19	Backarc spreading rate	H(>0), — prism accretion, — hinge asthenospheric intrusion	Differential velocity between two hangingwall plates
t2.20	Slab/mantle recycling	About 3 times higher than opposite	About 3 times lower than opposite
t2.21	Subduction mechanism	Slab-mantle wind interaction+far field plate velocities+slab density gradient relative to the country mantle	Far field plate velocities+slab density gradient relative to the country mantle

2372 orogen. A paradigm of plate tectonics is that the negative
 2373 buoyancy of slabs drives plate motions (e.g., [Conrad and](#)
 2374 [Lithgow-Bertelloni, 2003](#)), as suggested by the steeper
 2375 dip of the slab bearing old oceanic crust ([Forsyth and](#)
 2376 [Uyeda, 1975](#)), and the convergence rate at subduction
 2377 zones related to the age of the oceanic crust at the trench
 2378 (e.g., [Carlson et al., 1983](#)). However a number of
 2379 aforementioned counterarguments make the slab pull
 2380 weaker than so far accepted in the literature. For example
 2381 the energy required to pull the plates is far higher than the
 2382 strength that plates can afford under extension. Moreover
 2383 the asymmetry which is evident comparing the western
 2384 and the eastern Pacific subduction zones occurs also in
 2385 the Mediterranean subductions, regardless the age and
 2386 composition of the downgoing lithosphere ([Doglioni](#)
 2387 [et al., 1999a](#)). Moreover, [Lallemant et al. \(2005\)](#) and
 2388 [Cruciani et al. \(2005\)](#) have demonstrated that there is no
 2389 correlation between the slab dip and the age of the
 2390 subducting lithosphere. To this discussion we add here
 2391 the observation that there is no correlation between

convergence rate and age of the oceanic lithosphere at
 the trench ([Fig. 25](#)), suggesting that the negative
 buoyancy cannot be the primary driving force of plate
 tectonics. In the hotspot reference frame, the Africa plate
 moves westward ([Gripp and Gordon, 2002](#)) without any
 slab in its western side. Moreover, it moves opposite to a
 hypothetical Atlantic ridge push. The only slabs attached
 to Africa are in its northern margin, i.e., the Hellenic–
 Cyprus and Apennines subduction zones. Although
 problematic, another small, finger-like, east-dipping slab
 has been supposed beneath the Gibraltar arc ([Gutscher](#)
[et al., 2002](#)). The Hellenic–Cyprus slab is also dipping/
 directed NE-ward, opposite to the direction of motion of
 the Africa plate providing a kinematic evidence of no
 dynamic relationship. The Apennines slab is retreating
 and westward directed. These northern Africa subduc-
 tion zones are a small percentage of the plate boundaries
 surrounding Africa, and they dip in opposite directions
 with respect to the absolute motion of the plate.
 Therefore they cannot be the cause of its motion.

2412 The Apennines–Marianas and the Alps–Andes
2413 (continental and oceanic subduction zones) are repre-
2414 sentative of the two major classes of orogens where the
2415 subduction hinge migrates away from, and toward the
2416 upper plate respectively (Fig. 32). However, it has been
2417 shown that in the Apennines, a number of sub-settings
2418 can be described, and in the southern side of the arc the
2419 hinge migrates toward the upper plate, while in the rest
2420 of the arc the hinge migrates away (Fig. 18).

2421 The orogens of Alpine–Andean type have therefore
2422 slower subduction rates than the Apenninic–Marianas
2423 type when convergence is constant. The double verging
2424 Alpine–Andean type belt is composed mostly by upper
2425 plate rocks during the oceanic subduction, being the lower
2426 plate more extensively involved during the later colli-
2427 sional stage. The single verging Apennines–Marianas
2428 type belt is rather composed primarily by shallow rocks of
2429 the lower plate (Fig. 31). A wide variety of different
2430 geophysical, geological and volcanological signatures
2431 mark the two end members of orogens and subduction
2432 zones (Doglioni et al., 1999a). The two end-members
2433 where the subduction hinge migrates away or toward the
2434 upper plate largely match the two opposite cases of
2435 seismic decoupling or seismic coupling (e.g. Scholz and
2436 Campos, 1995). However, along the Apennines subduc-
2437 tion zone at least five different kinematic settings coexist,
2438 showing how a single subduction can have internal
2439 deviations from the standard model and variable veloc-
2440 ities as a function of the combination V_H and V_L .

2441 Relative to the mantle, the W-directed slab hinges are
2442 almost fixed, whereas they move west or southwest along
2443 E- or NE-directed subduction zones. When describing the
2444 plate motions relative to the mantle, e.g. in the hotspot
2445 reference frame, both Africa and Greece move south-
2446 westward with respect to the mantle (Greece faster). This
2447 implies that the slab is moving in the opposite direction of
2448 the subduction when studied relative to the mantle. The
2449 slab sinks because it is overridden by the faster upper plate
2450 (Fig. 23). This observation indicates that the slab pull
2451 cannot be the only driving force of neither the Hellenic
2452 subduction, nor of E- or NE-directed subduction zones
2453 in general, because it is moving SW-ward or W-ward
2454 relative to the mantle. Along this subduction zone, again,
2455 plate motions are not controlled by subduction rates, but
2456 vice-versa.

2457 Unlike E–NE-directed subduction zones, along W-
2458 directed subduction zones, the slab generally sinks faster
2459 than the convergence rate. However, the lower plate can
2460 converge or diverge from the upper plate. With respect to
2461 the mantle, W-directed slab should in general have a fixed,
2462 or anchored, hinge, whereas the hinge migrates eastward
2463 along the opposite subduction zones. In case the lower

2464 plate diverges faster than the hinge, the subduction rate
2465 is negative, i.e., the lower plate is escaping from the
2466 subduction (Fig. 14, 5W and 6W). This setting might
2467 represent a final evolution of the subduction zone and
2468 could be an alternative cause for the detachment of slab
2469 that is generally inferred as related to the sinking of the
2470 supposed denser lower part (e.g., Wortel and Spakman,
2471 2000). Alternatively, since once penetrated into the
2472 mantle, the slab cannot be re-exhumed, the detachment
2473 of the slab could rather occur because the top part of the
2474 lower plate L is moving away from the deeper (>100 –
2475 150 km?) segment (Fig. 14, 5W and 6W).

2476 W-directed subduction zones bring larger volumes of
2477 lithosphere back into the mantle than the opposite sub-
2478 duction zones.

2479 W-directed subduction zones have the rate of sinking
2480 controlled by the slab–mantle horizontal “easterly”-
2481 directed wind interaction, which mostly determines the
2482 retreat of the subduction hinge, plus the far field velocities
2483 of the plates, and the value of the negative slab buoyancy.

2484 Alternatively, E–NE–NNE-directed subduction
2485 zones have rather rates chiefly determined by the far
2486 field velocity of plates, being the subduction hinge
2487 generally advancing toward the upper plate and
2488 decreasing the subduction rate (Table 2).

2489 The analyzed kinematics frames suggest that sub-
2490 duction zones have rates of sinking controlled by far
2491 field plate velocities, hinge migration direction, and
2492 subduction polarity, claiming for a passive behavior of
2493 the slabs. This is more reasonable if the net “westward”
2494 rotation of the lithosphere is a global phenomenon rather
2495 than the simple average of plate motions (Scoppola
2496 et al., 2006). Tidal drag (Bostrom, 1971; Moore, 1973)
2497 combined with Earth’s rotation, mantle convection, and
2498 an ultra-low viscosity layer in the asthenosphere could
2499 trigger plate motions (Scoppola et al., 2006).

2500 The ridge push, related to the topographic excess,
2501 should be higher along elevated orogens, where on the
2502 contrary, plates converge rather than diverge. Boundary
2503 forces such as slab pull and ridge push could in principle
2504 generate a deceleration moving away from the energy
2505 source, but plates rather show internal homogeneous
2506 velocity (Fig. 34). Mantle convection could satisfy a
2507 steady state speed of the overlying lithosphere, assuming
2508 low or no decoupling at the asthenosphere interface.
2509 However, mantle convection is kinematically problematic
2510 in explaining the migration of plate boundaries and the
2511 occurrence of a decoupling surface at the lithosphere base.
2512 Although a combination of all forces acting on the
2513 lithosphere is likely, the decoupling between lithosphere
2514 and mantle suggests that a torque acts on the lithosphere
2515 independently of the mantle drag. Slab pull and ridge push

2516 are candidates for generating this torque, but, unlike these
 2517 boundary forces, the advantage of the Earth's rotation and
 2518 related tidal drag is to be a volume force, acting simul-
 2519 taneously and tangentially on the whole plates. Tidal drag
 2520 maintains the lithosphere under a permanent high
 2521 frequency vibration, polarized and sheared toward the

“west” (Fig. 37). Earth's rotation and the break exerted by
 the lag of the tidal bulge (Bostrom, 1971) can be efficient
 only if very low viscosity occur at the lithosphere–
 asthenosphere transition (Jordan, 1974), and growing
 evidences are emerging on the presence of an ultra-low
 viscosity layer at the very top of the asthenosphere (e.g.,

2522
 2523
 2524
 2525
 2526
 2527

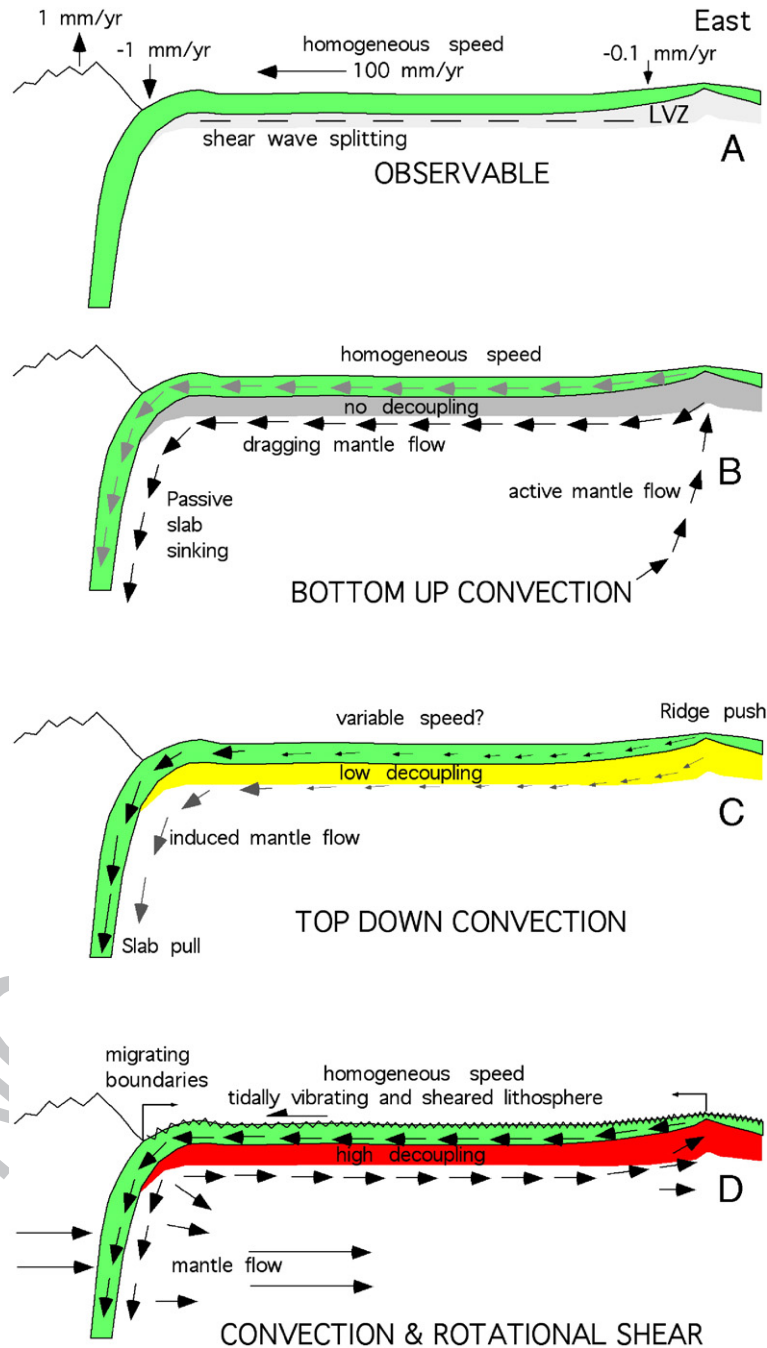


Fig. 37. The surface observables (A) are compared with three models of plate dynamics, where plate motion is induced by classic mantle convection (B), boundary forces (C), or the combination of the aforementioned mechanism plus the rotational drag (D).

2528 Rychert et al., 2005), possibly related also to higher fluids
 2529 concentration in the mantle. Lateral variations in the low-
 2530 velocity layer viscosity could control the different velo-
 2531 city of plates. The Earth's rotation contribution to move
 2532 the lithosphere could account for i) the homogeneous
 2533 internal velocity of each plate, ii) the decoupling
 2534 occurring at the lithosphere base, and iii) the westerly
 2535 polarized migration of the lithosphere and the plate
 2536 boundaries, consistent with the geological asymmetries of
 2537 subduction and rift zones as a function of the geographic
 2538 polarity. In this view, plate dynamics could be a com-
 2539 bination of mantle convection and the shear induced by
 2540 the tidal drag (Fig. 37).

2541 13. Uncited references

2542 Oliver, 1972
 2543 Shemenda, 1993

2544 Acknowledgments

2545 The article benefited of the critical reading by D.
 2546 Frizon de Lamotte and N. Kukowski. Discussions with
 2547 M. Battaglia, C. Chiarabba, M. Crespi, G. Dal Piaz, C.
 2548 Facenna, E. Garzanti, F. Innocenti, S. Lallemand, G.
 2549 Panza, and F. Riguzzi were very stimulating. Research
 2550 was supported by the University La Sapienza, Roma.

2551 References

2552 Ampferer, O., 1906. Über das Bewegungsbild von Faltengebirge,
 2553 Austria. Geol. Bundesanst. Jahrb. 56, 539–622.
 2554 Anderson, D.L., 1989. Theory of the Earth. Blackwell, pp. 1–366.
 2555 Anderson, D.L., 2001. Topside tectonics. *Science* 293, 2016–2018.
 2556 Anderson, D.L., 2002. The case for irreversible chemical stratification
 2557 of the mantle. *Int. Geol. Rev.* 44, 97–116.
 2558 Anderson, D.L., 2006. Speculations on the nature and cause of mantle
 2559 heterogeneity. *Tectonophysics* 416, 7–22.
 2560 Baldwin, S.L., Monteleone, B.D., Webb, L.E., Fitzgerald, P.G., Grove,
 2561 M., Hill, E.J., 2004. Pliocene eclogite exhumation at plate tectonic
 2562 rates in eastern Papua New Guinea. *Nature* 431, 263–267.
 2563 Bally, A.W., Burbi, L., Cooper, C., Ghelardoni, R., 1986. Balanced
 2564 sections and seismic reflection profiles across the central
 2565 Apennine. *Mem. Soc. Geol. Ital.* 35, 257–310.
 2566 Banerjee, P., Bürgmann, R., 2002. Convergence across the northwest
 2567 Himalaya from GPS measurements. *Geophys. Res. Lett.* 29, 13
 2568 (10.1029/2002GL015184).
 2569 Barruol, G., Deschamps, A., Coutant, O., 2004. Mapping upper mantle
 2570 anisotropy beneath SE France by SKS splitting indicates Neogene
 2571 asthenospheric flow induced by Apenninic slab roll-back and
 2572 deflected by the deep Alpine roots. *Tectonophysics* 394, 125–138.
 2573 doi:10.1016/j.tecto.2004.08.002.
 2574 Battaglia, M., Murray, M.H., Serpelloni, E., Bürgmann, R., 2004.
 2575 The Adriatic region: an independent microplate within the Africa–
 2576 Eurasia collision zone. *Geophys. Res. Lett.* 31, L09605. doi:10.1029/
 2577 2004GL019723.

Bercovici, D., 1998. Generation of plate tectonics from lithosphere-
 mantle flow and void-volatile self-lubrication. *Earth Planet. Sci.*
Lett. 154, 139–151. 2578
 Bernet, M., Zattin, M., Garver, J.I., Brandon, M.T., Vance, J.A., 2001. 2581
 Steady-state exhumation of the European Alps. *Geology* 29, 2582
 35–38. 2583
 Bevis, M., Taylor, F.W., Schutz, B.E., Recy, J., Isacks, B.L., Helu, S., 2584
 Singh, R., Kendrick, E., Stowell, J., Taylor, B., Calmant, S., 1995. 2585
 Geodetic observations of very rapid convergence and back-arc 2586
 extension at the Tonga arc. *Nature* 374, 249–251. 2587
 Bigi, S., Lenci, F., Doglioni, C., Moore, J.C., Carminati, E., Scrocca, 2588
 D., 2003. Decollement depth vs accretionary prism dimension in 2589
 the Apennines and the Barbados. *Tectonics* 22 (2), 1010. 2590
 doi:10.1029/2002TC001410. 2591
 Bina, C.R., 1996. Phase transition buoyancy contributions to stresses 2592
 in subducting lithosphere. *Geophys. Res. Lett.* 23, 3563–3566. 2593
 Bird, P., 2003. An updated digital model of plate boundaries. *Geochem.* 2594
Geophys. Geosyst. 4 (3), 1027. doi:10.1029/2001GC000252. 2595
 Bokelmann, G.H.R., 2002. Which forces drive North America? 2596
Geology 30, 1027–1030. doi:10.1130/0091-7613. 2597
 Bonatti, E., 1990. Not so hot “hot spots” in the oceanic mantle. *Science* 2598
 250, 107–111. 2599
 Bonatti, E., Ligi, M., Brunelli, D., Cipriani, A., Fabretti, P., Ferrante, 2600
 V., Ottolini, L., 2003. Mantle thermal pulses below the Mid 2601
 Atlantic Ridge and temporal variations in the oceanic lithosphere. 2602
Nature 423, 499–505. 2603
 Bostrom, R.C., 1971. Westward displacement of the lithosphere. 2604
Nature 234, 356–358. 2605
 Braun, M.G., Hirth, G., Parmentier, E.M., 2000. The effects of deep 2606
 damp melting on mantle flow and melt generation beneath mid- 2607
 ocean ridges. *Earth Planet. Sci. Lett.* 176, 339–356. 2608
 Brooks, D.A., Carlson, R.L., Harry, D.L., Melia, P.J., Moore, R.P., 2609
 Rayhorn, J.E., Tubb, S.G., 1984. Characteristics of back-arc 2610
 regions. *Tectonophysics* 102, 1–16. 2611
 Cadet, J.-P., Charvet, J., 1983. From subduction to paleosubduction in 2612
 Northern Japan. In: Hashimoto, M., Uyeda, S. (Eds.), *Accretion*
Tectonics in the Circum-Pacific Regions, pp. 135–148. 2613
 Calcagnile, G., Panza, G.F., 1981. The main characteristics of the 2614
 lithosphere–asthenosphere system in Italy and surrounding 2615
 regions. *Pure Appl. Geophys.* 119, 865–879. 2616
 Calcagnile, G., D’Ingeo, F., Farrugia, P., Panza, G.F., 1982. The 2617
 lithosphere in the central-eastern Mediterranean area. *Pure Appl.* 2618
Geophys. 120, 389–406. 2619
 Carlson, R.L., Hilde, T.W.C., Uyeda, S., 1983. The driving mechanism 2620
 of plate tectonics: relation to age of the lithosphere at trenches. 2621
Geophys. Res. Lett. 10, 297–300. 2622
 Carminati, E., Doglioni, C., Argnani, A., Carrara, G., Dabovski, C., 2623
 Dumurdzanov, N., Gaetani, M., Georgiev, G., Mauffret, A., Nazai, 2624
 S., Sartori, R., Scionti, V., Scrocca, D., Séranne, M., Torelli, L., 2625
 Zagorchev, I., 2004a. TRANSMED Transect III. In: Cavazza, W., 2626
 Roure, F., Spakman, W., Stampfli, G.M., Ziegler, P.A. (Eds.), *The*
TRANSMED Atlas — the Mediterranean Region from Crust to 2627
Mantle. Springer-Verlag, Berlin, p. 141. 2628
 Carminati, E., Doglioni, C., Scrocca, D., 2004b. Alps vs Apennines. 2629
Special Volume of the Italian Geological Society for the IGC 32
Florence-2004, pp. 141–151. 2630
 Carminati, E., Negrodo, A.M., Valera, J.L., Doglioni, C., 2005. 2631
 Subduction-related intermediate-depth and deep seismicity in 2632
 Italy: insights from thermal and rheological modeling. *Phys.* 2633
Earth Planet. Inter. 149, 65–79. 2634
 Catalano, R., Doglioni, C., Merlini, S., 2001. On the Mesozoic Ionian 2635
 basin. *Geophys. J. Int.* 144, 49–64. 2636
 2637
 2638
 2639

- 2640 Carlson, R.L., Melia, P.J., 1984. Subduction hinge migration. *Tectonophysics* 102, 399–411.
- 2641 Tectonophysics 102, 399–411.
- 2642 Chase, C.G., 1979. Subduction, the geoid, and lower mantle convection. *Nature* 282, 464–468.
- 2643 convection. *Nature* 282, 464–468.
- 2644 Chiarabba, C., Jovane, L., DiStefano, R., 2005. A new view of Italian seismicity using 20 years of instrumental recordings. *Tectonophysics* 395, 251–268.
- 2645 seismicity using 20 years of instrumental recordings. *Tectonophysics* 395, 251–268.
- 2646 physics 395, 251–268.
- 2647 Christova, C., Nikolova, S.B., 1993. The Aegean region: deep structures and seismological properties. *Geophys. J. Int.* 115, 635–653.
- 2648 and seismological properties. *Geophys. J. Int.* 115, 635–653.
- 2649 Clément, C., Hirn, A., Charvis, P., Sachpazi, M., Marnelis, P., 2000. Seismic structure and the active Hellenic subduction in the Ionian islands. *Tectonophysics* 329, 141–156.
- 2650 Seismic structure and the active Hellenic subduction in the Ionian islands. *Tectonophysics* 329, 141–156.
- 2651 islands. *Tectonophysics* 329, 141–156.
- 2652 Clift, P.D., MacLeod, C.J., 1999. Slow rates of subduction erosion estimated from subsidence and tilting of the Tonga forearc. *Geology* 27, 411–414.
- 2653 estimated from subsidence and tilting of the Tonga forearc. *Geology* 27, 411–414.
- 2654 Clift, P.D., Pecher, I., Kukowski, N., Hampel, A., 2003. Tectonic erosion of the Peruvian forearc, Lima Basin, by subduction and Nazca Ridge collision. *Tectonics* 22 (3), 1023. doi:10.1029/2002TC001386.
- 2655 Tectonic erosion of the Peruvian forearc, Lima Basin, by subduction and Nazca Ridge collision. *Tectonics* 22 (3), 1023. doi:10.1029/2002TC001386.
- 2656 erosion of the Peruvian forearc, Lima Basin, by subduction and Nazca Ridge collision. *Tectonics* 22 (3), 1023. doi:10.1029/2002TC001386.
- 2657 Nazca Ridge collision. *Tectonics* 22 (3), 1023. doi:10.1029/2002TC001386.
- 2658 Nazca Ridge collision. *Tectonics* 22 (3), 1023. doi:10.1029/2002TC001386.
- 2659 Conrad, C.P., Lithgow-Bertelloni, C., 2003. How mantle slabs drive plate tectonics. *Science* 298, 207–209.
- 2660 How mantle slabs drive plate tectonics. *Science* 298, 207–209.
- 2661 Crespi, M., Cuffaro, M., Doglioni, C., Giannone, F., Riguzzi, F., 2007. Space geodesy validation of the global lithospheric flow. *Geophys. J. Int.* doi:10.1111/j.1365-246X.2006.03226.x.
- 2662 Space geodesy validation of the global lithospheric flow. *Geophys. J. Int.* doi:10.1111/j.1365-246X.2006.03226.x.
- 2663 J. Int. doi:10.1111/j.1365-246X.2006.03226.x.
- 2664 Cruciani, C., Carminati, E., Doglioni, C., 2005. Slab dip vs. lithosphere age: no direct function. *Earth Planet. Sci. Lett.* 238, 2666–310.
- 2665 Slab dip vs. lithosphere age: no direct function. *Earth Planet. Sci. Lett.* 238, 2666–310.
- 2666 lithosphere age: no direct function. *Earth Planet. Sci. Lett.* 238, 2666–310.
- 2667 Cuffaro, M., Jurdy, D.M., 2006. Microplate motions in the hotspot reference frame. *Terra Nova* 18, 276–281. doi:10.1111/j.1365-3121.2006.00690.x.
- 2668 Microplate motions in the hotspot reference frame. *Terra Nova* 18, 276–281. doi:10.1111/j.1365-3121.2006.00690.x.
- 2669 reference frame. *Terra Nova* 18, 276–281. doi:10.1111/j.1365-3121.2006.00690.x.
- 2670 Cuffaro, M., Doglioni, C., in press. Global Kinematics in the Deep Vs Shallow Hotspot Reference Frames. In Foulger G., Jurdy D. (Eds), 2671 The Origins of Melting Anomalies: Plates, Plumes, and Planetary Processes.
- 2672 The Origins of Melting Anomalies: Plates, Plumes, and Planetary Processes.
- 2673 Processes.
- 2674 Cuffaro, M., Caputo, M., Doglioni, C., 2004. On the sub-rotation of a plate. *J. Virt. Expl.* 14 (2), 1–12.
- 2675 On the sub-rotation of a plate. *J. Virt. Expl.* 14 (2), 1–12.
- 2676 Cuffaro, M., Carminati, E., Doglioni, C., 2006. Horizontal versus vertical plate motions. *Earth Discuss.* 1, 1–18.
- 2677 Horizontal versus vertical plate motions. *Earth Discuss.* 1, 1–18.
- 2678 Dadson, S.J., Hovius, N., Chen, H., Dade, B., Hsieh, M.L., Willett, S.D., 2679 Hu, J.C., Horng, M.J., Chen, M.C., Stark, C.P., Lague, D., Lin, J.C., 2003. Links between erosion, runoff variability and seismicity in the Taiwan orogen. *Nature* 426, 648–651.
- 2680 Links between erosion, runoff variability and seismicity in the Taiwan orogen. *Nature* 426, 648–651.
- 2681 Taiwan orogen. *Nature* 426, 648–651.
- 2682 D'Agostino, N., Selvaggi, G., 2004. Crustal motion along the Eurasia–Nubia plate boundary in the Calabrian Arc and Sicily and active extension in the Messina Straits from GPS measurements. *J. Geophys. Res.* 109, B11402. doi:10.1029/2004JB002998.
- 2683 Crustal motion along the Eurasia–Nubia plate boundary in the Calabrian Arc and Sicily and active extension in the Messina Straits from GPS measurements. *J. Geophys. Res.* 109, B11402. doi:10.1029/2004JB002998.
- 2684 extension in the Messina Straits from GPS measurements. *J. Geophys. Res.* 109, B11402. doi:10.1029/2004JB002998.
- 2685 J. Geophys. Res. 109, B11402. doi:10.1029/2004JB002998.
- 2686 Dal Piaz, G.V., Hunziker, J.C., Martinotti, G., 1972. La Zona Sesia-Lanzo e l'evoluzione tettonico-metamorfica delle Alpi nordoccidentali interne. *Mem. Soc. Geol. Ital.* 11, 433–466.
- 2687 La Zona Sesia-Lanzo e l'evoluzione tettonico-metamorfica delle Alpi nordoccidentali interne. *Mem. Soc. Geol. Ital.* 11, 433–466.
- 2688 internal interne. *Mem. Soc. Geol. Ital.* 11, 433–466.
- 2689 Dal Piaz, G.V., Bistacchi, A., Massironi, M., 2003. Geological outline of the Alps. *Episodes* 26 (3), 175–180.
- 2690 Geological outline of the Alps. *Episodes* 26 (3), 175–180.
- 2691 Davis, D., Suppe, J., Dahlen, F.A., 1983. Mechanics of fold and thrust belt and accretionary wedge. *J. Geophys. Res.* 88, 1153–1172.
- 2692 Mechanics of fold and thrust belt and accretionary wedge. *J. Geophys. Res.* 88, 1153–1172.
- 2693 Debayle, E., Kennett, B., Priestley, K., 2005. Global azimuthal seismic anisotropy and the unique plate-motion deformation of Australia. *Nature* 433, 509–512.
- 2694 Global azimuthal seismic anisotropy and the unique plate-motion deformation of Australia. *Nature* 433, 509–512.
- 2695 Nature 433, 509–512.
- 2696 DeMets, C., Gordon, R.G., Argus, D.F., Stein, S., 1994. Effect of recent revisions to the geomagnetic reversal time scale on estimates of current plate motions. *Geophys. Res. Lett.* 21, 2191–2194.
- 2697 Effect of recent revisions to the geomagnetic reversal time scale on estimates of current plate motions. *Geophys. Res. Lett.* 21, 2191–2194.
- 2698 current plate motions. *Geophys. Res. Lett.* 21, 2191–2194.
- 2699 Denis, C., Schreider, A.A., Varga, P., Zavoti, J., 2002. Despinning of the Earth rotation in the geological past and geomagnetic paleointensities. *J. Geodyn.* 34, 667–685.
- 2700 Despinning of the Earth rotation in the geological past and geomagnetic paleointensities. *J. Geodyn.* 34, 667–685.
- 2701 paleointensities. *J. Geodyn.* 34, 667–685.
- Devoti, R., Ferraro, C., Gueguen, E., Lanotte, R., Luceri, V., Nardi, A., Pacione, R., Rutigliano, P., Sciarretta, C., Vespe, F., 2002. Geodetic control on recent tectonic movements in the central Mediterranean area. *Tectonophysics* 346, 151–167.
- Geodetic control on recent tectonic movements in the central Mediterranean area. *Tectonophysics* 346, 151–167.
- Dickinson, W.R., 1978. Plate tectonic evolution of North Pacific rim. *J. Phys. Earth* 26, 51–519 (Suppl.).
- Plate tectonic evolution of North Pacific rim. *J. Phys. Earth* 26, 51–519 (Suppl.).
- Doglioni, C., 1989. Notes on the tectonics of Morocco. 28th International Geological Congress, Washington, vol. 1, pp. 402–403.
- Notes on the tectonics of Morocco. 28th International Geological Congress, Washington, vol. 1, pp. 402–403.
- Doglioni, C., 1990. The global tectonic pattern. *J. Geodyn.* 12, 21–38.
- The global tectonic pattern. *J. Geodyn.* 12, 21–38.
- Doglioni, C., 1991. A proposal of kinematic modelling for W-dipping subductions — possible applications to the Tyrrhenian–Apennines system. *Terra Nova* 3 (4), 423–434.
- A proposal of kinematic modelling for W-dipping subductions — possible applications to the Tyrrhenian–Apennines system. *Terra Nova* 3 (4), 423–434.
- Doglioni, C., 1992. Main differences between thrust belts. *Terra Nova* 4 (2), 152–164.
- Main differences between thrust belts. *Terra Nova* 4 (2), 152–164.
- Doglioni, C., 1993. Geological evidence for a global tectonic polarity. *J. Geol. Soc. (Lond.)* 150, 991–1002.
- Geological evidence for a global tectonic polarity. *J. Geol. Soc. (Lond.)* 150, 991–1002.
- Doglioni, C., 1994. Foredeeps versus subduction zones. *Geology* 22 (3), 271–274.
- Foredeeps versus subduction zones. *Geology* 22 (3), 271–274.
- Doglioni, C., 1995. Geological remarks on the relationships between extension and convergent geodynamic settings. *Tectonophysics* 252 (1–4), 253–267.
- Geological remarks on the relationships between extension and convergent geodynamic settings. *Tectonophysics* 252 (1–4), 253–267.
- Doglioni, C., Harabaglia, P., Merlini, S., Mongelli, F., Peccerillo, A., Piromallo, C., 1999a. Orogens and slabs vs their direction of subduction. *Earth-Sci. Rev.* 45, 167–208.
- Orogens and slabs vs their direction of subduction. *Earth-Sci. Rev.* 45, 167–208.
- Doglioni, C., Gueguen, E., Harabaglia, P., Mongelli, F., 1999b. On the origin of W-directed subduction zones and applications to the western Mediterranean. *Geol. Soc. London, Spec. Publ.* 156, 541–561.
- On the origin of W-directed subduction zones and applications to the western Mediterranean. *Geol. Soc. London, Spec. Publ.* 156, 541–561.
- Doglioni, C., Merlini, S., Cantarella, G., 1999c. Foredeep geometries at the front of the Apennines in the Ionian sea (central Mediterranean). *Earth Planet. Sci. Lett.* 168 (3–4), 243–254.
- Foredeep geometries at the front of the Apennines in the Ionian sea (central Mediterranean). *Earth Planet. Sci. Lett.* 168 (3–4), 243–254.
- Doglioni, C., Agostini, S., Crespi, M., Innocenti, F., Manetti, P., Riguzzi, F., Savascin, Y., 2002. On the extension in western Anatolia and the Aegean sea. *J. Virt. Expl.* 7, 117–131.
- On the extension in western Anatolia and the Aegean sea. *J. Virt. Expl.* 7, 117–131.
- Doglioni, C., Carminati, E., Bonatti, E., 2003. Rift asymmetry and continental uplift. *Tectonics* 22 (3), 1024. doi:10.1029/2002TC001459.
- Rift asymmetry and continental uplift. *Tectonics* 22 (3), 1024. doi:10.1029/2002TC001459.
- Doglioni, C., Carminati, E., Cruciani, C., Cuffaro, M., 2005a. Opposite Kinematics, no Slab dip Vs Lithosphere age Correlation, and passive Behavior of Subduction zones. *Geophys. Res. Abstr.* 7 (SRRef-ID: 1607-7962/gra/EGU05-A-01985).
- Opposite Kinematics, no Slab dip Vs Lithosphere age Correlation, and passive Behavior of Subduction zones. *Geophys. Res. Abstr.* 7 (SRRef-ID: 1607-7962/gra/EGU05-A-01985).
- Doglioni, C., Green, D., Mongelli, F., 2005b. On the shallow origin of hotspots and the westward drift of the lithosphere. In: Foulger, G.R., Natland, J.H., Presnall, D.C., Anderson, D.L. (Eds.), *Plates, Plumes, and Paradigms. Geological Society of America Special Paper*, vol. 388, pp. 735–749.
- On the shallow origin of hotspots and the westward drift of the lithosphere. In: Foulger, G.R., Natland, J.H., Presnall, D.C., Anderson, D.L. (Eds.), *Plates, Plumes, and Paradigms. Geological Society of America Special Paper*, vol. 388, pp. 735–749.
- Doglioni, C., Carminati, E., Cuffaro, M., 2006a. Simple kinematics of subduction zones. *Int. Geol. Rev.* 48 (6), 479–493.
- Simple kinematics of subduction zones. *Int. Geol. Rev.* 48 (6), 479–493.
- Doglioni, C., Cuffaro, M., Carminati, E., 2006b. What moves plates? *Boll. Geofis. Teor. Appl.* 47 (3), 227–247.
- What moves plates? *Boll. Geofis. Teor. Appl.* 47 (3), 227–247.
- Dragert, H., Wang, K., James, T.S., 2001. A silent slip event on the deeper Cascadia subduction interface. *Science* 292, 1525–1528.
- A silent slip event on the deeper Cascadia subduction interface. *Science* 292, 1525–1528.
- Dziewonski, A.M., Anderson, D.L., 1981. Preliminary reference Earth model. *Phys. Earth Planet. Inter.* 25, 297–356.
- Preliminary reference Earth model. *Phys. Earth Planet. Inter.* 25, 297–356.
- England, P., Engdahl, R., Thatcher, W., 2004. Systematic variation in the depths of slabs beneath arc volcanoes. *Geophys. J. Int.* 156 (2), 377–408.
- Systematic variation in the depths of slabs beneath arc volcanoes. *Geophys. J. Int.* 156 (2), 377–408.
- Ernst, W.G., 2005. Alpine and Pacific styles of Phanerozoic mountain building: subduction-zone petrogenesis of continental crust. *Terra Nova* 17, 165–188. doi:10.1111/j.1365-3121.2005.00604.x.
- Alpine and Pacific styles of Phanerozoic mountain building: subduction-zone petrogenesis of continental crust. *Terra Nova* 17, 165–188. doi:10.1111/j.1365-3121.2005.00604.x.
- Faccenna, C., Piromallo, C., Crespo-Blanc, A., Jolivet, L., Rossetti, F., 2004. Lateral slab deformation and the origin of the western Mediterranean. *Arcs. Tectonics* 23, TC1012. doi:10.1029/2002TC001488.
- Lateral slab deformation and the origin of the western Mediterranean. *Arcs. Tectonics* 23, TC1012. doi:10.1029/2002TC001488.

- 2764 Farrugia, P., Panza, G.F., 1981. Continental character of the lithosphere
2765 beneath the Ionian sea. In: Cassinis, R. (Ed.), *The Solution of the*
2766 *Inverse Problem in Geophysical Interpretation*. Plenum Pub. Corp.,
2767 pp. 327–334.
- 2768 Forsyth, D., Uyeda, S., 1975. On the relative importance of driving
2769 forces of plate motion. *Geophys. J. R. Astron. Soc.* 43, 163–200.
- 2770 Foulger, G.R., Natland, J.H., Presnall, D.C., Anderson, D.L., 2005.
2771 Plates, plumes, and paradigms. *Geol. Soc. Am., Spec. Pap.* 388.
- 2772 Fowler, C.M.R., 2005. *The Solid Earth: An Introduction to Global*
2773 *Geophysics*. Cambridge University Press, New York, p. 685.
- 2774 Frepoli, A., Selvaggi, G., Chiarabba, C., Amato, A., 1996. State of
2775 stress in the Southern Tyrrhenian subduction zone from fault-plane
2776 solutions. *Geophys. J. Int.* 125, 879–891.
- 2777 Frizon De Lamotte, D., 2005. About the Cenozoic inversion of the
2778 Atlas domain in North Africa. *C. R. Geosci.* 337, 475–476.
- 2779 Frizon de Lamotte, D., Saint Bezar, B., Bracène, R., Mercier, E., 2000.
2780 The two main steps of the Atlas building and geodynamics of the
2781 western Mediterranean. *Tectonics* 19, 740–761.
- 2782 Garfunkel, Z., Anderson, C.A., Schubert, G., 1986. Mantle circulation
2783 and the lateral migration of subducted slabs. *J. Geophys. Res.* 91,
2784 7205–7223.
- 2785 Garzanti, E., Vezzoli, G., Andò, S., 2002. Modern sand from obducted
2786 ophiolite belts (Sultanate of Oman and United Arab Emirates).
2787 *J. Geol.* 110, 371–391.
- 2788 Garzanti, E., Doglioni, C., Vezzoli, G., Andò, S., in press. Orogenic
2789 Belts and Orogenic Sediment Provenances. *J. Geol.*
- 2790 Giardini, D., Woodhouse, J.H., 1986. Horizontal shear flow in the
2791 mantle beneath the Tonga arc. *Nature* 319 (6054), 551–555.
- 2792 Giunchi, C., Sabadini, R., Boschi, E., Gasperini, P., 1996. Dynamic
2793 models of subduction: geophysical and geological evidence in the
2794 Tyrrhenian sea. *Geophys. J. Int.* 126, 555–578.
- 2795 Goes, S., Giardini, D., Jenny, S., Hollenstein, C., Kahle, H.-G., Geiger,
2796 A., 2004. A recent tectonic reorganization in the south-central
2797 Mediterranean. *Earth Planet. Sci. Lett.* 226, 335–345.
- 2798 Gordon, R.G., 2000. Diffuse oceanic plate boundaries: strain rates,
2799 vertically averaged rheology, and comparison with narrow plate
2800 boundaries and stable plate interiors. *AGU, Geophys. Monogr.*
2801 121, 143–159.
- 2802 Gordon, R.G., Stein, S., 1992. Global tectonics and space geodesy.
2803 *Science* 256, 333–342.
- 2804 Gripp, A.E., Gordon, R.G., 2002. Young tracks of hotspots and current
2805 plate velocities. *Geophys. J. Int.* 150, 321–361.
- 2806 Gueguen, E., Doglioni, C., Fernandez, M., 1997. Lithospheric
2807 boudinage in the Western Mediterranean back-arc basins. *Terra*
2808 *Nova* 9 (4), 184–187.
- 2809 Gueguen, E., Doglioni, C., Fernandez, M., 1998. On the post 25 Ma
2810 geodynamic evolution of the western Mediterranean. *Tectonophy-*
2811 *sics* 298, 259–269.
- 2812 Gung, Y., Panning, M., Romanowicz, B., 2003. Global anisotropy and
2813 the thickness of continents. *Nature* 422, 707–711.
- 2814 Gutscher, M.-A., Malod, J., Rehault, J.-P., Contrucci, I., Klinghoefer,
2815 F., Mendes-Victor, L., Spakman, W., 2002. Evidence for active
2816 subduction beneath Gibraltar. *Geology* 30, 1071–1074.
- 2817 Hacker, B.R., Abers, G.A., Peacock, S.M., 2003. Subduction factory 1:
2818 theoretical mineralogy, densities, seismic wave speeds and H₂O con-
2819 tents. *J. Geophys. Res.* 108 (B1), 2029. doi:10.1029/2001JB001127.
- 2820 Hamilton, W.B., 2003. An alternative Earth. *GSA Today* 13 (11), 4–12.
- 2821 Hammond, W.C., Toomey, D.R., 2003. Seismic velocity anisotropy
2822 and heterogeneity beneath the Mantle Electromagnetic and
2823 Tomography Experiment (MELT) region of the East Pacific Rise
2824 from analysis of P and S body waves. *J. Geophys. Res.* 108 (B4),
2825 2176. doi:10.1029/2002JB001789.
- Hassani, R., Jongmans, D., Chery, J., 1997. Study of plate deformation
and stress in subduction processes using two-dimensional
numerical models. *J. Geophys. Res.* 102, 17951–17965.
- Heflin, M. et al., 2005. <http://sideshow.jpl.nasa.gov/mbh/series.html>.
- Hermann, J., 2002. Experimental constraints on phase relations in
subducted continental crust. *Contrib. Mineral. Petrol.* 143, 219–235.
- Heuret, A., Lallemand, S., 2005. Plate motions, slab dynamics and
back-arc deformation. *Phys. Earth Planet. Inter.* 149, 31–51.
- Hollenstein, Ch., Kahle, H.-G., Geiger, A., Jenny, S., Goes, S.,
Giardini, D., 2003. New GPS constraints on the Africa–Eurasia
plate boundary zone in southern Italy. *Geophys. Res. Lett.* 30 (18),
1935. doi:10.1029/2003GL017554.
- Hunstad, I., Selvaggi, G., D’Agostino, N., England, P., Clarke, P., Pierozzi,
M., 2003. Geodetic strain in peninsular Italy between 1875 and 2001.
Geophys. Res. Lett. 30 (4), 1181. doi:10.1029/2002GL016447.
- Husson, L., Ricard, Y., 2004. Stress balance above subduction:
application to the Andes. *Earth Planet. Sci. Lett.* 222, 1037–1050.
- Hyndman, R.D., Wang, K., Yuan, T., Spence, G.D., 1993. Tectonic
sediment thickening, fluid expulsion, and the thermal regime of
subduction zone accretionary prisms: the Cascadia margin off
Vancouver Island. *J. Geophys. Res.* 98, 21,865–21,876.
- IESG-IGETH, Italian Explosion Seismology Group, Institute of
Geophysics, ETH, Zürich, 1981. Crust and upper mantle structures
in the southern Alps from deep seismic sounding profiles (1977,
1978) and surface wave dispersion analysis. *Boll. Geofis. Teor.*
Appl. 23, 297–330.
- Innocenti, F., Kolios, N., Manetti, P., Rita, F., Villari, L., 1982. Acid
and basic late neogene volcanism in central Aegean Sea: its nature
and geotectonic significance. *Bull. Volcanol.* 45, 87–97.
- Innocenti, F., Kolios, N., Manetti, P., Mazzuoli, R., 1984. Evolution
and geodynamic significance of Tertiary orogenic volcanism in
Northeastern Greece. *Bull. Volcanol.* 47-1, 25–37.
- Isacks, B., Molnar, P., 1971. Distribution of stresses in the descending
lithosphere from a global survey of focal-mechanism solutions of
mantle earthquakes. *Rev. Geophys.* 9, 103–174.
- Jade, S., Bhatt, B.C., Yang, Z., Bendick, R., Gaur, V.K., Molnar, P., Anand,
M.B., Kumar, D., 2004. GPS measurements from the Ladakh
Himalaya, India: preliminary tests of plate-like or continuous
deformation in Tibet. *Geol. Soc. Amer. Bull.* 116 (11/12),
1385–1391. doi:10.1130/B25357.1.
- Jarrard, R.D., 1986. Relations among subduction parameters. *Rev.*
Geophys. 24, 217–284.
- Jordan, T.H., 1974. Some comments on tidal drag as a mechanism for
driving plate motions. *J. Geophys. Res.* 79 (14), 2141–2142.
- Jordan, T.H., 1988. Structure and formation of the continental
tectosphere. *J. Petrol. (Special Lithosphere Issue)* 11–37.
- Jouanne, F., Mugnier, J.L., Gamond, J.F., Le Fort, P., Pandey, M.R.,
Bollinger, L., Flouzat, M., Avouac, J.P., 2004. Current shortening
across the Himalayas of Nepal. *Geophys. J. Int.* 157, 1–14.
- Karig, D.E., 1971. Origin and development of marginal basins in the
Western Pacific. *J. Geophys. Res.* 76, 2542–2561.
- Karig, D.E., Sharman III, G.F., 1975. Subduction and accretion in
trenches. *Geol. Soc. Amer. Bull.* 86, 377–389.
- Kastens, K., et al., 1988. ODP Leg 107 in the Tyrrhenian Sea: insights
into passive margin and back-arc basin evolution. *Geol. Soc. Amer.*
Bull. 100, 1140–1156.
- Kelly, R.K., Kelemen, P.B., Jull, M., 2003. Buoyancy of the conti-
nental upper mantle. *Geochem. Geophys. Geosyst.* 4 (2), 1017.
doi:10.1029/2002GC000399.
- Kennedy, L.A., Russell, J.K., Kopylova, M.G., 2002. Mantle shear
zones revisited: the connection between the cratons and mantle
dynamics. *Geology* 30 (5), 419–422.

- 2888 Kennett, B.L.N., Engdahl, E.R., Bulland, R., 1995. Constraints on seismic
2889 velocities in the Earth from traveltimes. *Geophys. J. Int.* 122, 108–124.
- 2890 Kukowski, N., von Huene, R., Malavieille, J., Lallemand, S.E., 1994.
2891 Sediment accretion against a buttress beneath the Peruvian
2892 continental margin at 12 S as simulated with sandbox modeling.
2893 *Geol. Rundsch.* 83, 822–831.
- 2894 Kukowski, N., Hampel, A., Bialas, J., Huebscher, C., Barckhausen, U.,
2895 Bourgois, J., 2001. Tectonic erosion at the Peruvian margin:
2896 evidence from swath bathymetry data and process identification
2897 from 3D sandbox analogue modeling. *Eos, Trans. AGU* 82 (47)
2898 (Fall Meet. Suppl., Abstract T31A-0817).
- 2899 Lallemand, S., Heuret, A., Boutelier, D., 2005. On the relationships
2900 between slab dip, back-arc stress, upper plate absolute motion and
2901 crustal nature in subduction zones. *Geochem. Geophys. Geosyst.*
2902 6, Q09006. doi:10.1029/2005GC000917.
- 2903 Laubscher, H.P., 1988. The arcs of the Western Alps and the Northern
2904 Apennines: an updated view. *Tectonophysics* 146, 67–78.
- 2905 Laville, E., Petit, J.-P., 1984. Role of synsedimentary strike-slip faults in
2906 the formation of the Moroccan Triassic basins. *Geology* 12, 424–427.
- 2907 Lenci, F., Doglioni, C., in press. On some geometric prism asym-
2908 metries. Springer Verlag, IFP.
- 2909 Lenci, F., Carminati, E., Doglioni, C., Scrocca, D., 2004. Basal
2910 décollement and subduction depth vs. topography in the Apen-
2911 nines–Calabrian arc. *Boll. Soc. Geol. Ital.* 123, 497–502.
- 2912 Le Pichon, X., 1968. Sea-floor spreading and continental drift.
2913 *J. Geophys. Res.* 73 (12), 3661–3697.
- 2914 Liu, T.K., 1982. Tectonic implications of fission-track ages from the
2915 Central Range, Taiwan. *Proc. Geol. Soc. China* 25, 22–37.
- 2916 Liu, M., Yang, Y., Stein, S., Zhu, Y., Engeln, J., 2000. Crustal
2917 shortening in the Andes: why do GPS rates differ from geological
2918 rates? *Geophys. Res. Lett.* 27, 3005–3008.
- 2919 Liu, S., Wang, L., Li, C., Li, H., Han, Y., Jia, C., Wei, G., 2004.
2920 Thermal-rheological structure of lithosphere beneath the northern
2921 flank of Tarim Basin, western China: implications for geody-
2922 namics. *Sci. China, Ser. D: Earth Sci.* 47 (7), 659–672.
- 2923 Lithgow-Bertelloni, C., Richards, M.A., 1998. The dynamics of
2924 Cenozoic and Mesozoic plate motions. *Rev. Geophys.* 36, 27–78.
- 2925 Lustrino, M., 2005. How the delamination and detachment of lower
2926 crust can influence basaltic magmatism. *Earth-Sci. Rev.* 72, 21–38.
- 2927 Mantovani, E., Viti, M., Albarello, D., Babbucci, D., Tamburelli, C.,
2928 Cenni, N., 2002. Generation of backarc basins in the Mediterra-
2929 nean region: driving mechanisms and quantitative modelling. *Boll.*
2930 *Soc. Geol. Ital., Vol. Spec.* 1, 99–111.
- 2931 Margheriti, L., Lucente, F.P., Pondrelli, S., 2003. SKS splitting
2932 measurements in the Apenninic–Tyrrhenian domain (Italy) and
2933 their relation with lithospheric subduction and mantle convection.
2934 *J. Geophys. Res.* 108 (B4), 2218. doi:10.1029/2002JB001793.
- 2935 Mariotti, G., Doglioni, C., 2000. The dip of the foreland monocline in
2936 the Alps and Apennines. *Earth Planet. Sci. Lett.* 181, 191–202.
- 2937 Marotta, A., Mongelli, F., 1998. Flexure of subducted slabs. *Geophys.*
2938 *J. Int.* 132, 701–711.
- 2939 Mazzotti, S., Henry, P., Le Pichon, X., 2001. Transient and permanent
2940 deformation of central Japan estimated by GPS — 2. strain partitioning
2941 and arc–arc collision. *Earth Planet. Sci. Lett.* 184, 455–469.
- 2942 McKenzie, D.P., 1977. The initiation of trenches: a finite amplitude
2943 instability. In: Talwani, M., Pitman III, (Eds.), *Island Arcs, Deep*
2944 *Sea Trenches and Back-Arc Basins*. Maurice Ewing Ser., vol. 1.
2945 Am. Geophys. Un., Washington, D.C., pp. 57–61.
- 2946 Melosh, H., Raefsky, A., 1980. The dynamic origin of subduction zone
2947 topography. *Geophys. J. R. Astron. Soc.* 60, 333–354.
- 2948 Mitchell, A.H.G., Garson, M.S., 1981. *Mineral Deposits and Global*
2949 *Tectonic Settings*. Academic Press, London.
- Montario, M. J., 2001. Exhumation of the Cordillera Blanca, Northern
Peru, based on apatite fission track analysis. Department of Geology,
Union College, Schenectady, New York, Unpublished Thesis.
- Moore, G.W., 1973. Westward tidal lag as the driving force of plate
tectonics. *Geology* 1, 99–100.
- Moore, G.F., Shipley, T.H., Stoffa, P.L., Karig, D.E., Taira, A.,
Kuramoto, S., Tokuyama, H., Suyehiro, K., 1990. Structure of the
Nankai Trough accretionary zone from multichannel seismic
reflection data. *J. Geophys. Res.* 95, 8753–8765.
- Mueller, S., Panza, G.F., 1986. In: Wezel, F.C. (Ed.), *Evidence of a*
Deep-reaching Lithospheric Root under the Alpine Arc. *The*
Origin of Arcs, vol. 21. Elsevier, pp. 93–113.
- Mueller, R.D., Roest, W.R., Royer, J.Y., Gahagan, L.M., Sclater, J.G.,
1997. Digital isochrons of the world's ocean floor. *J. Geophys.*
Res. 102, 3211–3214.
- Negredo, A.M., Jiménez-Munt, I., Villasenor, A., 2004. Evidence for
eastward mantle flow beneath the Caribbean plate from neo-
tectonic modeling. *Geophys. Res. Lett.* 31, L06615. doi:10.1029/
2003GL019315.
- Nicolas, A., Boudier, B., Ildefonse, B., Ball, E., 2000. Accretion of
Oman and United Arab Emirates ophiolite: discussion of a new
structural map, with three structural maps, scale 1:500,000. In:
Boudier, F., Juteau, T. (Eds.), *The Ophiolite of Oman and United*
Arab Emirates. *Mar. Geophys. Res.*, vol. 21, pp. 147–179.
- Nishiwaki, C., Uyeda, S., 1983. Accretion tectonics and metallogene-
sis. In: Hashimoto, M., Uyeda, S. (Eds.), *Accretion Tectonics in*
the Circum-Pacific Regions, pp. 349–355.
- Niu, Y., O'Hara, M.J., Pearce, J.A., 2003. Initiation of subduction
zones as a consequence of lateral compositional buoyancy contrast
within the lithosphere: a petrological perspective. *J. Petrol.* 44 (5),
851–866.
- Norton, I.O., 2000. Global hotspot reference frames and plate motion.
In: Richards, M.A., Gordon, R.G., Van der Hilst, R.D. (Eds.), *The*
History and Dynamics of Global Plate Motions. *Geophysical*
Monograph, vol. 121, pp. 339–357.
- Oldow, J.S., Ferranti, L., Lewis, D.S., Campbell, J.K., D'Argenio, B.,
Catalano, R., Pappone, G., Carmignani, L., Conti, P., Aiken, C.,
2002. Active fragmentation of Adria, the north Africa promontory,
central Mediterranean orogen. *Geology* 30, 779–782.
- Oliver, J., 1972. Contributions of seismology to Plate Tectonics. *Am.*
Assoc. Pet. Geol. Bull. 56 (2), 214–225.
- Omori, S., Komabayashi, T., Maruyama, S., 2004. Dehydration and
earthquakes in the subducting slab: empirical link in interme-
diate and deep seismic zones. *Phys. Earth Planet. Inter.* 146,
297–311.
- Oxburgh, E.R., Parmentier, E.M., 1977. Compositional and density
stratification in oceanic lithosphere; causes and consequences.
J. Geol. Soc. (Lond.) 133 (4), 343–355.
- Panza, G.F., 1980. Evolution of the Earth's lithosphere. In: Davies, P.A.,
Runcorn, S.K. (Eds.), *Mechanisms of Continental Drift and Plate*
Tectonics. Academic Press, pp. 75–87.
- Panza, G.F., Mueller, S., 1978. The plate boundary between Eurasia
and Africa in the Alpine Area. *Mem. Soc. Geol. Ital.* 33, 43–50.
- Panza, G.F., Mueller, S., Calcagnile, G., Knopoff, L., 1982.
Delineation of the north central Italian upper mantle anomaly.
Nature 296, 238–239.
- Panza, G.F., Ponteviso, A., Chimera, G., Raykova, R., Aoudia, A.,
2003. The Lithosphere–Asthenosphere: Italy and surroundings.
Episodes 26 (3), 169–174.
- Panza, G., Raykova, R.B., Carminati, E., Doglioni, C., 2007. Upper
mantle flow in the western Mediterranean. *Earth Planet. Sci. Lett.*
doi:10.1016/j.epsl.2007.02.03.

- 3012 Papazachos, B.C., Dimitriadis, S.T., Panagiotopoulos, D.G., Papaza- 3074
 3013 chos, C.B., Papadimitriou, E.E., 2005. Deep structure and active 3075
 3014 tectonics of the southern Aegean volcanic arc. In: Fytikas, M., 3076
 3015 Vougioukalakis, G.E. (Eds.), *The South Aegean Active Volcanic* 3077
 3016 *Arc. Developments in Volcanology*, vol. 7. Elsevier, pp. 47–64. 3078
- 3017 Pepe, F., Sulli, A., Bertotti, G., Catalano, R., 2005. Structural highs 3079
 3018 formation and their relationship to sedimentary basins in the north 3080
 3019 Sicily continental margin (southern Tyrrhenian Sea): implication 3081
 3020 for the Drepano Thrust Front. *Tectonophysics* 409, 1–18. 3082
- 3021 Pertermann, M., Hirschmann, M.M., 2003. Anhydrous partial melting 3083
 3022 experiments on MORB-like eclogite: phase relations, phase 3084
 3023 compositions and mineral-melt partitioning of major elements at 3085
 3024 2–3 Gpa. *J. Petrol.* 44 (12), 2173–2201. 3086
- 3025 Piromallo, C., Morelli, A., 2003. P wave tomography of the mantle 3087
 3026 under the Alpine-Mediterranean area. *J. Geophys. Res.* 108 (B2), 3088
 3027 2065. doi:10.1029/2002JB001757. 3089
- 3028 Poli, S., Schmidt, M.W., 2002. Petrology of subducted slabs. *Annu.* 3090
 3029 *Rev. Earth Planet. Sci.* 20, 207–235. 3091
- 3030 Pollitz, F.F., Buegmann, R., Romanowicz, B., 1998. Viscosity of 3092
 3031 oceanic asthenosphere inferred from remote triggering of earth- 3093
 3032 quakes. *Science* 280, 1245–1249. 3094
- 3033 Pondrelli, S., Piromallo, C., Serpelloni, E., 2004. Convergence vs. 3095
 3034 retreat in Southern Tyrrhenian Sea: insights from kinematics. 3096
 3035 *Geophys. Res. Lett.* 31, L06611. doi:10.1029/2003GL019223. 3097
- 3036 Ranalli, G., 1995. *Rheology of the Earth*. Chapman and Hall, pp. 1–413. 3098
- 3037 Ranalli, G., Pellegrini, R., D’Offizi, S., 2000. Time dependence of 3099
 3038 negative buoyancy and the subduction of continental lithosphere. 3100
 3039 *J. Geodyn.* 30 (5), 539–555. 3101
- 3040 Ranero, C., von Huene, R., 2000. Subduction erosion along the Middle 3102
 3041 America convergent margin. *Nature* 344, 31–36. 3103
- 3042 Rehault, J.P., Mascle, J., Boillot, G., 1984. Evolution géodynamique de la 3104
 3043 Méditerranée depuis l’Oligocène. *Mem. Soc. Geol. Ital.* 27, 85–96. 3105
- 3044 Rehault, J.P., Boillot, G., Mauffret, A., 1985. The western Mediterranean 3106
 3045 basin. In: Stanley, D.J., Wezel, F.C. (Eds.), *Geological Evolution of* 3107
 3046 *the Mediterranean Basin*. Springer-Verlag, New York, pp. 101–130. 3108
- 3047 Regard, V., Faccenna, C., Martinod, J., Bellier, Q., Thomas, J.-C., 3109
 3048 2003. From subduction to collision: control of deep processes on 3110
 3049 the evolution of convergent plate boundary. *J. Geophys. Res.* 108 3111
 3050 (B4), 2208. doi:10.1029/2002JB001943. 3112
- 3051 Ricard, Y., Doglioni, C., Sabadini, R., 1991. Differential rotation 3113
 3052 between lithosphere and mantle: a consequence of lateral viscosity 3114
 3053 variations. *J. Geophys. Res.* 96, 8407–8415. 3115
- 3054 Riguzzi, F., Cuffaro, M., Crespi, M., Doglioni, C., Giannone, F., 2006. 3116
 3055 A model of plate motions. In: Sansò, F., Gil, A.J. (Eds.), *Geodetic* 3117
 3056 *Deformation Monitoring: From Geophysical to Engineering* 3118
 3057 *Roles*. International Association of Geodesy Symposia, vol. 131. 3119
 3058 Springer, pp. 200–208. 3120
- 3059 Rittmann, A., 1942. Zur Thermodynamik der Orogenese. *Geol.* 3121
 3060 *Rundsch.* 33, 485–498. 3122
- 3061 Robbins, J.W., Smith, D.E., Ma, C., 1993. Horizontal crustal 3123
 3062 deformation and large scale plate motions inferred from space 3124
 3063 geodetic techniques. *Contributions of Space Geodesy to Geody-* 3125
 3064 *namics: Crustal Dynamics*. Am. Geophys. Un., Geodynamics, 3126
 3065 vol. 23, pp. 21–36. 3127
- 3066 Roca, E., Frizon de Lamotte, D., Mauffret, A., Bracène, R., Vergés, J., 3128
 3067 Benaouali, N., Fernández, M., Muñoz, J.A., Zeyen, H., 2004. 3129
 3068 TRANSMED Transect II. In: Cavazza, W., Roure, F., Spakman, 3130
 3069 W., Stampfli, G.M., Ziegler, P.A. (Eds.), *The TRANSMED* 3131
 3070 *Atlas — The Mediterranean Region from Crust to Mantle*. 3132
 3071 Springer, Berlin Heidelberg. 3133
- 3072 Royden, L.H., 1993. The tectonic expression slab pull at continental 3134
 3073 convergent boundaries. *Tectonics* 12, 303–325. 3135
- Royden, L.H., Burchfiel, B.C., 1989. Are systematic variations in 3074
 thrust belt style related to plate boundary processes? (the western 3075
 Alps versus the Carpathians). *Tectonics* 8 (1), 51–62. 3076
- Ruff, L., Kanamori, H., 1980. Seismicity and the subduction process. 3077
Phys. Earth Planet. Inter. 23, 240–252. 3078
- Russo, R.M., Silver, P.G., 1994. Trench-parallel flow beneath the 3079
 Nazca plate from seismic anisotropy. *Science* 263, 1105–1111. 3080
- Rychert, C.A., Fischer, K.M., Rondenay, S., 2005. A sharp 3081
 lithosphere–asthenosphere boundary imaged beneath eastern 3082
 North America. *Nature* 436, 542–545. doi:10.1038/03904. 3083
- Sabadini, R., Vermeersen, B., 2004. *Global dynamics of the Earth*. 3084
 Springer, Mod. Approaches Geophys. 20, 1–344. 3085
- Schettino, A., 1999. Computational methods for calculating geomet- 3086
 rical parameters of tectonic plates. *Comput. Geosci.* 25, 897–9907. 3087
- Scholz, C.H., Campos, J., 1995. On the mechanism of seismic 3088
 decoupling and back arc spreading at subduction zones. 3089
J. Geophys. Res. 100 (B11), 22,103–22,115. 3090
- Scoppola, B., Boccaletti, D., Bevis, M., Carminati, E., Doglioni, C., 3091
 2006. The westward drift of the lithosphere: a rotational drag? 3092
Geol. Soc. Amer. Bull. 118 (1/2). doi:10.1130/B25734.1. 3093
- Scrocca, D., Doglioni, C., Innocenti, F., Manetti, P., Mazzotti, A., 3094
 Bertelli, Burbi, L., D’Offizi, S., 2003. CROP atlas: seismic reflection 3095
 profiles of the Italian crust. *Mem. Descr. Carta Geol. Ital.* 62, 194. 3096
- Scrocca, D., Carminati, E., Doglioni, C., 2005. Deep structure of the 3097
 Southern Apennines (Italy): thin-skinned or thick-skinned? 3098
Tectonics 24, TC3005. doi:10.1029/2004TC001634. 3099
- Secco, R.A., 1995. Viscosity of the outer core. *Mineral Physics and* 3100
Crystallography. A Handbook of Physical Constants. AGU 3101
 Reference Shelf, vol. 2, pp. 218–226. 3102
- Sella, G.F., Dixon, T.H., Mao, A., 2002. REVEL: a model for recent 3103
 plate velocity from space geodesy. *J. Geophys. Res.* 107 (B4), 3104
 2081. doi:10.1029/2000JB000033. 3105
- Seno, T., Yoshida, M., 2004. Where and why do large shallow intraslab 3106
 earthquakes occur? *Phys. Earth Planet. Inter.* 141, 183–206. 3107
- Serpelloni, E., Anzidei, M., Baldi, P., Casula, G., Galvani, A., 2005. 3108
 Crustal velocity and strain-rate fields in Taly and surrounding 3109
 regions: new results from the analysis of permanent and non- 3110
 permanent GPS networks. *Geophys. J. Int.* 161, 861–880. 3111
 doi:10.1111/j.1365-246X.2005.02618.x. 3112
- Shemenda, A.I., 1993. Subduction of the lithosphere and back-arc 3113
 dynamics: insights from physical modelling. *J. Geophys. Res.* 98, 3114
 16167–16185. 3115
- Sillitoe, R.H., 1977. Metallogeny of an Andean-type continental 3116
 margin in South Korea: implications for opening of the Japan Sea. 3117
 In: Talwani, M., Pitman III, (Eds.), *Island Arcs, Deep Sea* 3118
Trenches and Back-Arc Basins. AGU, Maurice Ewing Series, 3119
 vol. 1, pp. 303–310. 3120
- Silver, P.G., Holt, W.E., 2002. The mantle flow field beneath western 3121
 north America. *Science* 295, 1054–1057. 3122
- Smith, A.D., Lewis, C., 1999. The planet beyond the plume hypothesis. 3123
Earth-Sci. Rev. 48, 135–182. 3124
- Spence, W., 1987. Slab pull and the seismotectonics of subducting 3125
 lithosphere. *Rev. Geophys.* 25 (1), 55–69. 3126
- Spotila, J.A., Buscher, J.T., Meigs, A.J., Reiners, P.W., 2004. Long- 3127
 term glacial erosion of active mountain belts: example of the 3128
 Chugach–St. Elias Range, Alaska. *Geology* 32, 501–504. 3129
- Stampfli, G.M., Borel, G.D., 2002. A plate tectonic model for the 3130
 Paleozoic and Mesozoic constrained by dynamic plate boundaries 3131
 and restored synthetic oceanic isochrons. *Earth Planet. Sci. Lett.* 196 3132
 (1), 17–33. 3133
- Stein, S., Wysession, M., 2003. *Introduction to Seismology, Earth-* 3134
quakes, & Earth Structure. Blackwell Sci., p. 498. 3135

- 3136 Stern, R.J., 2002. Subduction zones. *Rev. Geophys.* 40, 1012.
3137 doi:10.1029/2001RG000108.
- 3138 Suyehiro, K., Takahashi, N., Arie, Y., Yokoi, Y., Hino, R., Shinohara,
3139 M., Kanazawa, T., Hirata, N., Tokuyama, H., Taira, A., 1996.
3140 Continental crust, crustal underplating, and low-Q upper mantle
3141 beneath an oceanic island arc. *Science* 272, 390–392.
- 3142 Syracuse, E.M., Abers, G.A., 2006. Global compilation of variations
3143 in slab depth beneath arc volcanoes and implications. *Geochem.*
3144 *Geophys. Geosyst.* 7, Q05017. doi:10.1029/2005GC001045.
- 3145 Tatsumi, Y., Eggins, S., 1995. Subduction zone magmatism. *Frontiers*
3146 in Earth Sciences. Blackwell Science, pp. 1–211.
- 3147 Taylor, B., Zellmer, K., Martinez, F., Goodliffe, A., 1996. Sea-floor
3148 spreading in the Lau back-arc basin. *Earth Planet. Sci. Lett.* 144,
3149 35–40.
- 3150 Teixell, A., Arboleya, M.-L., Julivert, M., Charroud, M., 2003.
3151 Tectonic shortening and topography in the central High Atlas
3152 (Morocco). *Tectonics* 22 (5), 1051. doi:10.1029/2002TC001460.
- 3153 Trampert, J., Deschamps, F., Resovsky, J., Yuen, D., 2004.
3154 Probabilistic tomography maps chemical heterogeneities through-
3155 out the lower mantle. *Science* 306, 853–856.
- 3156 TRANSALP Working Group, 2002. First deep seismic reflection images
3157 of the Eastern Alps reveal giant crustal wedges and transcrustal
3158 ramps. *Geophys. Res. Lett.* 29, 10 (10.1029/2002GL014911).
- 3159 Trümpy, R., 1975. On crustal subduction in the Alps. In: Mahel, M.
3160 (Ed.), *Tectonic Problems in the Alpine system*, Bratislava. Slovak
3161 Academy of Sciences, pp. 121–130.
- 3162 Turcotte, D.L., Schubert, G., 2002. *Geodynamics*. Cambridge
3163 University Press. 456 pp.
- 3164 Uyeda, S., Kanamori, H., 1979. Back-arc opening and the mode of
3165 subduction. *J. Geophys. Res.* 84 (B3), 1049–1061.
- 3166 Van der Hilst, R., 2004. Changing views on Earth's deep mantle.
3167 *Science* 306, 817–818.
- 3168 van Hinsbergen, D.J., Hafkenscheid, E., Spakman, W., Meulenkamp, J.E.,
3169 Wortel, R., 2005. Nappe stacking resulting from subduction of oceanic
3170 and continental lithosphere below Greece. *Geology* 33 (4), 325–328.
- 3171 Van Hunen, J., van den Berg, A.P., Vlaar, N.J., 2002. The impact of the
3172 South-American plate motion and the Nazca Ridge subduction on
3173 the flat subduction below South Peru. *Geophys. Res. Lett.* 29, 14
3174 (10.1029/2001GL014004).
- 3175 von Huene, R., 1986. Seismic images of modern convergent margin
3176 tectonic structure. *Am. Assoc. Pet. Geol. Stud.* 26, 1–60.
- 3177 von Huene, R., Lallemand, S., 1990. Tectonic erosion along the Japan
3178 and Peru convergent margins. *Geol. Soc. Amer. Bull.* 102 (6),
3179 704–720.
- 3222
- Wang, C.G., 1975. Are continents adrift, or driven? *New Asia College,*
Academic Annual, vol. XVII, pp. 347–354. 3180
- Warne, J.E., 1988. Evolution of the Jurassic High Atlas Rift, Morocco;
Transtension, structural and eustatic controls on carbonate deposi-
tion, tectonic inversion. *AAPG Mediterranean Basins Conference,*
Nice, France. Guidebook, Field Trip, vol. 9, p. 315. 3181
3182
3183
3184
3185
- Waschbusch, P., Beaumont, C., 1996. Effect of slab retreat on crustal
deformation in simple regions of plate convergence. *J. Geophys.*
Res. 101 (B12), 28,133–28,148. 3186
3187
3188
- Watts, A.B., Zhong, S., 2000. Observations of flexure and rheology of
oceanic lithosphere. *Geophys. J. Int.* 142, 855–875. 3189
3190
- Wdowinski, S., 1992. Dynamically supported trench topography.
J. Geophys. Res. 97, 17651–17656. 3191
3192
- Weber, J.C., Dixon, T.H., DeMets, C., Ambeh, W.B., Jansma, P.,
Mattioli, G., Saleh, J., Sella, G., Bilham, R., Pérez, O., 2001. GPS
estimate of relative motion between the Caribbean and South
American plates, and geologic implications for Trinidad and
Venezuela. *Geology* 29 (1), 75–78. 3193
3194
3195
3196
3197
- Willett, S.D., Brandon, M.T., 2002. On steady states in mountain belts.
Geology 30, 175–178. 3198
3199
- Winter, J., 2001. *An Introduction to Igneous and Metamorphic
Petrology*, Prentice Hall, New Jersey, p. 697. 3200
3201
- Wong A Ton, S.Y.M., Wortel, M.J.R., 1997. Slab detachment in
continental zones: an analysis of controlling parameters. *Geophys.*
Res. Lett. 24, 2095–2098. 3202
3203
3204
- Woodward, N.B., Boyer, S.E., Suppe, J., 1989. Balanced geological
cross-sections: an essential technique in geological research and
exploration. *Am. Geophys. Union, Short Course Geol.* 6, 132. 3205
3206
3207
- Wortel, M.J.R., Spakman, W., 2000. Subduction and slab detachment in
the Mediterranean–Carpathian region. *Science* 290, 1910–1917. 3208
3209
- Yamazaki, T., Seama, N., Okino, K., Kitada, K., Joshima, M., Oda, H.,
Naka, J., 2003. Spreading process of the northern Mariana Trough:
Rifting–spreading transition at 22 N. *Geochem. Geophys. Geophys.*
Geosyst. 4 (9), 1075. doi:10.1029/2002GC000492. 3210
3211
3212
3213
- Zhang, P.-Z., Shen, Z., Wang, M., Gan, W., Bürgmann, R., Molnar, P.,
Wang, Q., Niu, Z., Sun, J., Wu, J., Hanrong, S., Xinzhao, Y., 2004.
Continuous deformation of the Tibetan Plateau from global
positioning system data. *Geology* 32 (9), 809–812. doi:10.1130/
G20554.1. 3214
3215
3216
3217
3218
- Zhong, S., Gurnis, M., 1992. Viscous flow model of subduction zone
with a faulted lithosphere: long and short wavelength topography,
gravity and geoid. *Geophys. Res. Lett.* 19, 1891–1894. 3219
3220
3221